Characterization of Homeodomain - Leucine Zipper Genes in *Physcomitrella patens* with Reference to Evolution of Homeobox Genes in Land Plants

Keiko Sakakibara

PhD Dissertation

2002

Department of Molecular Biomechanics

School of Life Science

The Graduate University for Advanced Studies

TABLE OF CONTENTS

List of tables

Tables

List of figures

Figures

Abstract

Land plants have evolved multicellular bodies with specialized cell types in both gametophytes and sporophytes. In the last decade, the molecular mechanisms of sporophyte cell differentiation have been studied extensively, while those in gametophytes are mostly unknown. The moss Physcomitrella (*Physcomitrella patens*) is a model for studying gametophyte cell differentiation, because functional gene analysis techniques have been established and its gametophytes are easily observed at the cellular level. Although sporophytes and gametophytes acquired multicellular bodies independently, members of a common gene family may regulate cell differentiation in both gametophytes and sporophytes. To study gametophyte cell differentiation, we first screened Physcomitrella gametophytes for homeodomain-leucine zipper (HD-Zip) genes, which are involved in cell differentiation in angiosperm sporophytes.

Chapter 1 describes how 10 HD-Zip genes (named *Pphb1-10*) were isolated from Physcomitrella. Phylogenetic analyses comparing moss and angiosperm HD-Zip genes indicated that all the *Pphb* genes, except *Pphb3*, belong to three of the four HD-Zip subfamilies (HD-Zip I, II, and III), and that these subfamilies originated before the divergence of the vascular plant and moss lineages. RNA gel blot analyses showed that eight of the *Pphb* genes were expressed in gametophytes. One of the genes is further characterized in Chapter 2.

Chapter 2 explains how detailed expression analyses and the phenotype of disruptants of *Pphb7* showed that this gene is involved in rhizoid cell differentiation. Physcomitrella rhizoids are multicellular filaments that differentiate from epidermal cells of the stem in gametophytes. *Pphb7* is expressed in rhizoid initial cells and rhizoids. *Pphb7*-disrupted rhizoids have defective pigmentation and an increased number and size of chloroplasts, but the position and number of rhizoids do not differ from the wild type. The role of HD-Zip I genes in the diversification of cell types of moss gametophytes is discussed.

General Introduction

Metazoans and land plants likely evolved their multicellular organization from a unicellular common ancestor independently (Doolittle et al., 1996). Unlike metazoans, land plants have a multicellular body with specialized cell types in both gametophytes and sporophytes (Kenrick and Crane, 1997a,b).

Molecular genetic studies of individual specialized cell types in model plants, such as Arabidopsis (*Arabidopsis thaliana*), have provided information on the mechanism for the patterns of cell differentiation in plants (*e.g.*, vascular tissues: reviewed in Fukuda, 1996; Dengler, 2001; Ye, 2002; and epidermal cells: reviewed in Marks, 1997; Brownlee, 2000; Glover, 2000). Many previous studies have provided information on the molecular mechanisms of cell differentiation in sporophytes, but the mechanisms of cell differentiation in gametophytes remain mostly unknown.

Bryophytes and ferns have gametophytes with diverse cell types, which are suitable for studying cell differentiation in gametophytes. The moss Physcomitrella is a suitable model for studying the molecular mechanisms of cell differentiation in gametophytes (reviewed in Cove et al., 1997; Reski, 1998; Schaefer and Zrÿd, 2001) because it has the following two advantages:

(1) Molecular biological techniques for functional gene analysis have been established in Physcomitrella

Physcomitrella was the first moss to be transformed successfully (Schaefer et al., 1991), and the only land plant whose genes have been targeted by homologous recombination with high efficiency (Schaefer and Zrÿd, 1997; Schaefer, 2001). Several genes have been disrupted using the gene-targeting technique and their functions have been discussed according to the phenotypes of the transformants (Girke et al., 1998; Strepp et al., 1998; Girod et al., 1999; Imaizumi et al., 2002; Koprivova et al., 2002). Gene disruption and gene manipulation using the gene-targeting technique are useful tools for investigating gene function.

(2) Gametophyte cell differentiation is easily observed in Physcomitrella

Physcomitrella is easily cultured *in vitro*, and the life cycle is complete within approximately 3 months (Cove et al., 1997). Unlike vascular plants, gametophyte generation is dominant in Physcomitrella. The gametophytes consist of various cell types (Reski, 1998).

Two major developmental stages are observed in the gametophyte generation of Physcomitrella: the protonema, which is a filamentous network of the chloronemata (Fig. 1A) and caulonemata (Fig. 1B), and the gametophore (Fig. 1C). The gametophore is a leafy shoot that is derived from a side-branch initial cell, which arises from a sub-apical cell of the caulonema (Reski, 1998). A gametophore has a stem, rhizoids, and leaves that consist of one or a few cell layers. The simple structures of the protonemata and gametophore allow observation of developmental processes at the cellular level.

Although sporophytes originated at a different time from gametophytes (Graham, 1993), members of a common gene family may regulate cell differentiation in both gametophytes and sporophytes. To investigate this possibility, homeodomain-leucine zipper (HD-Zip) genes were selected as a gene family that is possibly involved in this process. Recent studies have revealed that several HD-Zip genes regulate cell differentiation of sporophytes in angiosperms (reviewed in Chan et al., 1998). HD-Zip genes are classified into four subfamilies (HD-Zip I, II, III, and IV) based on amino acid sequence similarities (Meijer et al. 1997). The functions of the HD-Zip genes are diverse among the different subfamilies, and even within the same subfamily (Chan et al. 1998).

The HD-Zip III and IV genes are involved in cell differentiation, according to mutant analyses in Arabidopsis. The HD-Zip IV gene *GL2* is involved in trichome and root hair differentiation (Rerie et al., 1994; Di Cristina et al., 1996), and several HD-Zip III genes affect cell differentiation in the stem (Zhong and Ye, 1999; Baima et al., 2001) and leaf (McConnell et al., 2001). Compared with the genes in these subfamilies, the functions of the HD-Zip I genes are obscure, because loss-of-function mutants are not available. Ectopic expression of the Arabidopsis HD-Zip I gene, *Athb1*, in tobacco, causes a defect in the palisade parenchyma (Aoyama et al., 1995), and other HD-Zip I genes are expressed in specific cell types (Tornero et al., 1996; Hiwatashi and Fukuda, 2000; Nishitani et al., 2001). Although no mutant from the HD-Zip II subfamily has been reported, *Oshox1*, a rice HD-Zip II gene, is thought to be involved in procambial cell fate commitment, based on an analysis of ectopic expression (Scarpella et al., 2000). These findings indicate that HD-Zip I and II genes are similar to HD-Zip III and IV genes, in that they are involved in the specification of cell types. Therefore, HD-Zip genes are good candidate genes for studying cell differentiation in gametophytes. Although several HD-Zip genes that are expressed in both gametophytes and sporophytes have been reported from the fern *Ceratopteris richardii* (Aso et al., 1999), the

Figure 1. Two major developmental stages in gametophyte generation of *Physcomitrella patens*.
(A) Chloronemal cells. (B) Caulonemal cells. (C) A gametophore with rhizoids. Arrows and the bracket indicate rhizoids. Bar in (A) = 50 μm for (A) and (B); bar in (C) = 500 μm.

functions of these genes are unknown, because no mutants of the genes are available. The functions of HD-Zip genes in gametophyte generation are still unknown.

As the first step in studying gametophyte cell differentiation, HD-Zip genes were isolated from Physcomitrella gametophytes. Chapter 1 details the phylogenetic analyses that were used to assess whether moss HD-Zip genes belong to the same subfamilies as angiosperm HD-Zip genes, and how the expression of these genes in gametophytes was investigated by RNA blot analysis. Chapter 2 reports that detailed functional analyses of one of the Physcomitrella HD-Zip genes, *Pphb7*, were carried out, to assess whether Physcomitrella HD-Zip genes are involved in cell differentiation of gametophytes. The results showed that the Physcomitrella HD-Zip I gene regulates rhizoid cell differentiation in gametophytes.

Chapter 1: Isolation of Homeodomain-Leucine Zipper Genes from the Moss *Physcomitrella patens* and the Evolution of Homeodomain-Leucine Zipper Genes in Land Plants

1-1. Summary

Homeobox genes encode transcription factors involved in many aspects of developmental processes. The HD-Zip genes, which are characterized by the presence of both a homeodomain and a leucine zipper motif, form a clade within the homeobox superfamily and are previously reported only from vascular plants. Here I report the isolation of 10 HD-Zip genes (named *Pphb1-10*) from the moss *Physcomitrella patens*. Based on a phylogenetic analysis of the 10 *Pphb* genes and previously reported vascular plant HD-Zip genes, all the *Pphb* genes except *Pphb3* belong to three of the four HD-Zip subfamilies (HD-Zip I, II, and III), indicating that these subfamilies originated before the divergence of the vascular plant and moss lineages. *Pphb3* is sister to HD-Zip II subfamily, and has some distinctive characteristics, including the difference of $\mathbf{a}_1$ and $\mathbf{d}_1$ sites of its leucine zipper motif, which are well conserved in each HD-Zip subfamily. Comparison of the genetic divergence of representative HD-Zip I and II genes showed that the evolutionary rate of HD-Zip I genes was faster than HD-Zip II genes.

1-2. Introduction

HD-Zip genes have been reported only from vascular plants (Bharathan et al., 1997; Aso et al., 1999), and are not found in the entire genome of either the metazoan *Caenorhabditis elegans* or the fungus *Saccharomyces cerevisiae*. Since genes with either a leucine zipper motif or a homeodomain have been reported in metazoa, fungi, and green plants, Schena and Davis (1992) speculated that the HD-Zip genes originated in the green plant lineage by exon shuffling between a gene encoding a homeodomain and another gene encoding a leucine zipper motif.

The functions of the HD-Zip genes are diverse among the different subfamilies, and even within the same subfamily (Chan et al., 1998). Although there has been a large number of studies of angiosperm HD-Zip genes, little is known about these genes in other green plants, and the origin of the HD-Zip genes is not yet well understood. Aso et al. (1999) reported HD-Zip I, II, and III genes from the fern *Ceratopteris richardii*, and indicated that the four HD-Zip subfamilies had already diverged before the divergence between the angiosperm and fern lineages approximately 400 million years ago (Stewart and Rothwell, 1993). In addition to these studies, analyses of HD-Zip genes in other land plants and green algae are necessary to further understand the evolution of the HD-Zip gene family.

In this chapter, I described the isolation of 10 HD-Zip genes from Physcomitrella, and included these in a phylogenetic analysis with previously reported HD-Zip genes isolated from vascular plants. I used the gene tree to determine the phylogenetic relationships of the HD-Zip genes, and whether four HD-Zip subfamilies were present in the last common ancestor of the mosses and vascular plants. The difference of evolutionary rates between the HD-Zip I and II subfamilies was reported, and the reason was discussed.

1-3. Materials and Methods

Strain and culture conditions

Physcomitrella patens (Hedw.) Bruch & Schimp subsp. *patens* Tan collected in Gransden Wood, Huntingdonshire, UK (Ashton and Cove, 1977) was used in this study as the Physcomitrella wild-type strain. Physcomitrella was grown on medium based on BCD medium (D. J. Cove, Univ. Leeds., UK; personal communication), which contains 1 mM $MgSO_4$, 10 mM KNO_3, 45 µM $FeSO_4$, 1.8 mM KH_2PO_4 adjusted pH to 6.5 with 4 M KOH, and trace elements (Knight et al., 1988). The trace elements include 0.22 µM $CuSO_4$, 0.19 µM $ZnSO_4$, 10 µM H_3BO_4, 0.10 µM Na_2MoO_4, 2 µM $MnCl_2$, 0.23 µM $CoCl_2$, and 0.17 µM KI. Growth supplements were added to the BCD medium for spore germination (10 mM $CaCl_2$ and 5 mM di-ammonium (+) –tartrate; S medium), for protonemata culture (1 mM $CaCl_2$ and 5 mM di-ammonium (+) –tartrate; P medium), and for induction and culture of gametophores (1 mM $CaCl_2$; G medium). These media were solidified with 0.8% (w/v) agar (A-9799, SIGMA, St. Louis, MO) in 9-cm petri dishes. The solidified medium was covered with a layer of cellophane (Futamura Chemical Industries Co., Ltd., Nagoya, Japan) to facilitate collection of the moss from the medium (Grimsley et al., 1977). Sporangia, each containing a few thousand spores, were stored at 4°C for several weeks to several years. The sporangia were sterilized with 1% (w/v) sodium hypochlorite (Wako Pure Chemical Industries, Ltd., Osaka, Japan) for 5 minutes, and rinsed four times with sterilized water. The sterilized sporangia were squashed with a sterile stick in a 1.5 ml plastic tube containing 1 ml of sterilized water, and 200 µl of this spore suspension was sown on the S medium. The dishes were stored at 25°C under continuous light (40 µmol photons $m^{-2}s^{-1}$). The spores usually germinated 2 or 3 days after inoculation and protonemata developed. The protonemata were collected 2 weeks after germination and were ground with a Polytron homogenizer (Kinematica, Littau, Switzerland) in approximately 8 ml of sterilized water at a speed setting of 4 and 2 ml of the suspended protonemata were transferred onto the P medium. To induce gametophores, the suspended protonemata were transferred to the G medium and grown at 25°C under continuous light (40 µmol photons $m^{-2}s^{-1}$) for 1 month after inoculation.

Cloning the HD-Zip genes

Using ISOGEN (Nippon Gene, Tokyo, Japan), total RNA was extracted from the wild-type protonemata 1 week after inoculation, and from gametophores grown for 1 month

after inoculation of protonemata onto G medium. Complementary DNA was synthesized from the total RNA with 3' RACE System using SuperScriptII reverse transcriptase and the adapter primer (5'-GGCCACGCGTCGACTAGTACTTTTTTTTTTTTTTTT-3') (Invitrogen, Carlsbad, CA). The synthesized cDNA was amplified with the adapter primer and one of two homeodomain-specific primers, HB1 (Bürglin et al., 1989) or HD1 (Aso et al., 1999) (Fig. 2) using ExTaq DNA polymerase (TaKaRa Shuzo Co., Ltd., Kyoto, Japan). Nucleotide sequences of the degenerate primers are 5'-CAUCAUCAUCAUAA(A/G)AT(A/T/G)TGGTT(C/T)CA(A/G)AA(C/T)GN(A/C)G-3' (HB1) and 5'-CAUCAUCAUCAUTGGTT(C/T)CA(A/G)AA(C/T)(A/C)GI(A/C)GIACN(A/C)G-3' (HD1). PCR cycle conditions consisted of 2 minutes at 94˚C, then 25 cycles of 94˚C for 30 seconds, 55˚C for 30 seconds, and 72˚C for 3 minutes, followed by 10 minutes at 72˚C. Further PCR was carried out with the universal amplification primer (5'-CUACUACUACUAGGCCACGCGTCGACTAGTAC-3') supplied by Invitrogen and the primer HB1 or HD1. These primers encode the amino acids KIWFQNRR and WFQNRRAR, respectively. The PCR products were separated on 1% (w/v) agarose gels (SeaKem GTG; FMC BioProducts, Rockland, ME). The DNA fragments between 0.5 and 2 kb were purified with the GeneClean III kit (BIO 101 Inc., La Jolla, CA), and cloned using the CLONEAMP pAMP1 system (Invitrogen). In all, 326 clones were obtained using HB1 (96 from the protonema cDNA and 230 from the gametophore cDNA), and 84 clones using HD1 (30 from the protonema cDNA and 54 from the gametophore cDNA). These candidate clones were sorted into 58 groups according to their digestion patterns using *Alu*I, and two or three clones from each group were sequenced with Dye Terminator Cycle Sequencing FS Ready Reaction Kit (Perkin-Elmer Applied Biosystems, Foster City, CA) or Big Dye Terminator Cycle Sequencing FS Ready Reaction Kit (Perkin-Elmer Applied Biosystems) using ABI PRISM 377 DNA sequencer (Perkin-Elmer Applied Biosystems). The 5' region of each gene encoding homeodomain was cloned using 5' RACE System (Invitrogen). Total RNA of protonemata and gametophores was treated with RNase-free DNase I (Invitrogen), and first strand cDNA was synthesized with SuperScriptII reverse transcriptase and the gene specific-primer for each *Pphb* gene shown in Table 1. The synthesized cDNA was amplified with the anchor primer (5'-CTACTACTACTAGGCCACGCGTCGACTAGTACGGGIIGGGIIGGGIIG-3') supplied by

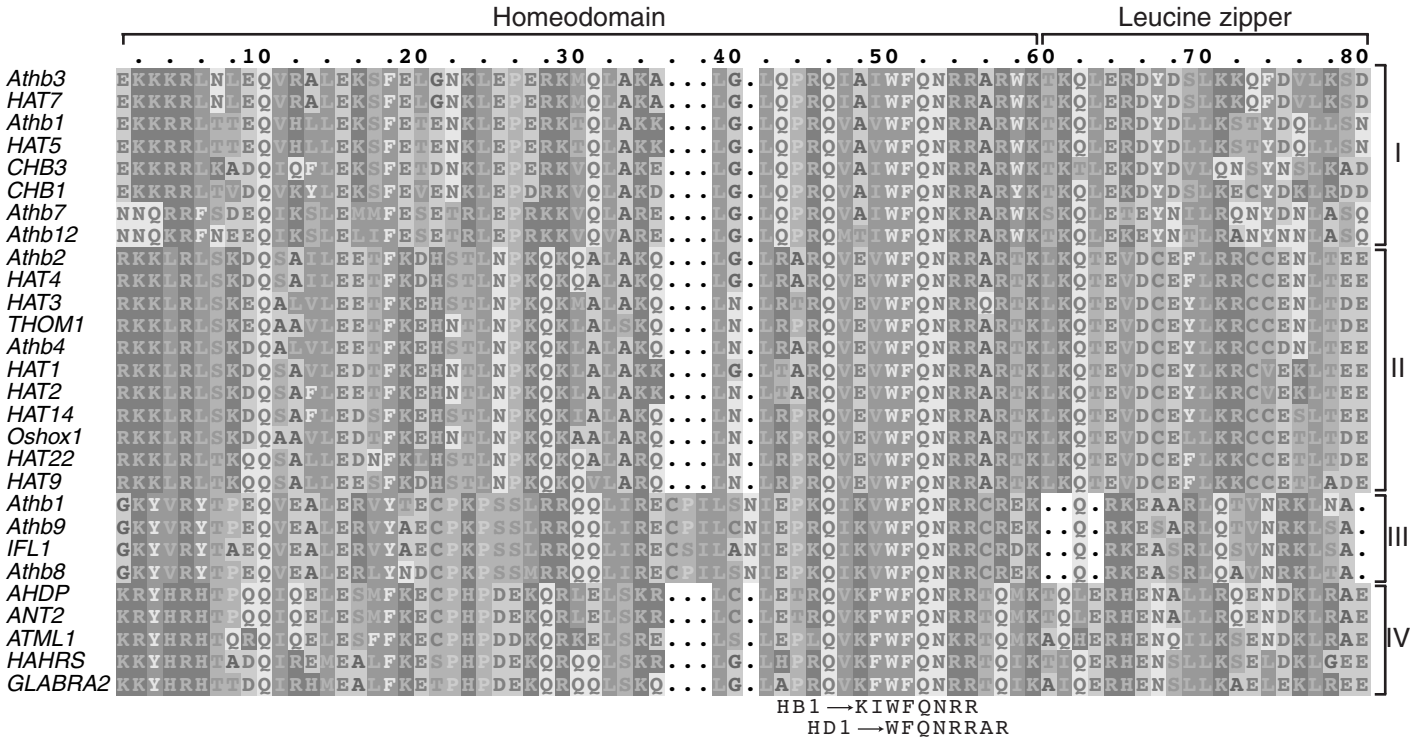

Figure 2. Positions of degenerate primers used for 3'RACE screening of HD-Zip genes.
An amino acid alignment of in homeodomain, and leucine zipper domain of HD-Zip genes. The positions of degenerate primers HB1 and HD1 are shown below the alignment. The brackets on the right indicate the different subfamilies of the HD-Zip gene family.

Table 1. List of primers cloning for *Pphb* genes.

Primer name	Primer Sequence (5' to 3')	length	Notes
5Pphb1-1	TCTCGTCCTGTAGCTCTTGC	20	Synthesized cDNA of *Pphb1* for 5' RACE
5Pphb1-2	CAUCAUCAUCAUGAGCCGGTTGTAATCCAAGGTA AGG	37	*Pphb1* 5' RACE product cloning
5Pphb2-1	GCTTCTCCTGCAACACAGCC	20	Synthesized cDNA of *Pphb2* for 5' RACE
5Pphb2-2	CAUCAUCAUCAUAAGCCGGTTGTAATCCAAAGTA AGG	37	*Pphb2* 5' RACE product cloning
5Pphb3-1	GGATGAGGTAGCTCAAATGG	20	Synthesized cDNA of *Pphb3* for 5' RACE
5Pphb3-2	CAUCAUCAUCAUCGCTGCCGTAAAACCTCACAGT CGG	37	*Pphb3* 5' RACE product cloning
Pphb3-51	GGGCAGGTAAATTGTGCAGGAT	22	*Pphb3* full length cloning
Pphb3-52	TAGCGGCCGCGCAGGATTACTCATCTGGAAAC	32	*Pphb3* full length cloning
Pphb3-31	TGTATTATAGGGGACCGACTGCC	23	*Pphb3* full length cloning
Pphb3-32	TAGCGGCCGCATATTCACCACGACCCACGCTAA	33	*Pphb3* full length cloning
5Pphb4-1	CTTCAGCGACTCGTAACACC	23	Synthesized cDNA of *Pphb4* for 5' RACE
5Pphb4-2	CAUCAUCAUCAUTTAAGCAACTCGCAGTCCACTT CGG	37	*Pphb4* 5' RACE product cloning
Pphb4-51	GCTGAGACATGGATAAGGTTGAG	23	*Pphb4* full length cloning
Pphb4-52	TAGCGGCCGCGGTTGAGCTGTGAAGAAGAAGTT	33	*Pphb4* full length cloning
Pphb4-31	CAAAATATTTTCTTTCGAATGAATT	25	*Pphb4* full length cloning
Pphb4-32	AAACTAAGAGAGAGTGCAAAATATT	25	*Pphb4* full length cloning
5Pphb5-1	ATGCTGGAACGTCTCTGGATT	21	Synthesized cDNA of *Pphb5* for 5' RACE
5Pphb5-2	CAUCAUCAUCAUCTTCAAGTGATTCTTCTCACTC AA	36	*Pphb5* 5' RACE product cloning
Pphb5-51	CGATCAATTCAGCGTTGGAATAA	23	*Pphb5* full length cloning
Pphb5-52	TAGCGGCCGCGTGAATACGCAGGCGGCCCATAT	33	*Pphb5* full length cloning
Pphb5-31	CAAGTCATAGCGCTCACCGAATT	23	*Pphb5* full length cloning
Pphb5-32	TAGCGGCCGCCAGGTGGAGGATGACTGCAGGTT	33	*Pphb5* full length cloning
5Pphb6-1	ATTTGATTGCCATCAGCACAA	21	Synthesized cDNA of *Pphb6* for 5' RACE

5Pphb6-2	CAUCAUCAUCAUATAGACGTTGCACCTCAGCTTT	34	*Pphb6* 5’ RACE product cloning
Pphb6-51	CGTTCAATGCGTGCATTCACATT	23	*Pphb6* full length cloning
Pphb6-52	TAGCGGCCGCCTGTGTTTGATCACCGTTTCAGG	33	*Pphb6* full length cloning
Pphb6-31	ACATCAACATGAGCCAATCTACC	23	*Pphb6* full length cloning
Pphb6-32	TAGCGGCCGCAAGAACATGCATCATGTGATCGG	33	*Pphb6* full length cloning
5Pphb7-1	CGTCGTCATTAGAGATTCCCTT	22	Synthesized cDNA of *Pphb7* for 5’ RACE
5Pphb7-2	CAUCAUCAUCAUTCACCTCAGCTTTAAGAGCACTT	35	*Pphb7* 5’ RACE product cloning
Pphb7-51	GTGTCGAGCGCGTCGGCAAGAG	22	*Pphb7* full length cloning
Pphb7-52	TAGCGGCCGCGGAAAGGGGAGGGAAGGGTGTAA	33	*Pphb7* full length cloning
Pphb7-31	AAAGAGGTGCCACTTTATTCCAT	23	*Pphb7* full length cloning
Pphb7-32	TAGCGGCCGCTCAGGGACGCACAACAGCGACAA	33	*Pphb7* full length cloning
5Pphb8-1	AGTCCTTCTCGCTCTGGGAA	20	Synthesized cDNA of *Pphb8* for 5’ RACE
5Pphb8-2	CAUCAUCAUCAUAGCTCGGCCTTGAGGACATCTT	34	*Pphb8* 5’ RACE product cloning
Pphb8-51	CTAGTCGCCAGTGCACTAGGCAT	23	*Pphb8* full length cloning
Pphb8-52	TAGCGGCCGCATTTAGCCATGTGACGGATACAA	33	*Pphb8* full length cloning
Pphb8-31	TCATGGATGCTCGTCACTACCTT	23	*Pphb8* full length cloning
Pphb8-32	TAGCGGCCGCTATCACACAAGTCGTTGGAGCAA	33	*Pphb8* full length cloning
5Pphb9-1	GTGGAAAGTTGGGACCTGCAA	21	Synthesized cDNA of *Pphb9* for 5’ RACE
5Pphb9-2	CAUCAUCAUCAUGCTGGGCTAACGGCTTCAAATT	34	*Pphb9* 5’ RACE product cloning
Pphb9-51	CACTTTATGCTTCCGGCTCGTAT	23	*Pphb9* full length cloning
Pphb9-52	TAGCGGCCGCGGCTAGAAGAACAGTGATGCACC	33	*Pphb9* full length cloning
Pphb9-31	TGATTTCTAACCCTCTTCCTGCC	23	*Pphb9* full length cloning
Pphb9-32	TAGCGGCCGCTGTGTGGAATTGTGAGCGGATAA	33	*Pphb9* full length cloning
5Pphb10-1	TCAAGAGCTTGTTAAGAGCTGTT	23	Synthesized cDNA of *Pphb10* for 5’ RACE
5Pphb10-2	CAUCAUCAUCAUCTGACCAACCTTGTTGCTTCTT	34	*Pphb10* 5’ RACE product cloning
Pphb10-51	TGACTTGTGTCCAACcTGAGG	21	*Pphb10* full length cloning

Pphb10-52	TAGCGGCCGCGAGGATTTGGAGGTTGAgGAGG	32	*Pphb10* full length cloning
Pphb10-31	GACCATGAGAGCACAGTACGCAA	23	*Pphb10* full length cloning
Pphb10-32	TAGCGGCCGCCCTGAATCCAGTCAGTCTGCTT	32	*Pphb10* full length cloning

Invitrogen and specific-primer for each *Pphb* gene. PCR cycles conditions consisted of 2 min at 94˚C, 25 cycles of 94˚C for 30 seconds, 60˚C for 30 seconds, and 72˚C for 3 minutes. Further PCR was carried out with the universal amplification primer (5'-CUACUACUACUAGGCCACGCGTCGACTAGTAC-3') supplied by Invitrogen and the gene specific primer for each *Pphb* gene.

Total genomic DNA was extracted from the wild type protonemata 1 week after inoculation using PHYTOPURE (Amersham Pharmacia Biotech, Uppsala, Sweden), and further purified using the CTAB method (Murray and Thompson, 1980).

Two gene specific primers located close to each end of the putative mRNA shown in Table 1 were synthesized. Nested PCR amplifications were performed with the cDNA or genomic DNA using these primers to obtain cDNA and genomic DNA clones. The PCR product was cloned into pBluescriptII SK+ (Stratagene, La Jolla, CA) or pGEM3z (Promega, Madison, WI).

To exclude PCR errors, at least two clones obtained from independent PCR were sequenced for each gene. When discrepancies were found, the majority from at least three independently amplified PCR products was selected.

Phylogenetic analysis

Plant HD-Zip genes similar to Physcomitrella HD-Zip genes were obtained from the nr and dbest datasets at NCBI using the programs blastx or tblastn (version 2.0.10) (Altschul et al., 1997). Genes containing undetermined amino acid residues within HD-Zip domain were not used for further analysis. Nucleotide sequences were translated to amino acid sequences based on the universal code. Genes with identical amino acid sequences in the region used for the analysis were treated as a single operational taxonomic unit. The deduced amino acid sequences of 96 HD-Zip genes used in this study were aligned using CLUSTAL W version 1.8 (Thompson et al., 1994), and then revised manually. Eighty-four amino acid sites without indels were used for the phylogenetic analysis.

To search the maximum likelihood (ML) tree, I used Neighbor-Joining (NJ) and most parsimonious (MP) trees as start trees for local rearrangement search (Adachi and Hasegawa, 1996). NJdist and ProtML programs were in the MOLPHY, version 2.3b3 package (Adachi and Hasegawa, 1996). A Neighbor-Joining (NJ) tree (Saitou and Nei, 1987) was obtained with NJdist based on the ML distance under the JTT model (Jones et al., 1992)

calculated with ProtML. Most parsimonious trees were obtained by the heuristic searches with the tree bisection and reconnection (TBR) using paup*4.0 b4a (Swofford, 2000). Three kinds of heuristic search were performed; (1) a heuristic search from a simple addition tree without the steepest descent option, (2) 84 searches from a random tree without the steepest descent option, and (3) 10 searches from a random tree with the steepest descent option. These analyses found totally 205,787 trees with 1,330 steps. Likelihood of all these trees was calculated using ProtML under JTT model and sorted with their Akaike Information Criterion (AIC) values (Adachi and Hasegawa, 1996). The best 1,000 trees were subject to further local rearrangement search (Adachi and Hasegawa, 1996). Further phylogenetic analyses constraining a monophyletic relationship of HD-Zip I genes were performed. The approximate likelihood (Adachi and Hasegawa, 1996) of all the 6,081,075 trees obtained under this constraint was calculated. For the best 10,000 trees, log likelihood was calculated. A ML tree found in this search was further subjected to a local rearrangement search.
The local bootstrap probability of each branch was estimated by using the resampling-of-estimated-log-likelihood (RELL) method (Kishino et al., 1990; Hasegawa and Kishino, 1994).

Difference of evolutionary rates between the HD-Zip I and II subfamilies

I examined whether the evolutionary rate in the HD-Zip I subfamily is higher than the HD-Zip II subfamily. Rate is the distance divided by the divergence time. If I focus on ortholog pairs of two defined species, the divergence time is a constant and the rate can be compared by comparing the distance. Every pair of species that has ortholog pairs in both HD-Zip I and II subfamilies was used. The ortholog pairs were determined according to the tree topology and species phylogeny. For each pair (i), the evolutionary distance (d_i) was calculated with ProtML under JTT model using –D option. The distance (d_i, d_j) of two pairs (i, j), one from the HD-Zip I subfamily and the other from the HD-Zip II subfamily, was compared. To test whether the distance was different between pairs i and j, i. e. $d_i > d_j$, the difference $d_i - d_j$ (D_{ij}) was tested against 0. D_{ij} was calculated for each set of amino acids data resampled in a bootstrap test, and standard deviations were calculated from 10,000 bootstrap samples.

RNA gel blot analyses

RNA gel blot analyses were performed as described in Hiwatashi et al. (2001). One microgram of poly $(A)^+$ RNA was electrophoresed on 1.0 %(w/v) agarose gels (SeaKem GTG) containing 2 M formaldehyde, 20 mM MOPS (pH 7.0), 5 mM CH_3COONa, and 1 mM EDTA, and transferred to Hybond N^+ nylon membrane (Amersham Biosciences Europe GmbH, Freiburg) using 10×SSC.

The plasmids that cloned 3' RACE products of *Physcomitrella* HD-Zip genes (p3Pphb1-10) were used for constructing probes to examine expression pattern of *Pphb* genes. A PCR fragment that was amplified with the Pphb1-P-5 (5'-AACCGCAATACCGAATTC-3') and Pphb1-P-3 (5'-TGCTCTTGCGATTGGCGC-3') primers using p3Pphb1 plasmid as the template was used as the *Pphb1* probe (Fig. 3). A *Aat*II/*Bsm*I-digested fragment of the plasmid p3Pphb2 was used as the *Pphb2* probe (Fig. 3). A PCR fragment that was amplified with the Pphb3-P-5 (5'-GCGAAGCGTAATGAGTCC-3') and Pphb3-P-3 (5'-TAGCGGCCGCATATTCACCACGACCCACGCTAA-3') primers using p3Pphb3 plasmid as the template was used as the *Pphb3* probe (Fig. 3). A PCR fragment that was amplified with the Pphb4-P-5 (5'-GGTTAGAGGTTAATTTCC -3') and Pphb4-P-3 (5'-TAGCGGCCGCGGTTGAGCTGTGAAGAAGAAGTT-3') primers using p3Pphb4 plasmid as the template was used as the *Pphb4* probe (Fig. 3). A PCR fragment that was amplified with the Pphb5-P-5 (5'-ATCCAGAGACGTTCCAGC-3') and Pphb5-P-3 (5'-TAGCGGCCGCAAGAACATGCATCATGTGATCGG-3') primers using p3Pphb5 plasmid as the template was used as the *Pphb5* probe (Fig. 3). A *Hinc*II-digested fragment of the plasmid p3Pphb6 was used as the *Pphb6* probe (Fig. 3). A *Bam*HI-digested fragment of the plasmid p3Pphb7 was used as the *Pphb7* probe (Fig. 3). A *Acc*I/*Aat*II-digested fragment of the plasmid p3Pphb8 was used as the *Pphb8* probe (Fig. 3). A PCR fragment that was amplified with the Pphb9-P-5 (5'-GGTCCCAACTTTCCACAT-3') and Pphb9-P-3 (5'-TAGCGGCCGCTGTGTGGAATTGTGAGCGGATAA-3') primers using p3Pphb9 plasmid as the template was used as the *Pphb9* probe (Fig. 3). A PCR fragment that was amplified with the Pphb10-P-5 (5'- AGATGATGGCTGGGAGGCTACGA-3') and Pphb10-P-3 (5'-CGGTAGCTAACAATCCCGCAGG-3') primers using p3Pphb10 plasmid as the template was used as the *Pphb10* probe (Fig. 3). A fragment of the *GAPDH* gene (Leech et al., 1993) was amplified with the PpgapC5' (5'-GAGATAGGAGCATCTGTACCGCTTGTGC-3') and PpgapC3' (5'-CATGGTGGGATCGGCTAAGATCAAGGTC-3') primers, using pPpGapC

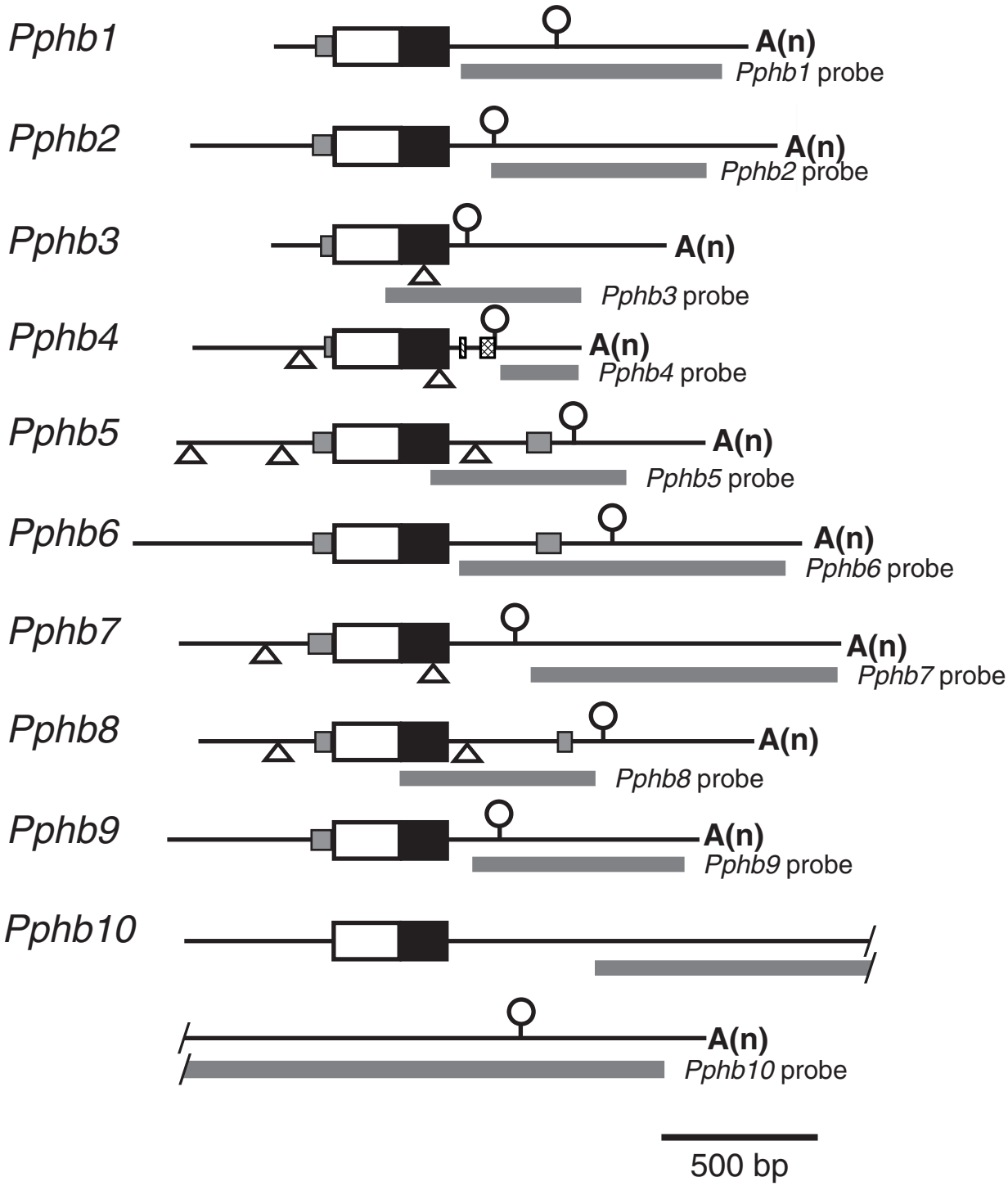

Figure 3. The structure of *Pphb1-Pphb10* cDNAs.
The circle and A (n) indicate the positions of the translation termination codon and the poly (A)+ tail, respectively. Genomic regions corresponding to the cDNA of *Pphb3-5* and *Pphb7-8* were sequenced and positions of introns are indicated by triangles. White, black, gray, hatched, and crosshatched boxes indicazte the homeodomain, leucine zipper motif, acidic region, CPSCE motif, and C-terminal end motif, respectively. *Pphb10* is separated into two lines connected by a slash. The probes used for the RNA blot analyses are indicated below each structure.

(Hiwatashi et al., 2001) as the template. The DNA fragments for probes were labeled using a Random Primer DNA labeling kit ver. 2.0 (TaKaRa Shuzo Co., Ltd.).

Hybridization was performed at 65°C for 16 hours in a hybridization buffer containing 0.5 M Na_2HPO_4 (pH 7.2), 1 mM EDTA, and 7% SDS and then washed at 65°C in a wash buffer containing 40 mM Na_2HPO_4 (pH 7.2), 1 mM EDTA, and 1 % SDS as described in Church and Gilbert (1984).

1-4. Results

Isolation of HD-Zip genes from Physcomitrella

Candidate HD-Zip cDNAs obtained by 3' RACE System using the homeobox specific primers were assigned to 10 genes named *Pphb1-10* (*Physcomitrella patens* homeobox genes; the accession numbers for the DNA database are AB028072 to AB028080, and AB032182, respectively). The 5' regions of the *Pphb* genes were obtained using the 5' RACE System with gene-specific primers for each HD-Zip gene. Every *Pphb* gene encodes both a homeodomain and a leucine zipper motif. The latter motif is adjacent to the C-terminus of the homeodomain (Fig. 3), and one of four amino acid residues (leucine, isoleucine, valine, or alanine) usually appears every seven amino acid in the motif ("d" positions in Fig. 4). One or two acidic regions, which are expected to be the transcriptional activation domains (Ptashne, 1988), were found adjacent to the N-terminus or C-terminus of the homeodomain and leucine zipper motif in every *Pphb* gene except *Pphb10* (Fig. 3). Putative repression domains, which were reported from *Oshox1* as high alanine/proline/glutamine content regions (Meijer et al., 1997), were not found in any *Pphb* genes. The CPSCE motif and C-terminal end consensus reported in HD-Zip II genes (Chan et al., 1998) were found in *Pphb4* (Fig. 3). The genomic regions of *Pphb3*, *4*, *5*, *7*, and 8 were amplified with primers located at the 5' or 3' end of each gene. Based on the comparison of the cDNA and genomic region of these *Pphb* genes, the locations of introns were inferred and are shown in figure 3.

Phylogenetic analysis of the HD-Zip genes

Eighty-six vascular plant HD-Zip genes obtained from the DNA database and the ten *Pphb* genes were aligned (Fig. 4), and 84 amino acid residues indicated in figure 5 were used for phylogenetic analysis (EMBL accession number: ds42823). Of the 84 sites, 73 sites were informative in parsimony analyses. I searched the ML tree using the NJ and MP trees as start trees for local rearrangements. The ML trees obtained from the NJ and MP trees had log likelihoods of -7,167.98 and -7,160.21, respectively. In the ML tree obtained from the MP trees, HD-Zip I subfamily unexpectedly does not form a monophyletic group, while HD-Zip I subfamily is always monophyletic in previous studies (Chan et al., 1998; Aso et al., 1999). Finally, a tree with a log likelihood of –7,155.93 ± 512.44 and AIC of 14,689.55 was obtained. The ML tree contains some short branches, and its AIC becomes better (14,673.63) by collapsing these branches. The ML tree with collapsed branches is shown in figure 5.

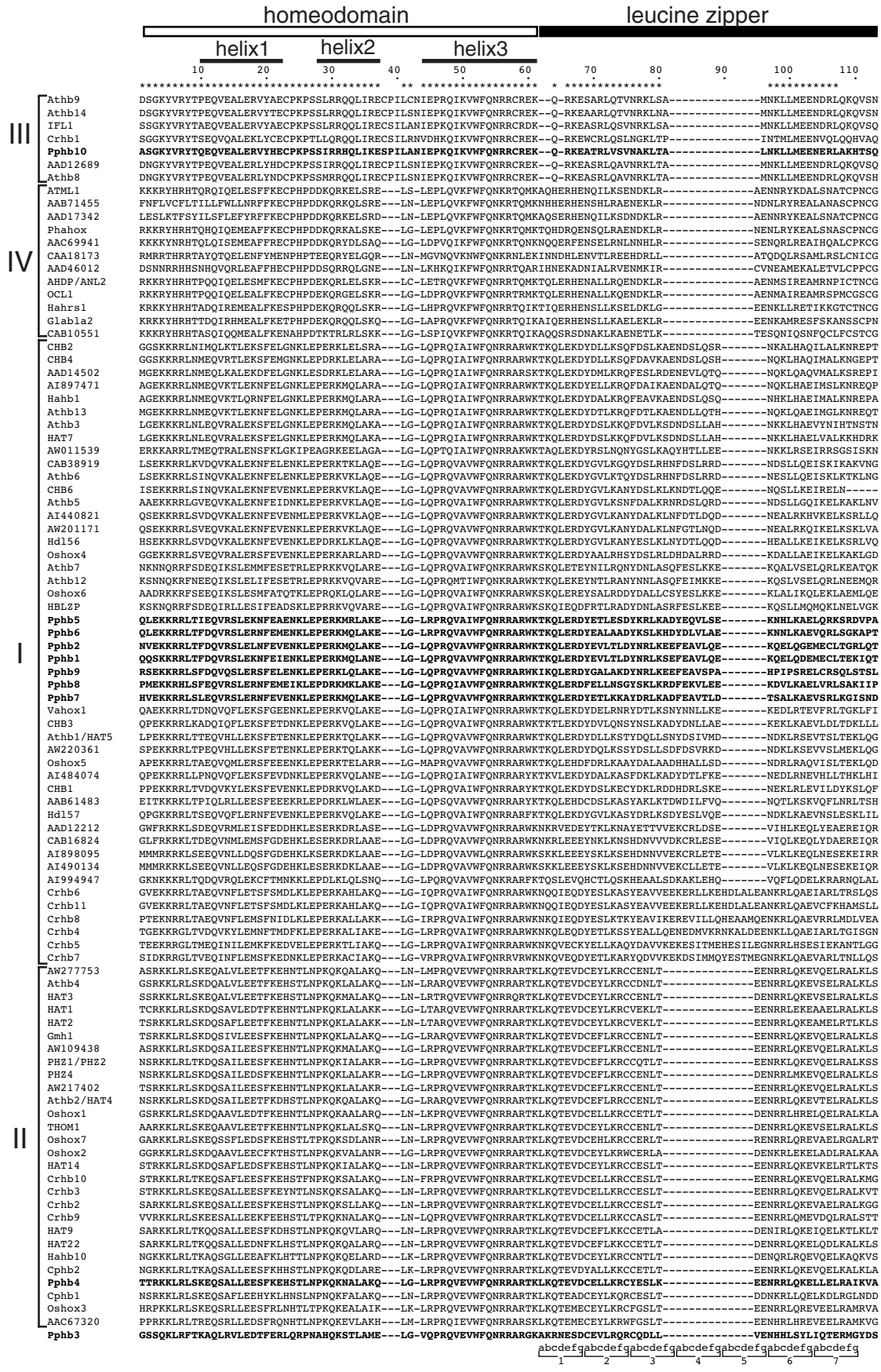
homeodomain
leucine zipper
helix1
helix2
helix3
III
IV
I
II
Athb9
Athb14
IFL1
Crhb1
Pphb10
AAD12689
Athb8
ATML1
AAB71455
AAD17342
Phahox
AAC69941
CAA18173
AAD46012
AHDP/ANL2
OCL1
Hahrs1
Glabla2
CAB10551
CHB2
CHB4
AAD14502
AI897471
Hahb1
Athb13
Athb3
HAT7
AW011539
CAB38919
Athb6
CHB6
Athb5
AI440821
AW201171
Hdl56
Oshox4
Athb7
Athb12
Oshox6
HBLZP
Pphb5
Pphb6
Pphb2
Pphb1
Pphb9
Pphb8
Pphb7
Vahox1
CHB3
Athb1/HAT5
AW220361
Oshox5
AI484074
CHB1
AAB61483
Hdl57
AAD12212
CAB16824
AI898095
AI490134
AI994947
Crhb6
Crhb11
Crhb8
Crhb4
Crhb5
Crhb7
AW277753
Athb4
HAT3
HAT1
HAT2
Gmh1
AW109438
PHZ1/PHZ2
PHZ4
AW217402
Athb2/HAT4
Oshox1
THOM1
Oshox7
Oshox2
HAT14
Crhb10
Crhb3
Crhb2
Crhb9
HAT9
HAT22
Hahb10
Cphb2
Pphb4
Cphb1
Oshox3
AAC67320
Pphb3
abcdefgabcdefgabcdefgabcdefgabcdefgabcdefgabcdefg
1
2
3
4
5
6
7

Figure 4. Alignment of amino acids sequences of the HD-Zip genes used to phylogenetic analyses. Dashes indicate gaps. The names of the subfamilies are shown to the left. *Pphb* genes cloned from *Physcomitrella patens* are indicated by bold type. The letter a-g indicate the position of each residue within the heptad of the leucine zipper motif, and typical amino acid residues (leucine, isoleucine, valine, or alanine) for the leucine zipper motif are usually observed in "d" positions. Asterisks above the alignment indicate the 85 amino acids used for the phylogenetic analysis. White and black boxes above the alignment indicate the homeodomain and leucine zipper motif, respectively. The black lines below the white box indicate helix 1, 2, and 3, respectively. The brackets on the left indicate the different subfamilies of the HD-Zip family. Accession numbers of genes are *Athb9* (Y10922), *Athb14* (Y11122), *IFL1* (AF188994), *Crhb1* (AB013791), *Pphb10* (AB032182), *Athb8* (Z50851), *ATML1* (U37589), *Phahox* (U34743), *AHDP* (U85254), *ANL2* (AAD47139), *OCL1* (CAB51059), *Hahrs1* (L76588), *Glabra2* (L32873), *CHB2* (D26574), *CHB4* (D26576), *Hahb1* (L22847), *Athb13* (AAF20996), *Athb3* (X62644), *HAT7* (U09340), *Athb6* (X67034), *CHB6* (D26578), *Athb5* (X67033), *Hdl56* (AAF01764), *Oshox4* (AAD37697), *Athb7* (X67032), *Athb12* (AF001949), *Oshox6* (AAD37699), *HBLZP* (AAD38144), *Pphb5* (AB028076), *Pphb6* (AB028077), *Pphb2* (AB028073), *Pphb1* (AB028072), *Pphb9* (AB028080), *Pphb8* (AB028079), *Pphb7* (AB028078), *Vahox1* (X94947), *CHB3* (D26575), *Athb1* (X58821), *HAT5* (M90416), *Oshox5* (AAD37698), *CHB1* (D26573), *Hdl57* (AAF01765), *Crhb6* (AB013796), *Crhb11* (AB013801), *Crhb8* (AB013798), *Crhb4* (AB013794), *Crhb5* (AB013795), *Crhb7* (AB013797), *Athb4* (Y09582), *HAT3* (U09338), *HAT1* (U09332), *HAT2* (U09335), *Gmh1* (X92489), *PHZ1* (X95193), *PHZ2* (X94375), *PHZ4* (X94449), *Athb2* (X68146), *HAT4* (M90394), *Oshox1* (X96681), *THOM1* (S76820), *Oshox7* (AAD37700), *Oshox2* (AAD37695), *HAT14* (U09334), *Crhb10* (AB013800), *Crhb3* (AB013793), *Crhb2* (AB013792), *Crhb9* (AB013799), *HAT9* (U09342), *HAT22* (U09336), *Hahb10* (L48485), *Cphb2* (AJ005833), *Pphb4* (AB028075), *Cphb1* (AJ005820), *Oshox3* (AAD37696), *Pphb3* (AB028074).

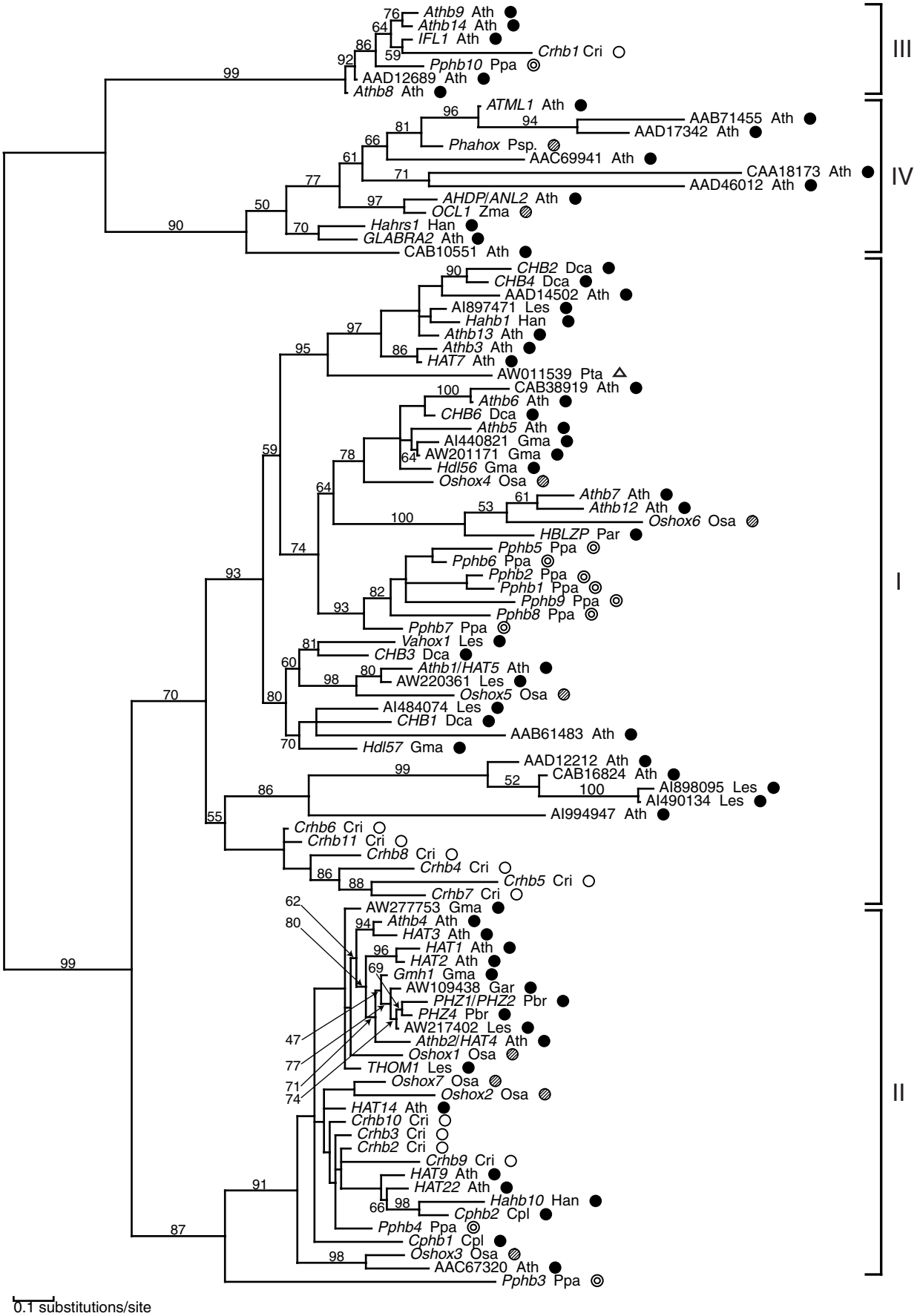
Athb9 Ath
Athb14 Ath
IFL1 Ath
Crhb1 Cri
Pphb10 Ppa
AAD12689 Ath
Athb8 Ath
ATML1 Ath
AAB71455 Ath
AAD17342 Ath
Phahox Psp.
AAC69941 Ath
CAA18173 Ath
AAD46012 Ath
AHDP/ANL2 Ath
OCL1 Zma
Hahrs1 Han
GLABRA2 Ath
CAB10551 Ath
CHB2 Dca
CHB4 Dca
AAD14502 Ath
AI897471 Les
Hahb1 Han
Athb13 Ath
Athb3 Ath
HAT7 Ath
AW011539 Pta
CAB38919 Ath
Athb6 Ath
CHB6 Dca
Athb5 Ath
AI440821 Gma
AW201171 Gma
Hdl56 Gma
Oshox4 Osa
Athb7 Ath
Athb12 Ath
Oshox6 Osa
HBLZP Par
Pphb5 Ppa
Pphb6 Ppa
Pphb2 Ppa
Pphb1 Ppa
Pphb9 Ppa
Pphb8 Ppa
Pphb7 Ppa
Vahox1 Les
CHB3 Dca
Athb1/HAT5 Ath
AW220361 Les
Oshox5 Osa
AI484074 Les
CHB1 Dca
AAB61483 Ath
Hdl57 Gma
AAD12212 Ath
CAB16824 Ath
AI898095 Les
AI490134 Les
AI994947 Ath
Crhb6 Cri
Crhb11 Cri
Crhb8 Cri
Crhb4 Cri
Crhb5 Cri
Crhb7 Cri
AW277753 Gma
Athb4 Ath
HAT3 Ath
HAT1 Ath
HAT2 Ath
Gmh1 Gma
AW109438 Gar
PHZ1/PHZ2 Pbr
PHZ4 Pbr
AW217402 Les
Athb2/HAT4 Ath
Oshox1 Osa
THOM1 Les
Oshox7 Osa
Oshox2 Osa
HAT14 Ath
Crhb10 Cri
Crhb3 Cri
Crhb2 Cri
Crhb9 Cri
HAT9 Ath
HAT22 Ath
Hahb10 Han
Cphb2 Cpl
Pphb4 Ppa
Cphb1 Cpl
Oshox3 Osa
AAC67320 Ath
Pphb3 Ppa
III
IV
I
II
0.1 substitutions/site

Figure 5. The maximum likelihood tree of the 96 HD-Zip genes found by local rearrangement search.
Local bootstrap probability is shown on or below branches where available. This is an unrooted tree. The horizontal branch length is proportional to the estimated evolutionary distance. The species from which the gene was isolated, is indicated by an abbreviation after the gene name; Ath (*Arabidopsis thaliana*), Cri (*Ceratopteris richardii*), Cpl (*Craterostigma plantagineum*), Dca (*Daucas carota*), Gma (*Glycine max*), Han (*Helianthus annuus*), Les (*Lycopersicon esculentum*), Osa (*Oryza sativa*), Psp. (*Phalaenopsis* sp.), Ppa (*Physcomitrella patens*), Pbr (*Pimpinella brachycarpa*), Par (*Prunus armeniaca*), Zma (*Zea mays*). Symbols after the abbreviated species name indicate the higher classification: eudicots (black circles), monocots (hatched circles), gymnosperms (triangles), ferns (open circles), and mosses (double circles). The brackets on the right indicate the different subfamilies of the HD-Zip gene family.

The HD-Zip family has been classified into four subfamilies, namely HD-Zip I, II, III, and IV, based on amino acid sequences (Sessa et al., 1993; Chan et al., 1998; Aso et al., 1999). *Pphb1*, *2*, *5*, *6*, *7*, *8*, and *9* form a clade with 93% of local bootstrap support, which is included in the HD-Zip I subfamily. In this subfamily, seven additional amino acid residues in the latter half of the leucine zipper motif distinguish the fern *Ceratopteris richardii* HD-Zip I genes, *Crhb4*, *5*, *6*, *7*, *8*, and *11* (Aso et al., 1999). The *Pphb* genes do not have these additional residues and are similar to angiosperm HD-Zip I genes (Fig. 4).

Pphb4 clusters in the HD-Zip II subfamily, whose monophyly is supported with high local bootstrap probability (91%). *Pphb3* is sister to all other members of the HD-Zip II subfamily with 87% local bootstrap support. *Pphb10* clusters in the HD-Zip III subfamily, whose monophyly has 99% local bootstrap support. No gene that clusters with the HD-Zip IV subfamily was found in this study.

Difference of evolutionary rates between the HD-Zip I and II subfamilies

Six species pairs had ortholog pairs in both HD-Zip I and II subfamilies. The compared ortholog pairs and the result of comparisons are shown in Tables 2–7. In comparisons of distance between ortholog pairs a eudicot (*Arabidopsis*, *Glycine*, or *Lycopersicon*) and a monocot (*Oryza*), every HD-Zip I ortholog pair had larger distance than any HD-Zip II ortholog pair. In most comparisons, more than 95% of differences in the bootstrap samples was positive, and the minimum bootstrap proportion was 79%. On the other hand, some comparisons in species pairs between eudicots were negative, but not significantly different from 0.

The leucine zipper motif of *Pphb* genes

The leucine zipper motif consists of several heptad repeats. Each site in a heptad repeat is assigned an alphabetical letter from **a** to **g** (Fig. 4). The leucine residues are usually found in the **a** and **d** sites and play important roles in protein dimerization (Hu et al., 1990; Gonzalez et al., 1997).

In the angiosperm HD-Zip I genes, the $\mathbf{a_1}$ and $\mathbf{d_1}$ sites are mainly occupied by threonine and leucine, respectively. In the fern HD-Zip I genes, the $\mathbf{a_1}$ site is occupied by asparagine instead of threonine and the $\mathbf{d_1}$ site is variable and occupied by leucine, valine, or isoleucine (Aso et al., 1999). The $\mathbf{a_1}$ sites of the *Pphb* genes in the HD-Zip I subfamily are all

Table 2. The difference of evolutionary distances from HD-Zip I gene to HD-Zip II gene (*Arabidopsis* and *Oryza* orthologous pairs).

		HD-Zip I											
		CAB38919–*Oshox4*		*Athb5–Oshox4*		*Athb6–Oshox4*		*Athb7–Oshox6*		*Athb12–Oshox6*		*Athb1/HAT5–Oshox5*	
HD-Zip II		[0.36 ± 0.09]		[0.36 ± 0.10]		[0.44 ± 0.12]		[0.44 ± 0.12]		[0.50 ± 0.12]		[0.31 ± 0.07]	
Athb4–Oshox1	[0.19± 0.06]	0.17 ± 0.10	(98)	0.17 ± 0.10	(98)	0.16 ± 0.10	(98)	0.25 ± 0.12	(100)	0.31 ± 0.11	(100)	0.12 ± 0.08	(94)
HAT3–Oshox1	[0.22 ± 0.07]	0.14 ± 0.09	(96)	0.14 ± 0.10	(96)	0.12 ± 0.10	(95)	0.21 ± 0.12	(99)	0.28 ± 0.12	(100)	0.09 ± 0.08	(87)
HAT1–Oshox1	[0.24 ± 0.07]	0.13 ± 0.10	(95)	0.12 ± 0.10	(95)	0.11 ± 0.10	(96)	0.20 ± 0.12	(99)	0.26 ± 0.12	(100)	0.08 ± 0.08	(86)
HAT2–Oshox1	[0.23 ± 0.07]	0.13 ± 0.10	(96)	0.13 ± 0.10	(96)	0.12 ± 0.10	(96)	0.21 ± 0.12	(99)	0.27 ± 0.12	(100)	0.09 ± 0.07	(89)
Athb2/HAT4–Oshox1	[0.24 ± 0.07]	0.12 ± 0.10	(91)	0.12 ± 0.10	(92)	0.11 ± 0.10	(91)	0.20 ± 0.12	(98)	0.26 ± 0.12	(99)	0.07 ± 0.08	(79)
AAC67320–*Oshox3*	[0.24 ± 0.07]	0.12 ± 0.09	(94)	0.12 ± 0.09	(96)	0.11 ± 0.10	(95)	0.20 ± 0.12	(99)	0.26 ± 0.12	(100)	0.08 ± 0.08	(81)

[a] The number in brackets indicates the evolutionary distance.

[b] The number in parentheses indicates percentage of bootstrap samples where the distance of HD-Zip I gene is larger than that of HD-Zip II gene.

Table 2. The difference of evolutionary distances from HD-Zip I gene to HD-Zip II gene (*Arabidopsis* and *Oryza* orthologous pairs).

		HD-Zip I					
		CAB38919–*Oshox 4*		*Athb5–Oshox4*		*Athb6–Oshox4*	
HD-Zip II		[0.36 ± 0.09]		[0.36 ± 0.10]		[0.44 ± 0.12]	
Athb4–Oshox1	[0.19± 0.06]	0.17 ± 0.10	(98)	0.17 ± 0.10	(98)	0.16 ± 0.10	(98)
HAT3–Oshox1	[0.22 ± 0.07]	0.14 ± 0.09	(96)	0.14 ± 0.10	(96)	0.12 ± 0.10	(95)
HAT1–Oshox1	[0.24 ± 0.07]	0.13 ± 0.10	(95)	0.12 ± 0.10	(95)	0.11 ± 0.10	(96)
HAT2–Oshox1	[0.23 ± 0.07]	0.13 ± 0.10	(96)	0.13 ± 0.10	(96)	0.12 ± 0.10	(96)
Athb2/HAT4–Oshox1	[0.24 ± 0.07]	0.12 ± 0.10	(91)	0.12 ± 0.10	(92)	0.11 ± 0.10	(91)
AAC67320–*Oshox3*	[0.24 ± 0.07]	0.12 ± 0.09	(94)	0.12 ± 0.09	(96)	0.11 ± 0.10	(95)

[a] The number in brackets indicates the evolutionary distance.

[b] The number in parentheses indicates percentage of bootstrap samples where the distance of HD-Zip I gene is larger than that of HD-Zip II gene.

Table 3. The difference of evolutionary distances from HD-Zip I gene to HD-Zip II gene (*Glycine* and *Oryza* orthologous pairs).

		HD-Zip I					
		AI440821–*Oshox4*		AW201171–*Oshox4*		*Hdl56–Oshox4*	
HD-Zip II		[0.35 ± 0.11]		[0.30 ± 0.08]		[0.31 ± 0.11]	
Gmh1–Oshox1	[0.21 ± 0.06]	0.14 ± 0.10	(99)	0.09 ± 0.08	(93)	0.10 ± 0.11	(95)
AW277753–*Oshox1*	[0.16 ± 0.06]	0.19 ± 0.09	(100)	0.14 ± 0.07	(98)	0.14 ± 0.10	(99)

[a] The number in brackets indicates the evolutionary distance.

[b] The number in parentheses indicates percentage of bootstrap samples where the distance of HD-Zip I gene is larger than that of HD-Zip II gene.

Table 4. The difference of evolutionary distances from HD-Zip I gene to HD-Zip II gene (*Lycopersicon* and *Oryza* orthologous pairs).

		HD-Zip I	
		AW220361–*Oshox5*	
HD-Zip II		[0.32 ± 0.07]	
AW217402–*Oshox1*	[0.20 ± 0.06]	0.12 ± 0.07	(95)
THOM1–*Oshox1*	[0.19 ± 0.06]	0.13 ± 0.07	(97)

[a] The number in brackets indicates the evolutionary distance.

[b] The number in parentheses indicates percentage of bootstrap samples where the distance of HD-Zip I gene is larger than that of HD-Zip II gene.

Table 5. The difference of evolutionary distances from HD-Zip I gene to HD-Zip II gene (*Arabidopsis* and *Glycine* orthologous pairs).

		HD-Zip I					
		Athb5–AI440821		*Athb5*–AW201171		AAB61483–*Hdl57*	
HD-Zip II		[0.22 ± 0.09]		[0.16 ± 0.06]		[0.60 ± 0.13]	
Athb2/*HAT4*–*Gmh1*	[0.12± 0.05]	0.10 ± 0.10	(95)	0.04 ± 0.07	(79)	0.49 ± 0.13	(100)
Athb4–AW277753	[0.10 ± 0.04]	0.11 ± 0.09	(97)	0.06 ± 0.08	(84)	0.50 ± 0.13	(100)
HAT3–AW277753	[0.09 ± 0.04]	0.13 ± 0.10	(98)	0.07 ± 0.07	(91)	0.51 ± 0.14	(100)
HAT1–AW277753	[0.22 ± 0.06]	0.00 ± 0.09	(63)	-0.06 ± 0.08	(27)	0.39 ± 0.13	(100)
HAT2–AW277753	[0.17 ± 0.05]	0.04 ± 0.10	(84)	-0.01 ± 0.08	(52)	0.43 ± 0.13	(100)

[a] The number in brackets indicates the evolutionary distance.

[b] The number in parentheses indicates percentage of bootstrap samples where the distance of HD-Zip I gene is larger than that of HD-Zip II gene.

Table 6. The difference of evolutionary distances from HD-Zip I gene to HD-Zip II gene (*Arabidopsis* and *Lycopersicon* orthologous pairs).

		HD-Zip I					
		AAD14502–AI897471		*Athb13*–AI897471		*Athb1*/*HAT5*–AW220361	
HD-Zip II		[0.26 ± 0.09]		[0.09 ± 0.04]		[0.09 ± 0.04]	
Athb2/*HAT4*–AW217402	[0.12 ± 0.04]	0.15 ± 0.09	(99)	-0.02 ± 0.06	(35)	-0.02 ± 0.05	(31)

Table 7. The difference of evolutionary distances from HD-Zip I gene to HD-Zip II gene (*Glycine* and *Lycopersicon* orthologous pairs).

		HD-Zip I	
		Hdl57–AI484074	
HD-Zip II		[0.31 ± 0.10]	
Gmh1–AW217402	[0.05 ± 0.03]	0.26 ± 0.10	(100)
AW277753–AW217402	[0.14 ± 0.05]	0.17 ± 0.11	(98)
Gmh1–*THOM1*	[0.15 ± 0.05]	0.17 ± 0.11	(99)
AW277753–*THOM1*	[0.08 ± 0.03]	0.24 ± 0.11	(100)

[a] The number in brackets indicates the evolutionary distance.

[b] The number in parentheses indicates percentage of bootstrap samples where the distance of HD-Zip I gene is larger than that of HD-Zip II gene.

threonine, except for *Pphb9*, which has isoleucine. Leucine residues occupy the $\mathbf{d_1}$ sites as observed in angiosperm HD-Zip I genes.

The $\mathbf{a_1}$ and $\mathbf{d_1}$ sites of HD-Zip II genes are fixed with leucine and threonine, respectively. As in the angiosperms, the $\mathbf{a_1}$ and $\mathbf{d_1}$ sites of *Pphb4* are threonine and leucine, respectively. The $\mathbf{a_1}$ and $\mathbf{d_1}$ sites of *Pphb3* are alanine and asparagine, respectively, unlike any other HD-Zip genes.

Expression of *Pphb* genes

The spatial patterns of *Pphb* gene expression in gametophytes were assessed by RNA gel blot analyses. The transcript of the *Pphb1*, *2*, *3*, *6*, *7*, *8*, and *9* are 1.7, 1.7, 1.4, 1.7, 1.7, 1.7, and 1.7 kb in length, respectively (Fig. 6). The signal of *Pphb2* was mainly detected in protonemata, while those of the other genes were in gametophores (Fig. 6). Two length of transcripts of *Pphb10* (2.2 and 2.9 kb) were detected in gametophores. Although *Pphb4* and *Pphb5* were cloned by RT-PCR using total RNA and PCR using genomic DNA derived from gametophyte tissues, expression of *Pphb4* and *Pphb5* was not detectable in protonemata and gametophores by RNA gel blot analyses.

The expression of *Pphb* genes in sporophyte generation is unknown, because it is difficult to obtain sufficient sporophyte tissues for RNA gel blot analyses.

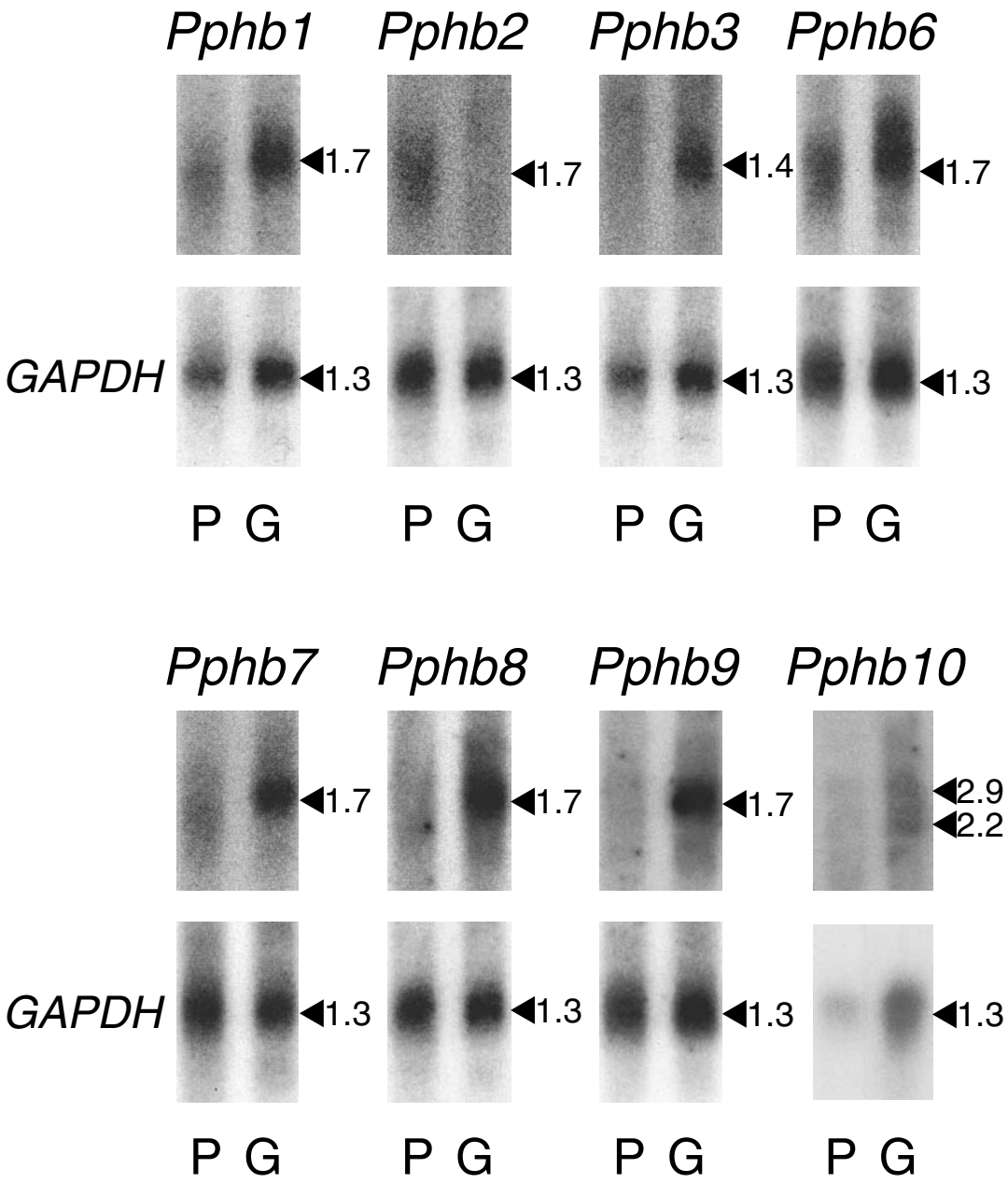

Figure 6. RNA gel blot analyses of *Pphb1–3* and *Pphb6–10*.
Poly $(A)^+$ RNA of 1.0 μg from protonemata (P) and from gametophores with rhizoids (G) of wild-type *P. patens* was hybridized with each gene specific probe for *Pphb1–Pphb3* and *Pphb6–Pphb10* shown in Figure 3. As an internal control, the DNA fragment encoding glyceraldehyde 3-phosphate dehydrogenase (*GAPDH*) was used as a probe (Leech et al., 1993).

1-5. Discussion

Phylogenetic relationships among HD-Zip subfamilies of Physcomitrella

Previously, HD-Zip genes were known only in vascular plants and not in other multicellular organisms. In this chapter, I described the isolation of 10 HD-Zip genes from the moss, Physcomitrella. This is the first report of HD-Zip genes isolated from non-vascular green plants, suggesting that HD-Zip genes originated before the divergence of the mosses and vascular plants. Previous studies suggested that the HD-Zip gene family divided into four subfamilies, HD-Zip I, II, III, and IV, before the seed plants and ferns split (Aso et al., 1999). The HD-Zip gene tree in figure 5 indicates that the divergence of the four subfamilies occurred before the split of the mosses. *Pphb3* is sister to the HD-Zip II subfamily, and has two unique characters: 1) the large distance separating *Pphb3* from its sister, the HD-Zip II subfamily, and 2) the divergence of amino acid residues in the otherwise conserved $\mathbf{a_1}$ and $\mathbf{d_1}$ sites of the leucine zipper motif. This will be confirmed by further screening the HD-Zip genes in other plants.

The fact that the mosses have HD-Zip I and II genes is not surprising, because their roles in angiosperms (e.g. light, ABA, and auxin signal transduction networks) are likely general to all plants, including mosses. A phytochrome gene, which encodes a photo-sensor pigment of plants has been cloned in Physcomitrella (Kolukisaoglu et al., 1993), and some phototropic responses that should be caused by the light signal transduction network have also been reported in mosses (Russell et al., 1998). The desiccation stress response networks mediated by ABA, which involve angiosperm HD-Zip I or II genes is likely conserved between Physcomitrella and angiosperms (Knight et al., 1995). Auxin is an important developmental regulator in both angiosperms and mosses (reviewed in Cove 1992), although its roles in development are different in the two because of their developmental and morphological differences. It is unclear whether these plants use similar cascades for light-, ABA-, and auxin- mediated networks, and further characterization of Physcomitrella HD-Zip I and II gene functions and comparison with angiosperm HD-Zip genes are necessary.

Most angiosperm HD-Zip III genes are involved in the differentiation of vascular tissue (Baima et al., 1995; Zhong and Ye, 1999; Baima et al., 2001). Some mosses, including Physcomitrella, have water conducting hydroids and nutrient conducting leptoids in the gametophyte similar to the tracheids and sieve elements of vascular plants, respectively (Bell, 1992). However, the homologies of these cells are ambiguous, because in vascular plants

tracheids and sieve elements are formed in the sporophyte generation. Furthermore, the cell wall thickening common to tracheids does not occur in hydroids, although the leptoids are similar to sieve elements at the ultrastructural level (Schofield and Hébant, 1984). Determining the function of *Pphb10*, the moss HD-Zip III gene, may give insights into the evolution of vascular tissue in land plants.

Differences of evolutionary rates between the HD-Zip I and II subfamilies

The amino acid residues in the homeodomain and leucine zipper motif of the HD-Zip I subfamily appear less conserved than those of the HD-Zip II subfamily in the alignment (Fig. 4). Chan et al. (1998) pointed out the possibility that the evolutionary rate was higher in the former subfamily than in the latter. Comparison of the evolutionary distances for the ortholog pairs of eudicots and rice indicated that HD-Zip I genes evolved faster than HD-Zip II genes after the split of eudicots and monocots (Tables 2-4). Within eudicots, the differences are not clear, which may be because the difference has not accumulated enough to be significant (Tables 5-7). Some metazoan homeobox genes have been reported to function as a complex with other cofactors that regulate the homeobox gene (Mann and Chan 1996; Bürglin 1998; González-Crespo et al. 1998; Mann and Affolter 1998). The leucine zipper motif also plays a role in protein-protein interaction (O'Shea et al., 1991). HD-Zip II genes may evolve slowly because HD-Zip II genes interact with cofactors that regulate the function of HD-Zip II genes strictly, while HD-Zip I genes may evolve faster because these genes do not interact with cofactors, and have relaxed specificity. In animals, helix 3 of the homeodomain is essential for DNA recognition (Kissinger et al., 1990), while helices 1 and 2 are involved in less stringent interactions with other proteins (Chan et al., 1994; Zappavigna et al., 1994; Grueneberg et al., 1995). Figure 4 shows that the amino acid residues of helix 3 of HD-Zip I and II genes are highly conserved throughout HD-Zip I and II genes, while helices 1 and 2 of HD-Zip I genes have more variety than HD-Zip II genes. This suggests that a difference in the protein-protein interactions of the HD-Zip I and II subfamilies may be one of the reasons for the difference in their respective evolutionary rates.

Some HD-Zip genes are reported to dimerize via the leucine zipper motif and bind DNA *in vitro* (Sessa et al., 1993; Gonzalez et al., 1997; Sessa et al., 1998). The $\mathbf{a_1}$ and $\mathbf{d_1}$ sites of the leucine zipper motif are important for determining the dimerization partner (Gonzalez et al., 1997). Amino acids in the $\mathbf{a_1}$ and $\mathbf{d_1}$ sites of HD-Zip I genes vary, while those of HD-

Zip II genes are always leucine and threonine, respectively. Given that the amino acids of HD-Zip II genes are highly conserved, these genes likely select their dimerization partner more strictly than HD-Zip I genes, perhaps to maintain specificity of pairing. Further studies on the protein interactions of HD-Zip genes are required to test this hypothesis.

Pphb genes may be involved in specific developmental processes

The observation that none of *Pphb* genes are expressed in both of protonemata and gametophores indicates these HD-Zip genes are required for specific developmental processes (Fig. 6). Most of *Pphb* genes are expressed in gametophores. A protonema is two-dimensional in growth and differentiates few cell types, while the gametophore, on the other hand, is three-dimensional and has complex organs (stems, leaves, and rhizoids) with many specialized cell types (Fig. 1). Several HD-Zip genes of angiosperms are likely involved in specification of cell types in vascular tissues or epidermal cells (Rerie et al., 1994; Di Cristina et al., 1996; Zhong and Ye, 1999; Scarpella et al., 2000). *Physcomitrella* HD-Zip genes may be also involved in specific cell types and more *Pphb* genes are likely expressed in the gametophore than protonemata, because the gametophore is composed of more cell-types. Detailed expression analyses and functional analyses of each *Pphb* gene will elucidate the possibility.

Chapter 2: Involvement of Auxin and a Homeodomain-Leucine Zipper I Gene in Epidermal Cell Differentiation of the Moss *Physcomitrella patens*

2-1. Summary

Differentiation of epidermal cells is important for immobile plants because they are in direct contact with the biotic and abiotic environments. Rhizoids are multicellular filaments that differentiate from the epidermis; they have functions similar to root hairs in vascular plants in that they support the plant body and are involved in the absorption of water and nutrients. Rhizoids are observed in a wide range of plants, including pteridophytes, bryophytes, and green algae. In this study, I examined the mechanisms underlying rhizoid differentiation in the moss *Physcomitrella patens*. This moss is the only land plant in which high-frequency gene targeting is possible using homologous recombination. I found that rhizoid differentiation could be split into two processes: determination and characterization. Two types of rhizoids with distinct differentiation patterns (basal and mid-stem rhizoids) were recognized. The differentiation of basal rhizoids from epidermal cells was induced by exogenous auxin, while that of mid-stem rhizoids required an unknown factor in addition to exogenous auxin. Once an epidermal cell was fated to become a rhizoid initial cell, expression of the homeodomain-leucine zipper I gene *Pphb7* was induced. Analysis of *Pphb7* disruptant lines showed that *Pphb7* regulates the induction of pigmentation and the increase in the number and size of chloroplasts, but not the position or number of rhizoids. This is the first report on the involvement of a homeodomain-leucine zipper I gene in epidermal cell differentiation.

2-2. Introduction

Multicellular organisms are composed of diverse cell types and the definition of the molecular mechanism of cell-type determination is one of the fundamental problems in developmental biology (Alberts et al., 2002). In land plants, the epidermis is the outermost cell layer, which functions as a barrier to retain water and to defend against pathogens and predators. The compact arrangement of small cells with thick cell walls and the presence of a tough cuticle of the epidermis provide the mechanical strength to withstand gravity and the extracellular environment (Bold et al., 1987; Esau, 1977; Glover, 2000). Parts of the epidermal cells of land plants are specialized. Stomatal guard cells are specialized for gas exchange, trichomes and scales are for protection against environmental changes and predators, and root hairs in vascular plants and rhizoids in pteridophytes and non-vascular plants including green algae are for the absorption of water and nutrients. Rhizoid morphology varies from unicellular to multicellular filamentous structures. In addition to absorption, the rhizoid functions as an organ that attaches the plant body to the substratum, a function that is especially important in the gametophytes of pteridophytes and non-vascular plants, which do not have roots (Bell, 1992; Bold et al., 1987; Raghavan, 1989).

Molecular genetic studies of individual specialized cell types in angiosperms have provided information on the mechanism behind the patterns of cell differentiation (Brownlee, 2000; Hülskamp et al., 1994; Marks, 1997). The positioning of presumptive cells is likely regulated by cell-cell communication *via* molecular signals, such as the plant hormone ethylene or its precursor, which function in root hair formation (Tanimoto et al., 1995), and the serine protease subtilisin, which participates in stomatal guard cell differentiation (Berger and Altmann, 2000). The factors involved in trichome and rhizoid differentiation, as well as the additional determinants of root hair and stomatal guard cell differentiation, are unknown. Communication usually occurs between clonally unrelated cells in root hairs and trichomes, while the determination of stomatal guard cells occurs *via* cell-cell interactions among clonally related cells (Brownlee, 2000; Glover, 2000). Such cell-cell communication triggers signal transduction cascades and induces the transcription of downstream genes that are involved in the later events of cell differentiation. Various classes of transcription factors are involved in these cascades (Lee and Schiefelbein, 1999; Oppenheimer et al., 1991; Payne et al., 2000; Wada et al., 1997). *GLABRA2* (*GL2*), which is a member of the homeodomain-leucine zipper (HD-Zip) gene family, functions in the promotion and repression of

specialization in trichome and root hair cells, respectively (Di Cristina et al., 1996; Rerie et al., 1994), in co-operation with other transcription factors (Lee and Schiefelbein, 1999; Oppenheimer et al., 1991; Payne et al., 2000; Wada et al., 1997).

The HD-Zip genes, which are characterized by a homeodomain (McGinnis et al., 1984) and a leucine zipper motif (Landschulz et al., 1988) that lies adjacent to the C-terminus of the homeodomain, form four subfamilies (Meijer et al., 1997), and are found only in green plants (the HD-Zip I-IV subfamilies; Aso et al., 1999). In addition to *GL2* of the HD-Zip IV subfamily, some members of the HD-Zip gene family are involved in cell differentiation in certain parts of the plant body. Overexpression of the HD-Zip I gene *Athb-1* produces pleiotropic effects on leaf cell differentiation (Aoyama et al., 1995), and most members of the HD-Zip III subfamily play roles in the cellular differentiation of stems (Baima et al., 2001; Zhong and Ye, 1999) and leaves (McConnell et al., 2001).

Rhizoids are widely observed in green plants, but their development has not been studied at the molecular level, mainly because a useful model system was lacking. The moss *Physcomitrella patens* is a suitable plant in which to study rhizoid differentiation, since techniques for transformation and gene targeting by homologous recombination have been established during the last decade (Cove et al., 1997; Schaefer, 2001; Schaefer and Zrÿd, 1997). The rhizoids of *P. patens* are multicellular filamentous structures that differentiate from the epidermal cells of the stem of a leafy shoot (gametophore). The rhizoids function in the attachment of leafy shoots to the substratum and in the uptake of nutrients (Bates and Bakken, 1998; Duckett et al., 1998). Auxin is reported to increase the number of rhizoids (Ashton et al., 1979), although the details of their spatial patterns are unknown.

In this study, I report that rhizoid differentiation is dissected into two processes, determination and characterization. The cell-cell communication *via* auxin and unknown factor(s) regulates the former process, while a member of the HD-Zip subfamily, *Pphb7* induced by auxin is involved only in the latter process. A model for rhizoid differentiation is proposed.

2-3. Materials and Methods

Strain and culture conditions

Physcomitrella patens (Hedw.) Bruch & Schimp subsp. *patens* Tan was collected in Gransden Wood, Huntingdonshire, UK (Ashton and Cove, 1977) and used as the Physcomitrella wild-type strain. The culture conditions were as described in Chapter 1 under 16 hours light and 8 hours dark conditions. G medium described in Chapter 1 was used as a standard medium. In order to observe juvenile gametophores, the protonemata were inoculated in 6-cm petri dishes with 5 ml of 0.5×BCD medium without agar (liquid BCD medium; Nishiyama et al., 2000) that contained 0.1 mM $CaCl_2$ and 2% (w/v) sucrose, and cultured for 1 week. To examine the effects on rhizoid differentiation of short-term treatment with exogenous auxin, gametophores that had been grown on standard medium for 6 weeks were cultured for 1 week in water that contained 0, 0.1, 1, or 10 µM 1-naphthalene acetic acid (NAA) (N1641, Sigma Chemical Co., St. Louis, MO). To examine the effects of long-term exposure to exogenous auxin, protonemata were cultured for 6 weeks on standard medium that contained 0.1, 1, or 10 µM NAA. To test whether the applications of plant hormones change the expression level of *Pphb7* mRNA, gametophores were cultured for 4 weeks on standard medium covered with cellophane (Futamura Chemical Industries Co., Ltd.). The cellophane sheets with gametophores were transferred to petri dishes with 10 ml of water that contained 0.1, 1, 10 µM NAA, 10 µM 6-benzylamino purine (BA) (B-3274, Sigma Chemical Co.), 10 µM gibberellin A3 (GA) (Wako Pure Chemical Industries, Ltd.), 10 µM abcisic acid (ABA) (A1049, Sigma Chemical Co.), or 10 µM aminocyclopropanol-1-1carboxylate (ACC) (A0430, Sigma Chemical Co.). To examine whether dehydration and osmotic stress effect *Pphb7* expression, the cellophane sheets with gametophores were transferred to an empty petri dish and a petri dish with 10 ml of 6% mannitol, respectively. These gametophores were collected 1, 6, or 24 hours later, and used for RNA blot analyses. To examine the effects of treatment with exogenous auxin and cytokinin, gametophores that had been grown on standard medium for 6 weeks were cultured for 1, 6, 24, or 48 hours in water that contained 0, 0.1, 1, or 10 µM NAA or 1, or 10 µM BA.

Transformation

PEG-mediated transformation of Physcomitrella was performed according to Schaefer et al. (1991). To isolate protoplasts, 5 days-old protonema was incubated at 25˚C for

30 minutes in a solution of 4% (w/v) Driserase (Kyowa Hakko Kogyo Co., Ltd., Tokyo, Japan) and 8% (w/v) mannitol, and filtered through 50 µm nylon mesh. Freshly isolated protoplasts were centrifuged (2 minutes, 180×g) and suspended in 8 % (w/v) mannitol. This washing procedure was repeated twice. Finally suspended protoplasts were counted with hemocytometor, and resuspended at 1.6×10^6 ml^{-1} in MMM solution [15 mM $MgCl_2$, 0.1% (w/v) MES, 8% (w/v) mannitol, pH 5.6]. Protoplast suspension (300 µl) and PEG solution [300 µl; 4%(w/v) PEG6000, 100 mM $Ca(NO_3)_2$, 100 mM Tris-HCl, pH 8.0] was added to Falcon 2057 tube (Becton Dickinson, Franklin Lakes, USA) containing 30 µl of plasmid DNA and mixed gently. The plasmid DNA was purified with phenol/chloroform extraction, followed by PEG precipitation, and were resuspended in TE [10 mM Tris-HCl, 1mM EDTA, pH 8.0] at a concentration of 1 µg $µl^{-1}$. The transformation mixture was incubated at 45˚C for 5 minutes and at 20˚C for 10 minutes. Subsequently, the solution was diluted by adding 300 µl of protoplast liquid medium [5 mM $Ca(NO_3)_2$, 1 mM $MgSO_4$, 45 µM $FeSO_4$, 0.18 mM KH_2PO_4 (pH 6.5 adjusted with KOH), 1 ml of alternative TES per liter, 5 mM d-ammonium (+) tartrate, 6.6% (w/v) mannitol, and 0.5% (w/v) glucose] every 5 minutes at 5 times and 1 ml of protoplast liquid medium every 5 minutes at 5 times. The diluted protoplast solution was poured into a 6 cm-dish and incubated at 25˚C in darkness over night. Protoplasts were centrifuged (2 minutes, 180×g), resuspended in 8 ml of PRM/T medium [BCD medium suspended with 5 mM d-ammonium (+) tartrate, 10 mM $CaCl_2$, and 8% (w/v) mannitol]. Two ml of protoplast suspension was poured on a 9 cm-dish containing PRM/T medium [BCD medium suspended with 5 mM d-ammonium (+) tartrate, 9 mM $CaCl_2$, and 6% (w/v) mannitol], and incubated at 25˚C for 3 days under continuous daylight with a light flux of 50 µmol m^{-2} s^{-1}. Cultures were transferred to BCDAT medium supplemented with 50 mg l-1 or 20 mg l-1 G418 (Invitrogen) for the selection of transformants, and incubated at 25˚C for 4 weeks under continuous daylight. Each transformant regenerated from protoplast under G418 selection was transferred to antibiotic-free BCDAT medium and cultured at 25˚C for 1 week. After an incubation of 1 week, each transformant was re-transferred to BCDAT medium supplemented with 50 mg l^{-1} or 20 mg l^{-1} G418 (Invitrogen). Transformants that were able to survive on selection medium were selected as stable transformants.

Microscopy

Live gametophores were carefully removed from culture medium, transferred to

either a petri dish that contained agar medium or to a slide glass that contained a drop of distilled water, and observed using a stereomicroscope or light microscope. An epi-fluorescence microscope (Leica DMLB HC; Leica Microsystems, Heerbrugg, Switzerland) with an A filter (UV excitation for chlorophyll) and a GFP filter (blue excitation for GFP) was used to detect fluorescence from chlorophyll and green fluorescence protein (GFP), respectively. Chloroplast nucleoids were stained with 1×SYBR Green I (Molecular Probes, Inc., Eugene, OR) in 2% glutaraldehyde for 30 minutes, and was observed using the epi-fluorescence microscope with the GFP filter. The histochemical detection of β-glucuronidase (GUS) activity was performed as described by Jefferson et al. (1987) with slight modification. Tissues were fixed in a solution of 0.3% (v/v) formalin, 0.3 M mannitol, and 0.2% (w/v) MES (pH 5.6) for 30 minutes at room temperature and washed 3 times with 50 mM NaH_2PO_4 (pH 7.0). The tissues were infiltrated for 30 minutes in a substrate solution [50 mM NaH_2PO_4 (pH 7.0), 0.5 mM 5-bromo-4-chloro-3-indolyl β-D-glucurunic acids (X-Gluc, Wako Pure Chemical), 0.5 mM $K_3Fe(CN)_6$, 0.5 mM $K_4Fe(CN)_6$ and 0.3% (v/v) Triton X-100] and were incubated at 37˚C for 2 hours. After the incubation, the tissues were fixed in 2% (v/v) formalin for 10 minutes. The tissues were dehydrated through an ethanol series. Leaves were observed after clearing with chloral hydrate according to Tsuge et al. (1996).

Images of a rhizoid cell were digitized with a CCD camera (CoolSNAP, Roper Scientific Photometrics, Germany) to quantify rhizoid pigmentation. The mean light intensities of the red, green and blue channels in an area of 2500 pixels on and outside the rhizoid were determined using Adobe Photoshop 6.0 (Adobe Systems Incorporated, San Jose, CA). Light transmittance was calculated as the ratio of the mean light intensity on the rhizoid to that outside the rhizoid in each channel. In order to quantify chloroplast size, an outline of the chloroplast was traced on the image using Adobe Photoshop 6.0, and the area was calculated with the NIH Image 1.62f program (NIH, Bethesda, MD; http://rsb.info.nih.gov/nih-image/).

For the sectioning of resin-embedded tissues, gametophores were fixed in 2.5% formaldehyde and 2% glutaraldehyde in 0.1 M sodium phosphate buffer (pH 7.0), dehydrated in a graded ethanol series, and embedded in Technovit 7100 (Heraeus Kulzer, Wehrheim, Germany). Sections (5-μm thick) were made with a microtome and stained with 0.05% (w/v) toluidine blue in 0.1 M sodium phosphate buffer (pH 7.0).

For scanning electron microscopy, gametophores grown on the standard medium for

6 weeks were fixed with modified Karnovsky's fixative [3% glutaraldehyde, 1.5% (w/v) paraformaldehyde in 0.1 M sodium phosphate buffer (pH 7.4); Karnovsky, 1965] for 2 hours, and soaked in 1% (w/v) tannic acid overnight. The samples were then fixed in 2% osmium tetroxide for 2 hours and in 1% uranyl acetate overnight before dehydration through a graded ethanol series. The fixed preparations were soaked once in an isoamyl acetate and ethanol mixture (1:1) for 30 minutes and twice in isoamyl acetate for 30 minutes, and were critical-point dried using carbon dioxide. The dried tissues were mounted on stubs and coated with gold with an ion spatter (model IB-3; EIKO Engineering Co., Ltd., Tokyo, Japan). The preparations were observed using a scanning electron microscope (S-800; Hitachi Ltd., Tokyo, Japan).

For transmission electron microscopy of rhizoids, gametophores were carefully removed from standard medium and fixed with the same fixative as scanning electron microscopy for 2 hours and followed by 2% osmium tetroxide for 2 hours. These were stained with 1% uranyl acetate en bloc before dehydration, and embedded with Epon. Electron microscope observations were done with a JEM 100CX (JEOL Ltd., Akishima, Japan) operating at 100 kV.

Cloning of *Pphb7*

A partial cDNA fragment that covered the region downstream of the HD-Zip domain of *Pphb7* was cloned into the pAMP1 vector (Invitrogen) to generate the plasmid p3Pphb7. To clone the 5'-region of the *Pphb7* mRNA, first-strand cDNA was synthesized with the 5'-RACE system using SuperScriptII reverse transcriptase (Invitrogen) and the 5Pphb7-1 (5'-CGTCGTCATTAGAGATTCCCTT-3'). The synthesized cDNA was amplified with the anchor primer and 5Pphb7-2 primers (5'-CAUCAUCAUCAUTCACCTCAGCTTTAAGAGCACTT-3') using Ex Taq DNA Polymerase (TaKaRa Shuzo Co., Ltd.). PCR cycles conditions consisted of 2 min at 94˚C, 25 cycles of 94˚C for 30 seconds, 60˚C for 30 seconds, and 72˚C for 3 minutes. Further PCR was carried out with the universal amplification primer (5'-CUACUACUACUAGGCCACGCGTCGACTAGTAC-3') supplied by Invitrogen and 5Pphb7-2 primers. PCR conditions were as in the previous reaction. PCR products were cloned into pAMP1 (Invitrogen).

Based on the nucleotide sequences of these partial 5'- and 3'- cDNA fragments,

nested primers (Pphb7-51 and Pphb7-52 for the 5'-end, and Pphb7-31 and Pphb7-32 for the 3'-end) were used to amplify most of the *Pphb7* cDNA (1787 bp) sequence. The primer sequences were shown in Table 1. The amplified fragment was cloned into pGEM3z (Promega, Madison, WI), thereby generating pcPphb7. A 2851-bp genomic DNA fragment that corresponded to the *Pphb7* cDNA (Fig. 7A) was amplified using the aforementioned primers and Physcomitrella genomic DNA as the template, and cloned into pGEM3z, to give pgPphb7. A 780-bp genomic DNA fragment that bordered the 5'-end of the *Pphb7* cDNA was obtained by the TAIL-PCR method (Liu et al., 1995) using the arbitrary primer A3 (5'-(A/T)GTGNAG(A/T)ANCANAGA-3') and three gene-specific primers (5Pphb7tail1, 5'-CAAATCTAATCACGTATGCCCA-3'; 5Pphb7tail2, 5'-AAGCAGAGAAATCAGAGTGTCG-3'; and 5Pphb7tail3, 5'-ACCATCGTTTGTTCCCTGATCT-3'), and cloned into the pGEM-T vector (Promega).

Gene targeting

Pphb7-GUS was constructed as follows: genomic DNA fragment that encompassed the *Pphb7*-coding region was amplified with the reverse primer (5'-AGCGGATAACAATTTCACACAGG-3') and the SalI-Pphb7S primer (5'-ACGCGTCGACTCCGAGCTCGATGGTTAAG-3'), using pgPphb7 as the template. The fragment was digested with *Sal*I, and the 693-bp fragment was cloned into the *Sal*I site of the pGUS-NPTII-2 plasmid, which contained the coding sequence of the GUS gene (*uidA*), the nopaline synthase polyadenylation signal (nos-ter), and the NPTII expression cassette (nptII; Nishiyama et al., 2000), thereby creating an in-frame fusion of the *Pphb7* and *uidA* genes (Fig. 7B). A 1.2-kb *Xba*I fragment of pgPphb7 that contained the 3'-region of *Pphb7* was inserted into this plasmid and the recombinant plasmid was designated as pPphb7-GUS. This plasmid was linearized by digestion with *Apa*I and *Not*I, and used for gene targeting (Fig. 7B).
The plasmid pKS1, which contained nos-ter and nptII, was used for the construction of GFP-Pphb7. The coding sequence of sGFP was amplified from pTH-2 (Chiu et al., 1996) using the M13-21 and Apa-Sal/mGFPend primers (5'-TGTAAAACGACGGCCAGT-3' and 5'-GAGGGCCCGGTCGACTTGTACAGCTCGTC-3', respectively). The PCR product was digested with *Sal*I, and the 746-bp fragment was cloned into the *Sal*I site (located upstream of nos-ter) of pKS1. The pgPphb7 plasmid was digested with *Bam*HI, blunt-ended, digested with *Not*I, and the 891-bp DNA fragment that contained the 3'-untranslated region of *Pphb7* was

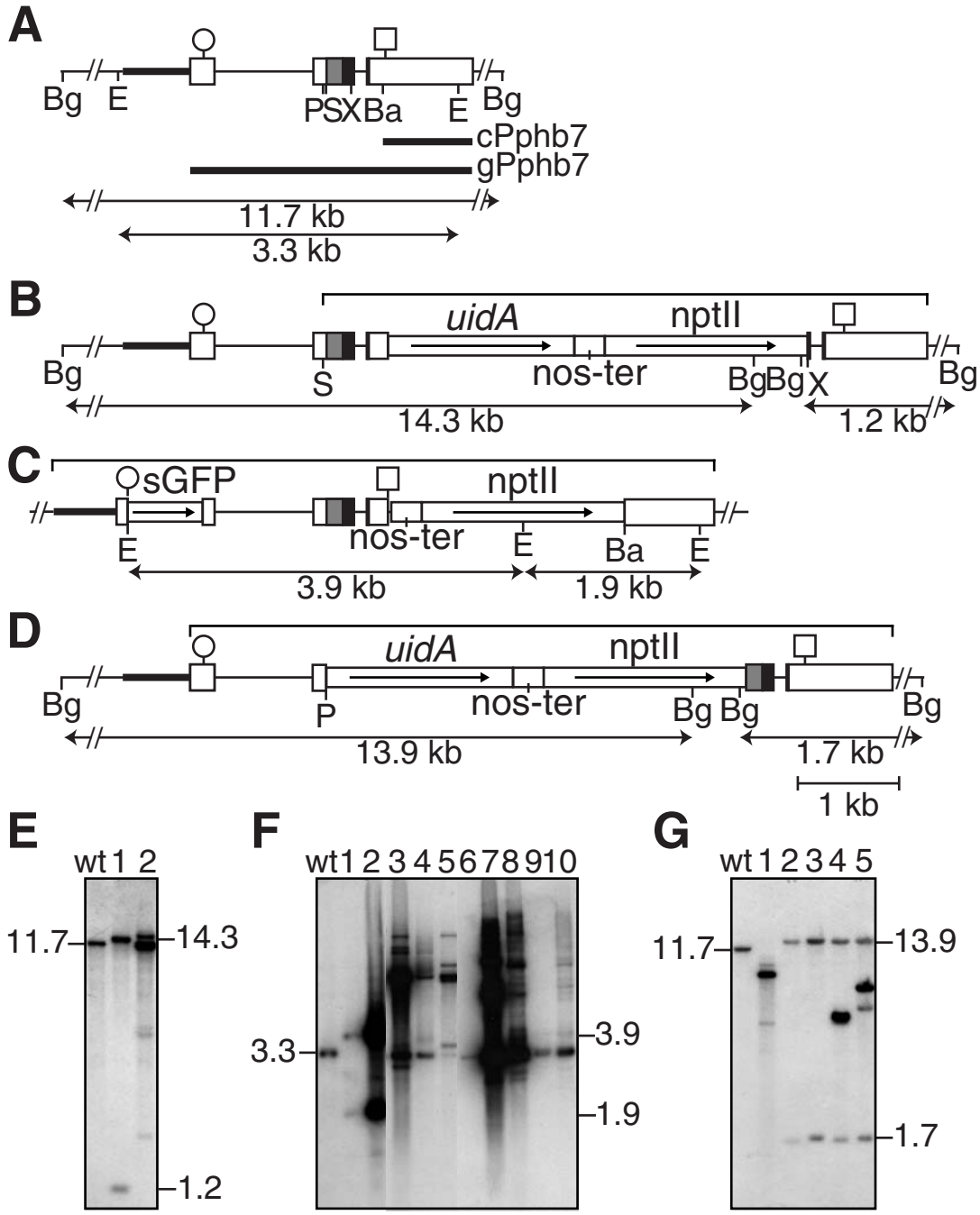

Figure 7. Genomic structures of *Pphb7* in the wild-type and transformant lines.
Genomic structure of *Pphb7* in the wild type (A), Pphb7-GUS (B), GFP-Pphb7 (C), and *Pphb7* disruptant (D). (A) The boxes and the lines between the boxes indicate the exons and introns, respectively. A bold line represents the genomic DNA fragment isolated using the TAIL-PCR method. The circle and square indicate putative start and stop codons, respectively. The gray and black boxes indicate a homeodomain and a leucine zipper motif, respectively. The cPphb7 and gPphb7 probes for RNA and DNA gel blot analyses are shown as bold lines under the genomic structure. (B-D) The *uidA*, sGFP, nos-ter, and nptII designations represent the uidA-coding region, the GFP-coding region, the nopaline synthase polyadenylation signal, and an NPTII expression cassette, respectively. Each bracket above the genome structure indicates the region contained in a plasmid used for gene targeting. P, *Pma*CI, S, *Sal*I, X, *Xba*I, Ba, *Bam*HI, Bg, *Bgl*II, E, *Eco*T14I. (E-G) DNA gel blot analyses to confirm gene targeting. Genomic DNA from the wild type (wt) and from transformants was digested with *Bgl*II (E,G) or *Eco*T14I (F). The gPphb7 probe was used. (E) Wild type and Pphb7-GUS-1 and -2 lines (lanes 1 and 2); (F) Wild type and GFP-Pphb7-1 to -10 lines (lanes 1-10); (G) Wild type and Pphb7dis-1 to -5 lines (lanes 1-5). The numbers listed next to the blots are the fragment lengths in kb.

inserted into the *Sph*I (blunt-ended)-*Not*I site located downstream of nptII. The 1842-bp *Pphb7*-coding region and the 740-bp 5'-flanking region were amplified by PCR using the pgPphb7 and p5Pphb7tail plasmids as templates. The amplified fragments were inserted into the *Eco*RV and *Kpn*I-*Apa*I sites of their respective cloning vectors. The 1842-bp fragment was connected in-frame to the sGFP-coding sequence. The following primers were used for the PCR amplification: Pphb7start (5'-GATGGTAGTCCCTAGTTTACCCGC-3') and Pphb7stop (5'-GCTTCACTTGAGATGCAAGTGACTG-3') for the 1842-bp fragment; and KpnI-5Pphb7F (5'-TAGGTACCTCCCCGCCTGATGCTGAA-3') and ApaI-5Pphb7R (5'-TAGGGCCCAATTCACTAGTGATTACCAT-3') for the 740-bp fragment. The recombinant plasmid was linearized with *Kpn*I and *Not*I, and used for gene targeting (Fig. 7C).
A plasmid that carried a disruption of the *Pphb7* gene was made as follows: the 4.4-kb fragment that encompassed *uidA*, nos-ter, and nptII was excised from pTN9 using *Xho*I, blunt-ended, and cloned into the *Pma*CI site of pgPphb7. The resulting plasmid was digested with *Not*I and used for gene targeting (Fig. 7D).

Transformants with the modified *Pphb7* locus were identified by PCR amplification of genomic DNA using the Pphb7-51 and Pphb7-31 primers.

RNA and DNA gel blot analyses

The protocols used for the extraction of poly $(A)^+$ RNA and DNA, blotting, and hybridization were performed as described in Chapter 1. A *Bam*HI-digested fragment of the plasmid p3Pphb7 was used as the cPphb7 probe for RNA gel blot analysis (Fig. 7A). A PCR fragment that was amplified with the Pphb7-52 and Pphb7-32 primers using pgPphb7 plasmid as the template was used as the gPphb7 probe (Fig. 7A). Radioactivity of hybridization signals was quantified with FUJIX BAS2000 Bio Analyzer (Fuji Photo Film Co. Ltd., Tokyo, Japan). Relative expression level was calculated as the ratio of the intensity of each lane to that of a lane with no treatment.

Reverse transcription-polymerase chain reaction (RT-PCR)

Gametophores cultured on the standard medium for 6 weeks under continuous light. Total RNA of the gametophores or rhizoids was extracted using RNeasy Plant mini kit (QIAGEN, Stanford Valencia, CA) and the first strand of cDNA was synthesized using oligo$(dT)_{20}$ primer and mixed primers oligo$(dT)_{20}$, PpchlB-RT (5'-

CAGATGGCTCGATTCGAGCAA-3'), PprbcL-RT (5'-GCAGCAGCTAATTCAGGACTCCA-3'), and PppsbA-RT(5'-TCTAGAGGGAAGTTGTGAGCGT-3') for nucleus gene and chloroplast, respectively. Sequences of *chlB* and *psbA* were kindly provided by Dr. M. Sugita, Nagoya Univ., Japan. PCR was performed using *PfuTurbo* Hotstart DNA polymerase. Sample concentrations were normalized for equal amplification of DNA fragments with PpgapC5' and PpgapC3' primers. PCR was performed under the same conditions except that the primers were specific for cDNA of each gene. For semi-quantitative of mRNAs, I examined DNA fragments that had been amplified during increasing numbers of cycles during a series of PCRs. The products of PCR were analyzed by agarose-gel electrophoresis and sequenced directly using both primers using for amplification. The primer pairs were as follows: for *PpPOR1*, PpPOR1-F (5'-CATTCGGGCTCAGGGTGTTG-3') and PpPOR1-R (5'-CCCATCAGCATATTAGCCAAGAGGA-3'); for *PpPOR2*, PpPOR2-F (5'-GCCAGCGTACAATCATCAGCA-3') and PpPOR2-R (5'-TGAGGACAGATCACAGTGCATCA-3'); for *PprbcS1*, PprbcS1-F (5'-TTGGCTGCATTGCCCTTGCGAT-3') and PprbcS1-R (5'-ATCAAAGCTACTGCTACCCGACC-3'); for *chlB*, PpchlB-F (5'-AGTAATTCCTGAAGGAGGCTCTGT-3') and PpchlB-R (5'-CGAGTTATTGAAGCTGCGTGAGT-3'); for *rbcL* (AB066207), PprbcL-F (5'-TACCCATTAGATTTATTTGAAGAAGGTTC-3') and PprbcL-R (5'-CGTTCCCCTTCAAGTTTACCTACTACAGT-3'); and for *psbA*, PppsbA-F (5'-CTTGCTACATGGGTCGTGAGTG-3') and PppsbA-R (5'-TGCTGATACCTAATGCAGTGAACC-3').

2-4. Results

Two developmentally different types of rhizoid

Two distinct developmental stages are observed in the haploid generation of Physcomitrella: the protonema, which is a filamentous network of the chloronemata (Fig. 1A) and caulonemata (Fig. 1B); and the gametophore (Fig. 1C), which is a leafy shoot (Reski, 1998). The gametophore is derived from a side-branch initial cell, which arises from a sub-apical cell of the caulonema. The gametophore leaves are divided into juvenile and adult leaves according to the absence and presence of a midrib, respectively (Fig. 8E,F). Adult leaves start to appear after several juvenile leaves have formed. A gametophore with only juvenile leaves is designated as a juvenile gametophore, and a gametophore with mature adult leaves is termed an adult gametophore.

Rhizoids are brown-pigmented filaments that differentiate from epidermal cells of a gametophore stem. The first rhizoid formed at the base of a gametophore, below the first juvenile leaf (Fig. 8A). Subsequent rhizoids differentiated from the gametophore stem epidermal cells below the subsequent juvenile leaves (Fig. 8B,M). I use the term 'basal rhizoid' to describe a rhizoid that was accompanied by a juvenile leaf. The basal rhizoids differentiated from stem epidermal cells below the juvenile leaves. Other spatial distribution patterns were not observed.

A rhizoid also formed below the adult leaf, and was named the 'mid-stem rhizoid'. The two types of rhizoids were distinguishable by position but not by morphology. While the basal rhizoids were formed concomitant with the growth of juvenile leaves, the mid-stem rhizoids differentiated with a stereotypic spatial pattern once the growth of the corresponding adult leaf ceased. When a gametophore grew with approximately 8 adult leaves that were longer than 300 μm, the first mid-stem rhizoid started to differentiate on the gametophore stem, below the first adult leaf and above the uppermost juvenile leaf (Fig. 8C,D). Scanning electron microscopy showed that mid-stem rhizoids differentiated from stem epidermal cells of the same longitudinal cell files as abaxial epidermal cells of a midrib (Fig. 8D). The positions of the rhizoid cells in relation to leaf traces were examined by serial sectioning. The midrib contained abaxial and adaxial epidermal cells, hydroids with thin cell walls, stereids, which are small cells with thick cell walls, and conducting parenchymal elements (deuters), which contain fewer chloroplasts and have thick cell walls (Wiencke and Schulz, 1983; Fig. 8I,J). Adult leaves merged with stems, and parts of the hydroids and stereids in the midrib

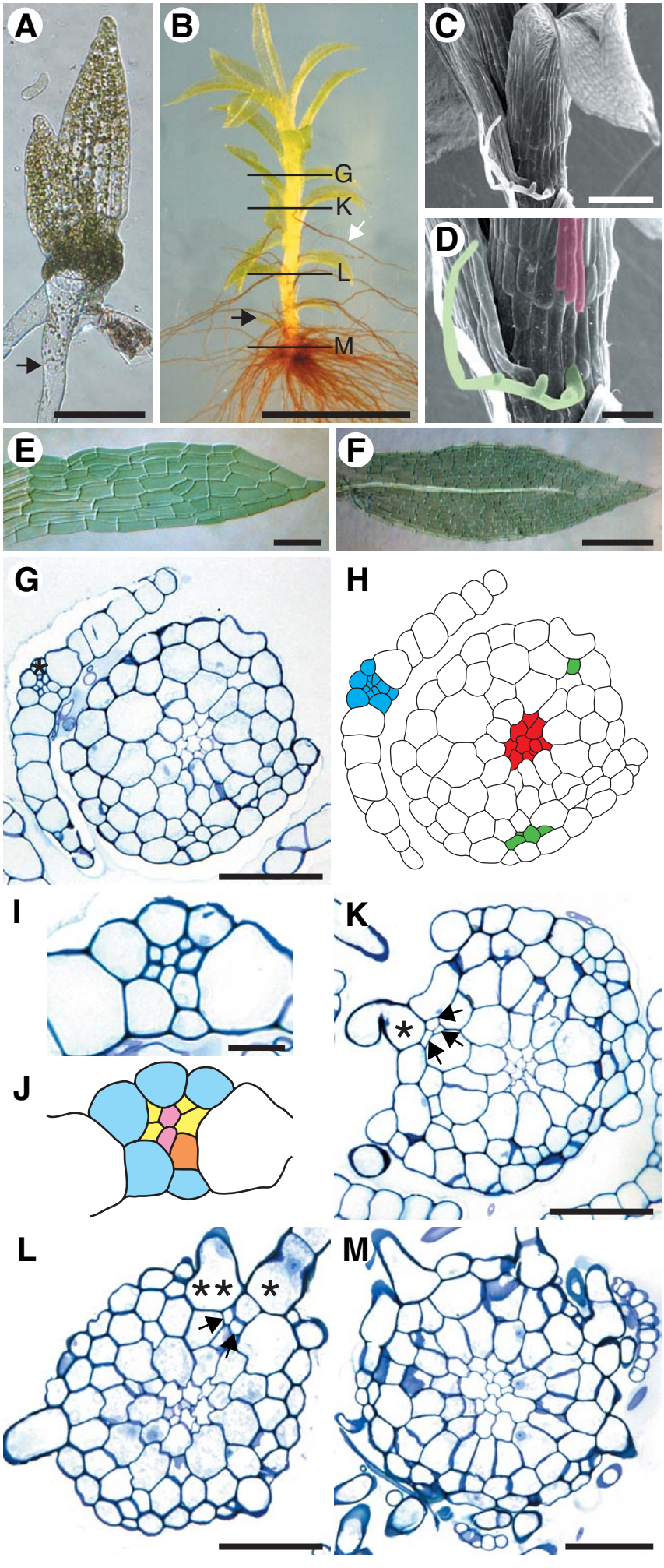
A
B
G
K
L
M
C
D
E
F
G
H
I
J
K
L
M

Figure 8. Rhizoid differentiation in the wild type.
(A) A juvenile gametophore with juvenile leaves. The arrow indicates the first rhizoid. (B) An adult gametophore with 17 leaves. Lines G, K, L, and M indicate the positions of the transverse sections shown in (G), (K), (L), and (M), respectively. The white and black arrows indicate the uppermost mid-stem rhizoid and the uppermost juvenile leaf, respectively. (C) A scanning electron micrograph showing a mid-stem rhizoid formed below an adult leaf. (D) A higher magnification of (C). The midrib cells and a mid-stem rhizoid are colored pink and green, respectively. (E) A juvenile leaf. (F) An adult leaf. (G,K-M) Transverse sections of a gametophore with 18 leaves in various positions relative to the gametophore axis. The positions of the sections are indicated in (B). (G) Above the uppermost mid-stem rhizoid. (K) At the uppermost mid-stem rhizoid. (L) At mid-stem rhizoids adjacent to a leaf trace, below the uppermost mid-stem rhizoid. (M) At the gametophore base where basal rhizoids formed. The asterisk in (G) indicates the abaxial epidermal cell of a midrib in the same longitudinal cell file as the uppermost mid-stem rhizoid. The asterisk in (K) indicates the uppermost mid-stem rhizoid. The single and double asterisks in (L) indicate the first rhizoid and the second rhizoid, respectively, which are differentiated at the same position. The arrows in (K) and (L) indicate leaf trace cells. (H) A line drawing of (G). Hydroids in the center of the stem, leaf traces, and a midrib are colored red, green, and blue, respectively. (I) A higher magnification of the transverse section of the midrib shown in (G). (J) A line drawing of (I). Epidermal cells, stereids, hydroids, and deuters are colored light blue, yellow, pink, and orange, respectively. Bar in (A) = 50 μm; bar in (B) = 1 mm; bars in (C) and (F) = 250 μm; bars in (D), (E), (G), (K), (L), and (M) = 100 μm; bar in (I) = 20 μm.

were connected to leaf traces in the stem. The leaf traces were not connected to hydroid cells in the centers of the stems (Fig. 8G,H). The mid-stem rhizoid differentiated from a stem epidermal cell that lay adjacent to a leaf trace (Fig. 8K). Serial sectioning also confirmed that the rhizoid-forming cell was located in the same cell file as the abaxial epidermal cell of a midrib (Fig. 8G,K). Following mid-stem rhizoid differentiation, the next rhizoid differentiated from an adjacent epidermal cell (Fig. 8L).

The first step in rhizoid differentiation was the protrusion of an epidermal cell from the gametophore stem. The protrusion elongated by tip growth, and divided into a rhizoid apical cell and a rhizoid subapical cell, which were separated by an oblique septum (Fig. 9A). Rhizoids continued to elongate with the division of apical cells, so that a filamentous rhizoid with several cells was formed. The third cell from the apical cell began to attain a brown pigmentation, which became more extensive (Fig. 9B-D). Compared to protonemal cells, the development of chloroplasts was poor, even in mature rhizoid cells, although some chloroplasts could be identified by fluorescence microscopy (Fig. 9D).

Effect of exogenous auxin on rhizoid differentiation

Ashton et al. (1979) mentioned an increase in the number of rhizoids following treatment with exogenous auxin. In this study, I observed spatial patterns of increased rhizoids. When adult gametophores with 12-16 leaves were cultured in 0, 0.1, 1, or 10-µM NAA for 1 week, the numbers of mid-stem rhizoids per gametophore increased relative to increases in NAA concentration (Table 8; Fig. 10A,B). With exogenous auxin, the uppermost rhizoids formed in the more apical part of gametophores, and the number of leaves above the uppermost mid-stem rhizoid decreased (Table 8). The additional rhizoids differentiated from stem epidermal cells in the cell files of the midrib cells, as was the case with non-treated gametophores (Fig. 10B). Adventitious gametophores were formed from gametophore stems, and several rhizoids were observed on the adventitious gametophore (Fig. 10A).

The long-term effects of NAA treatment were also examined. Gametophores with leaves formed on the 0.1-µM NAA medium (Fig. 10C) as on NAA-free medium. However, leafless gametophores with numerous rhizoids formed on medium that contained either 1 or 10 µM NAA (Fig. 10D,E). The leafless gametophores grown on 10-µM NAA were taller than those grown on 1-µM NAA medium (Fig. 10D,E). The total number of rhizoids per

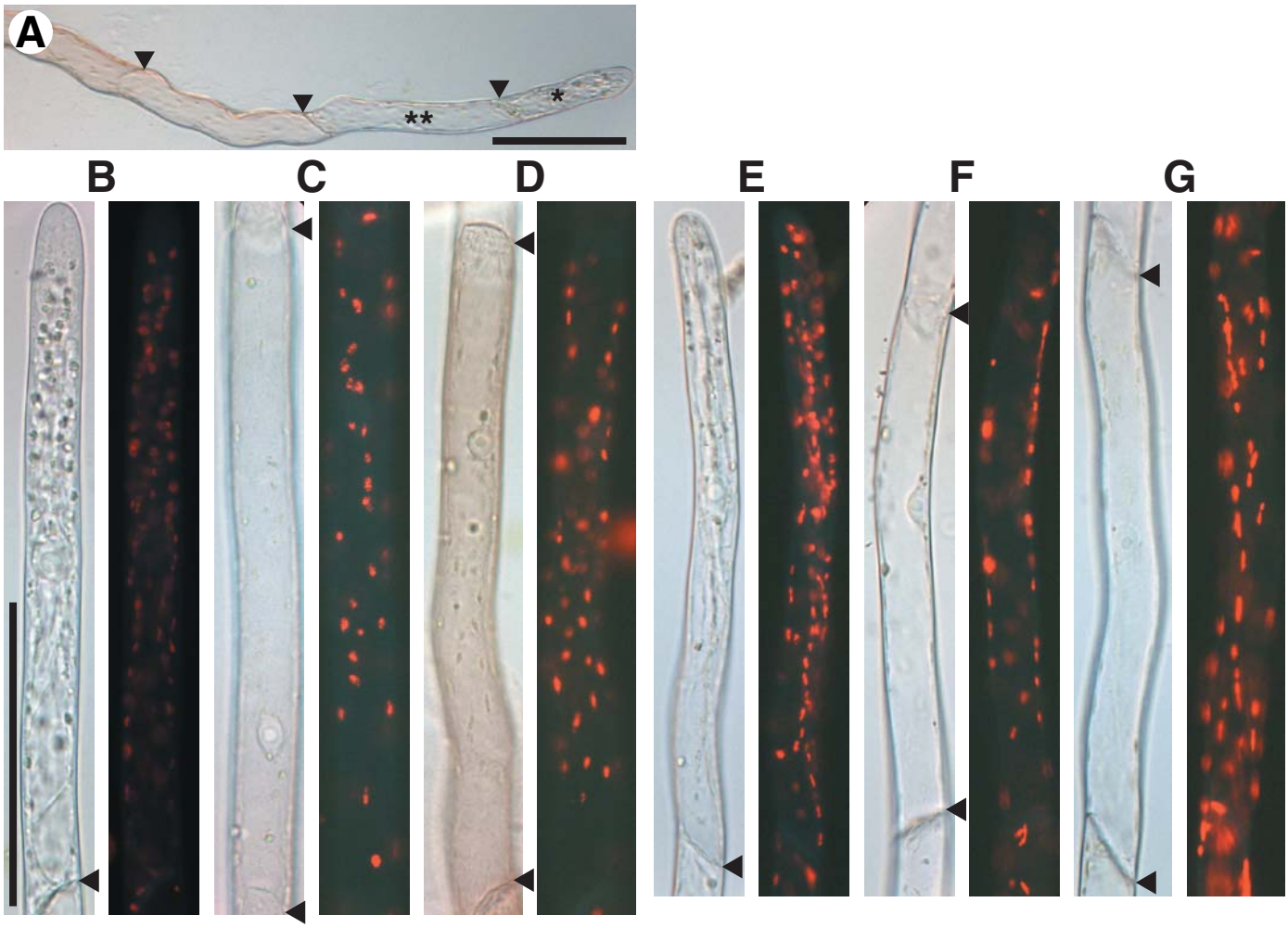

Figure 9. Rhizoid cells of the wild type and the *Pphb7* disruptant.
(A) A wild-type rhizoid composed of 4 cells, viewed with Nomarski optics. The arrowheads indicate septa between the cells. The single and double asterisks indicate rhizoid apical and rhizoid subapical cells, respectively. (B-D) A wild-type rhizoid composed of 8 cells. The apical cell (B), third cell (C), and fifth cell (D) viewed with Nomarski optics (left), and images under UV excitation (right). (E-G) A Pphb7dis-3 rhizoid composed of 8 cells. The apical cell (E), third cell (F), and fifth cell (G) viewed with Nomarski optics (right), and the corresponding fluorescence images under UV excitation (left). The black arrowheads indicate the septa. Bar in (A) = 100 μm; bar in (B) = 50 μm for (B-G).

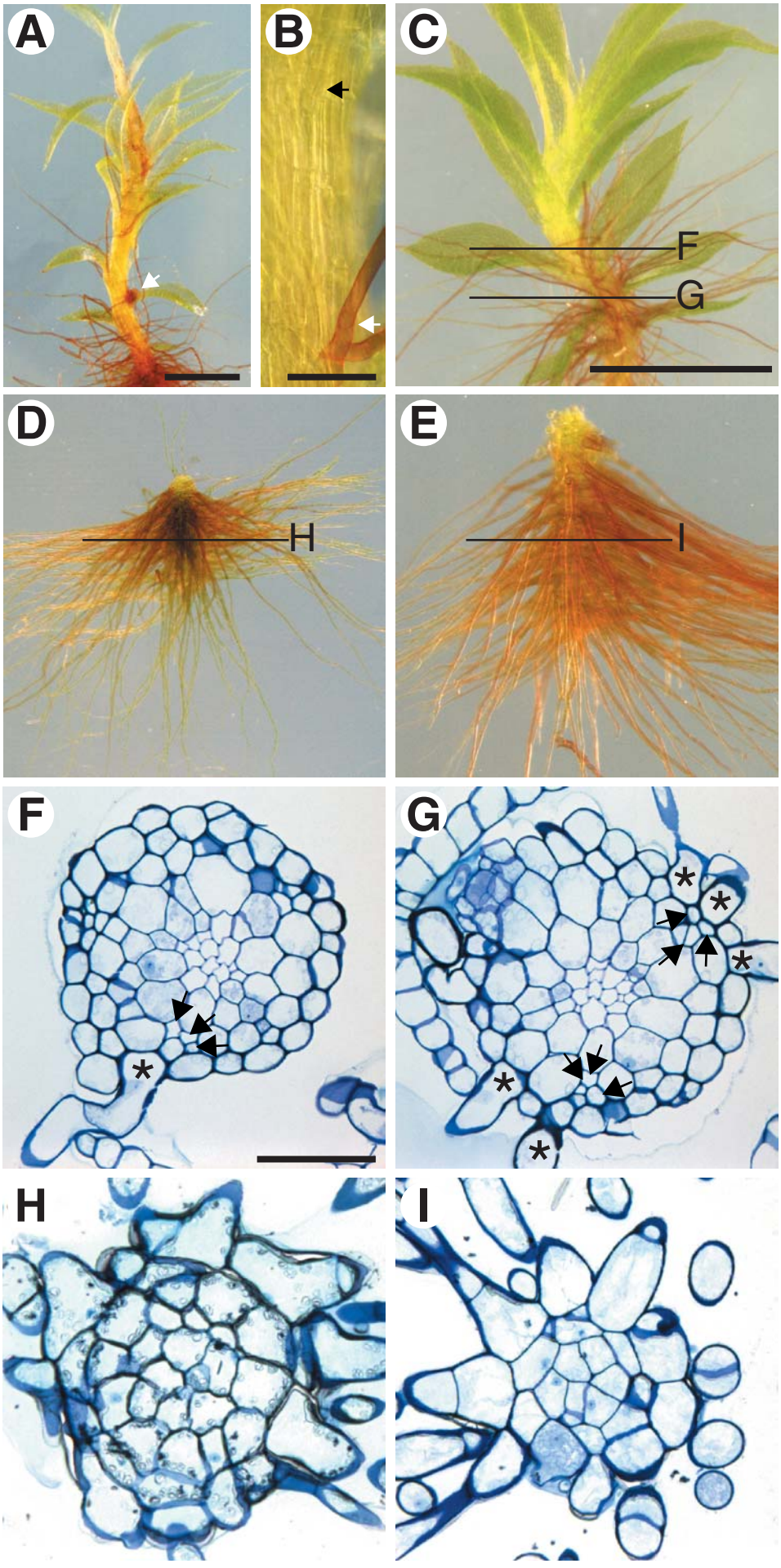
A
B
C
F
G
D
H
E
I
F
G
H
I

Figure 10. The effects of exogenous auxin on the differentiation of wild-type rhizoids. (A) A gametophore that was cultured in 1-μM NAA for 1 week. The white arrow indicates an adventitious gametophore. (B) The uppermost mid-stem rhizoid of the gametophore in (A). The black and white arrows indicate a midrib and the uppermost mid-stem rhizoid in the same cell file as a midrib, respectively. (C-E) Gametophores that were grown in the presence of 0.1- (C), 1- (D), and 10-μM (E) NAA for 6 weeks. Lines F, G, H, and I indicate the positions of the transverse sections shown in (F), (G), (H), and (I), respectively. (F,G) Transverse sections of a gametophore that was cultured in the presence of 0.1-μM NAA medium at the position of the uppermost mid-stem rhizoid (F), and at the position of the mid-stem rhizoids close to a leaf trace that lay below the uppermost mid-stem rhizoid (G). The asterisks and arrows indicate rhizoids and cells of the leaf traces, respectively. (H,I) Transverse sections of leafless gametophores that were cultured on medium that contained 1 (H) and 10 μM (I) NAA, respectively. Bars in (A) and (C) = 1 mm for (A) and (C-E); bars in (B) and (F) = 100 μm for (B) and (F-I).

Table 8. The number of rhizoids per gametophore in wild-type and the *Pphb7* disruptants following treatment with NAA for 1 week.

		Medium			
		0 µM NAA	0.1 µM NAA	1 µM NAA	10 µM NAA
Wild-type	Mid-stem rhizoids	14.0±8.2 (n = 10)	26.4±9.2 [a] (n = 10)	41.0±15.6 [a] (n = 10)	52.0±28.0 [a] (n = 10)
	Basal rhizoids	40.4±6.2 (n = 10)	38.7±13.3 (n = 10)	40.5±18.3 (n = 10)	36.8±21.0 (n = 10)
	Leaves[*]	8.2±2.5 (n = 10)	5.3±1.3 [a] (n = 10)	2.0±3.3 [a] (n = 10)	1.9±0.7 [a] (n = 10)
Pphb7dis-2	Mid-stem rhizoids	16.1±9.1 (n = 10)	28.4±10.8 [a] (n = 10)	41.2±9.0 [a] (n = 10)	52.4± 15.7 [a] (n = 10)
	Basal rhizoids	40.0±10.6 (n = 10)	37.4±7.1 (n = 10)	39.5±12.7 (n = 10)	35.1± 12.9 (n = 10)
	Leaves[*]	8.3±2.3 (n = 10)	5.7±1.4 [a] (n = 10)	3.3±1.7 [a] (n = 10)	1.5± 0.5 [a] (n = 10)
Pphb7dis-3	Mid-stem rhizoids	17.9±9.8 (n = 10)	26.6±10.3 [a] (n = 10)	43.1±19.3 [a] (n = 10)	53.3± 25.5 [a] (n = 10)
	Basal rhizoids	38.1±5.2 (n = 10)	35.1±6.3 (n = 10)	37.4±18.3 (n = 10)	36.8± 12.9 (n = 10)
	Leaves[*]	7.5±2.4 (n = 10)	5.8±1.5 [a] (n = 10)	3.0±3.1 [a] (n = 10)	1.6± 1.2 [a] (n = 10)

Gametophores were grown on the standard medium for 6 weeks, and then cultured for 1 week in water that contained 0, 0.1, 1, or 10 µM NAA. The means and standard deviations for the numbers of rhizoids are indicated. n, total number of gametophores examined; [*] number of adult leaves above the uppermost mid-stem rhizoid that measured more than 300 µm in length. [a] The values are significantly different by the Student's *t*-test ($P<0.05$) from those obtained following treatment with 0 µM NAA.

gametophore was increased by exogenous auxin in a dose-dependent manner (Table 9). The numbers of both mid-stem and basal rhizoids increased in gametophores that were grown on 0.1-µM NAA compared to gametophores that were grown on NAA-free medium (Table 9), although the rhizoids of leafless gametophores could not be classified into mid-stem and basal rhizoids. The additional, NAA-induced mid-stem rhizoids differentiated from epidermal cells that were located close to a leaf trace (Fig. 10F,G), as was the case when no exogenous auxin was added (Fig. 8K).

Regular gametophore stems consisted of epidermal cells, parenchyma cells, and hydroids, which had thin cell walls (Fig. 8G,H). These cells differentiated in the leafy gametophores grown on 0.1-µM NAA (Fig. 10F,G). On the other hand, the leafless gametophores grown on 1- and 10-µM NAA lacked central strands, and almost all of the epidermal cells differentiated into rhizoids (Fig. 10H,I).

Pphb7 is expressed in rhizoid cells

Several HD-Zip genes have been reported to be involved in cell differentiation in certain parts of the plant body (Rerie et al., 1994; Aoyama et al., 1995; Di Cristina et al., 1996; Zhong and Ye, 1999; Baima et al., 2001; McConnell et al., 2001). I isolated partial cDNA clones of ten HD-Zip genes of Physcomitrella as reported in Chapter 1. During preliminary expression analysis of these genes, I found that *Pphb7* was expressed in rhizoids. The *Pphb7* cDNA and corresponding genomic DNA were isolated and sequenced. The *Pphb7* gene consisted of three exons and two introns, and had two cDNA variants with different splice-acceptor sites in the first intron, which produced four amino acid differences (Fig. 7A; AB084623). *Pphb7* contained a homeodomain (McGinnis et al., 1984) and a leucine zipper motif (Landschulz et al., 1988), which was located adjacent to the C-terminus of the homeodomain.

RNA gel blot analysis of *Pphb7* was performed using poly $(A)^+$ RNA from protonemata and from gametophores with rhizoids. A cDNA fragment (cPphb7; Fig. 7A) that lacked the conservative HD-Zip motif was used as a probe to avoid cross-hybridization. The expression of *Pphb7* mRNA was detected in gametophores that contained rhizoids, but not in protonemata (Fig. 6). The mRNA was approximately 1.7 kb long, which was consistent with the size of the cloned cDNA.

Table 9. The number of rhizoids per gametophore in wild-type and the *Pphb7* disruptants following growth for 6 weeks in media that contained various concentrations of NAA.

		Medium			
		0 µM NAA	0.1 µM NAA	1 µM NAA	10 µM NAA
Wild-type	Mid-stem rhizoids	5.0±2.0 (n = 10)	16.2±3.4 [a] (n = 10)	n.d.	n.d.
	Basal rhizoids	37.1±8.5 (n = 10)	62.5±13.0 [a] (n = 10)	n.d.	n.d.
	Total number of rhizoids	42.1±8.6 (n = 10)	78.7±13.0 [a] (n = 10)	89.3±19.4 [a] (n = 10)	113.3±19.3 [a] (n = 10)
Pphb7dis-2	Mid-stem rhizoids	5.3±2.0 (n = 10)	16.9±2.3 [a] (n = 10)	n.d.	n.d.
	Basal rhizoids	36.3±7.2 (n = 10)	62.6±13.0 [a] (n = 10)	n.d.	n.d.
	Total number of rhizoids	41.6±8.1 (n = 10)	79.5±13.2 [a] (n = 10)	88.1±24.0 [a] (n = 10)	110.9±21.3 [a] (n = 10)
Pphb7dis-3	Mid-stem rhizoids	5.6±1.9 (n = 10)	16.5±3.1 [a] (n = 10)	n.d.	n.d.
	Basal rhizoids	34.7±11.9 (n = 10)	66.8±10.9 [a] (n = 10)	n.d.	n.d.
	Total number of rhizoids	40.3±12.6 (n = 10)	83.3±12.1 [a] (n = 10)	89.1±24.8 [a] (n = 10)	108.1±20.7 [a] (n = 10)

Protonemata were cultured for 6 weeks on standard medium that was supplemented with 0, 0.1, 1, or 10 µM NAA. The means and standard deviations for rhizoid numbers are indicated. n, total number of gametophores examined; n.d., no leafy gametophores were differentiated. [a] The values are significantly different ($P<0.001$) from those obtained following treatment with 0 µM NAA.

In order to characterize the detailed expression pattern of *Pphb7*, the coding sequence of β-glucuronidase (GUS; Jefferson et al., 1987) was inserted in-frame just before the stop codon of *Pphb7* by homologous recombination (Fig. 7B), so that the GUS activity of the Pphb7-GUS fusion protein could be detected histochemically. Physcomitrella protoplasts were transformed using the PEG method (Schaefer et al., 1991; Nishiyama et al., 2000). Stable transformants (17 and 18 in two separate experiments) were obtained, two of which had the fusion targeted to the *Pphb7* locus, as judged by PCR analysis. The insertion was confirmed by DNA gel blot analysis (Fig. 7E). Genomic DNA was isolated from the wild type and from the two transformed lines, and used for DNA gel blot analysis with the gPphb7 probe (Fig. 7A,E). The blot showed that one line (Pphb7-GUS-1) contained a single copy of the fusion inserted in the *Pphb7* locus (Fig. 7B,E). The *Pphb7*-coding region in Pphb7-GUS-1 was sequenced to confirm that there were no mutations in the region and that integration had occurred *via* homologous recombination. The second transformant contained multiple copies of the fusion construct, because extra bands were detected in the DNA gel blot and the signal intensity for this line was much higher than that for the wild type or Pphb7-GUS-1 (Fig. 7E). Since the GUS activity patterns of the two Pphb7-GUS lines were not distinguishable, the results for Pphb7-GUS-1 are shown (Fig. 11).

Initially, GUS activity was detected in the epidermal cells at the base of the juvenile gametophore (Fig. 11B). No signal was detected in juvenile gametophores before the differentiation of the first rhizoid (Fig. 11A). GUS activity was detected in the base of the adult gametophore, which corresponds to the rhizoid initial cells (Fig. 11E). In the case of mid-stem rhizoids, one cell below the leaf midrib showed a stronger GUS signal than the surrounding cells (Fig. 11C). Cells with protrusions also showed GUS signals (Fig. 11D). Given the coincidence of cells in which rhizoids were formed and in which GUS activity was observed, GUS-positive cells that lacked protrusions could be considered rhizoid initial cells. The initial cell of a basal rhizoid was round and displayed whole-cell staining (Fig. 11B), while the mid-stem rhizoid initial cell was slender and was stained only in its basal half (Fig. 11C). GUS signals were detected in several rhizoid cells that were close to the rhizoid apical cell (Fig. 11G), while the signals were weaker in rhizoid cells that were mature and contained brown pigment (Fig. 11E). Although the chloronemata and caulonemata are filamentous tissues like the rhizoids, no signal was detected in either of these tissues (Fig. 11 H,I).

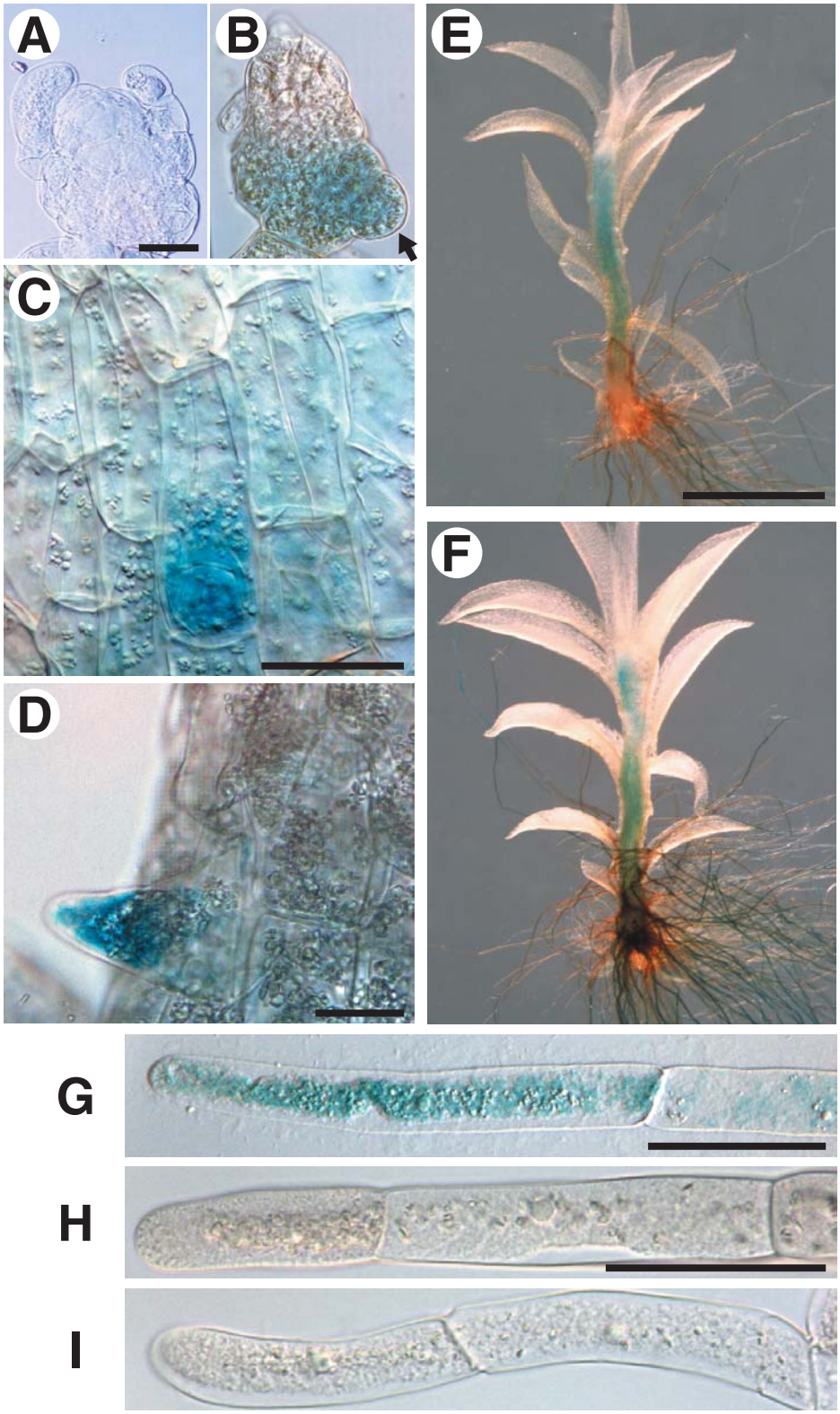

Figure 11. Histochemical detection of GUS activity in the Pphb7-GUS-1 line.
(A) A juvenile gametophore without a rhizoid. (B) A juvenile gametophore with a basal rhizoid protrusion (arrow). (C) Epidermal cells of an adult gametophore stem. (D) A rhizoid initial cell with protrusion of a mid-stem rhizoid. (E) A gametophore cultured for 6 weeks on G medium. (F) Gametophores cultured in 10-μM NAA solution for 6 hours. (G) The apical (left) and subapical (right) cells of a rhizoid with 8 cells. (H,I) Apical parts of a chloronema (H) and a caulonema (I). Bars in (A), (C), and (H) = 50 μm for (A,B), (C), and (H,I); bar in (D) = 25 μm; bar in (E) = 1 mm for (E,F); bar in (G) = 100 μm.

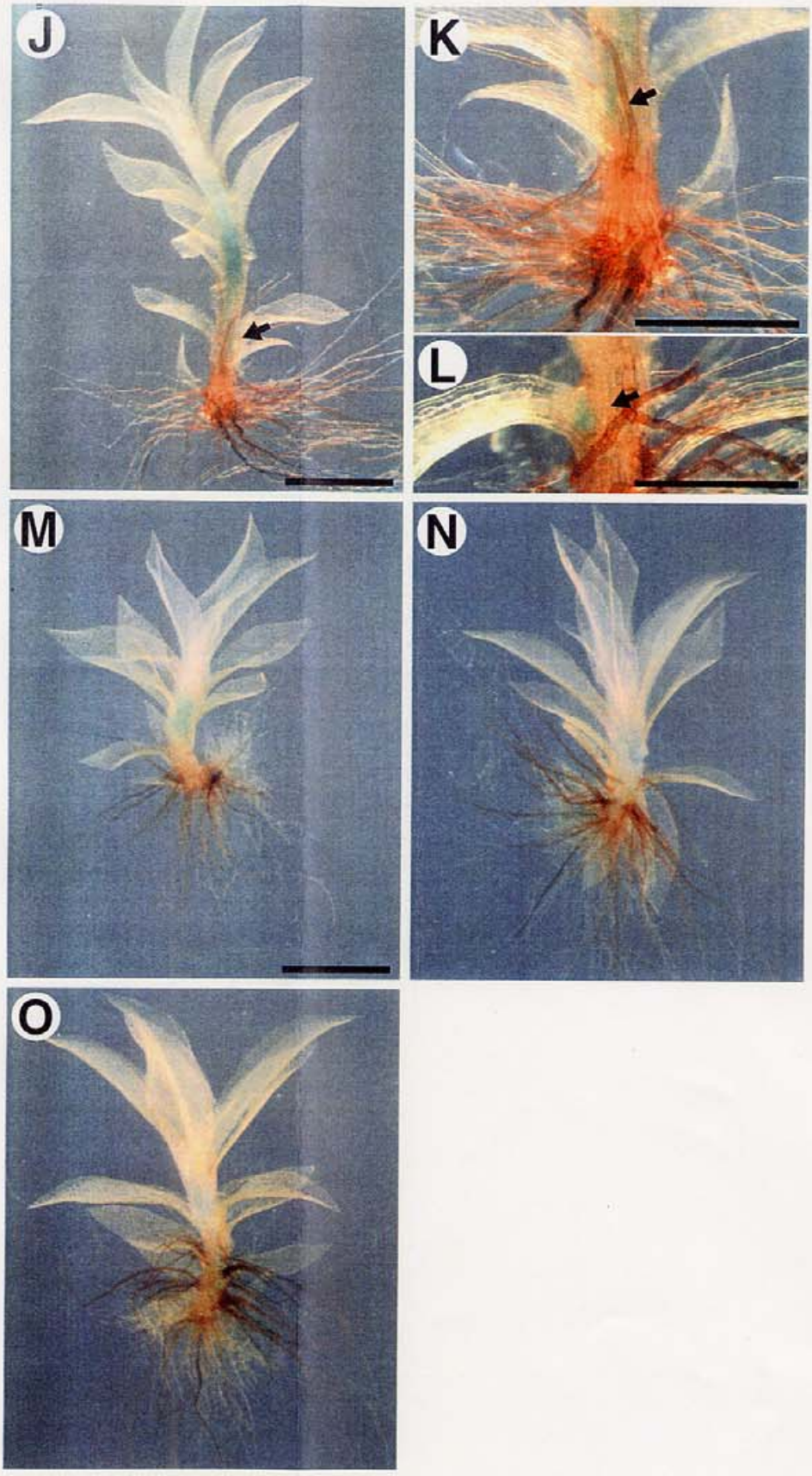

(J-L) Gametophores cultured in 10-μM BA solution for 24 (J), 48 (K), and 72 (L) hours. Arrows indicate adventitious buds. (M-P) Gametophores cultured in 10-μM GA (M), ABA (N), and ACC (O) solution for 24 hours. Bars in (J) and (M) = 1 mm for (J) and (M-O); bars in (K) and (L) = 500 μm for (K) and (L).

Subcellular localization of the Pphb7 protein

The Pphb7-GUS fusion protein was detected in the rhizoid cells. The subcellular localization of the protein was not readily detected in the histochemical GUS staining of Pphb7-GUS lines, because the subcellular membranes were broken during staining with the detergent. To detect the subcellular localization of Pphb7, the GFP-Pphb7 fragment, in which the coding sequence of sGFP (Chiu et al., 1996) was inserted in-frame just before the start codon of *Pphb7*, was introduced into Physcomitrella. Five separate transformation experiments with the GFP-Pphb7 fragment resulted in the isolation of 94 stable transformants (1, 24, 11, 26, and 32 lines, respectively). Ten of these lines contained the GFP fusion integrated into the *Pphb7* locus, as detected by PCR. DNA gel blot analysis of the wild type and of 10 GFP-Pphb7 lines showed that one line (GFP-Pphb7-1) contained a single copy of the insertion in the *Pphb7* locus, while all the other lines contained multiple copies of the inserted fusion construct (Fig. 7C,F). The *Pphb7*-coding region in GFP-Pphb7-1 was sequenced to confirm that it lacked any mutation, and the subcellular localization of the GFP-Pphb7-1 fusion protein was observed. The intercellular localization of GFP-Pphb7-2 and -3 was not distinguishable from that of GFP-Pphb7-1 (data not shown).

GFP signals in the initial cells of each basal and stem rhizoid were not clearly detected because of high background (data not shown). We could not confirm whether the difference of GUS signals between these two types of initial cells is significant. Once rhizoids protrude from the stem, the background becomes lower. Green fluorescence was detected in the nucleus and cytoplasm of rhizoid apical cells (Fig. 12A), but the nuclear signal was stronger than that of cytoplasm. The nuclear GFP signal was equally strong in the second cell (Fig. 12B), but weaker in subsequent cells (Fig. 12C,D). GFP fluorescence was detected in both the nucleus and cytoplasm of a rhizoid in which the intact GFP was expressed under the control of the GH3 promoter (Li et al., 1999; Fig. 12E-G). The wild-type rhizoid emitted very weak fluorescence under the conditions of observation (Fig. 12H-I).

Regulation of the level of *Pphb7* mRNA expression

Rhizoid formation was induced by exogenous auxin (Tables 8, 9). I examined whether the expression of *Pphb7* mRNA was induced by auxin using RNA gel blot analysis. Exogenous auxin increased the level of *Pphb7* mRNA expression in a dose-dependent manner

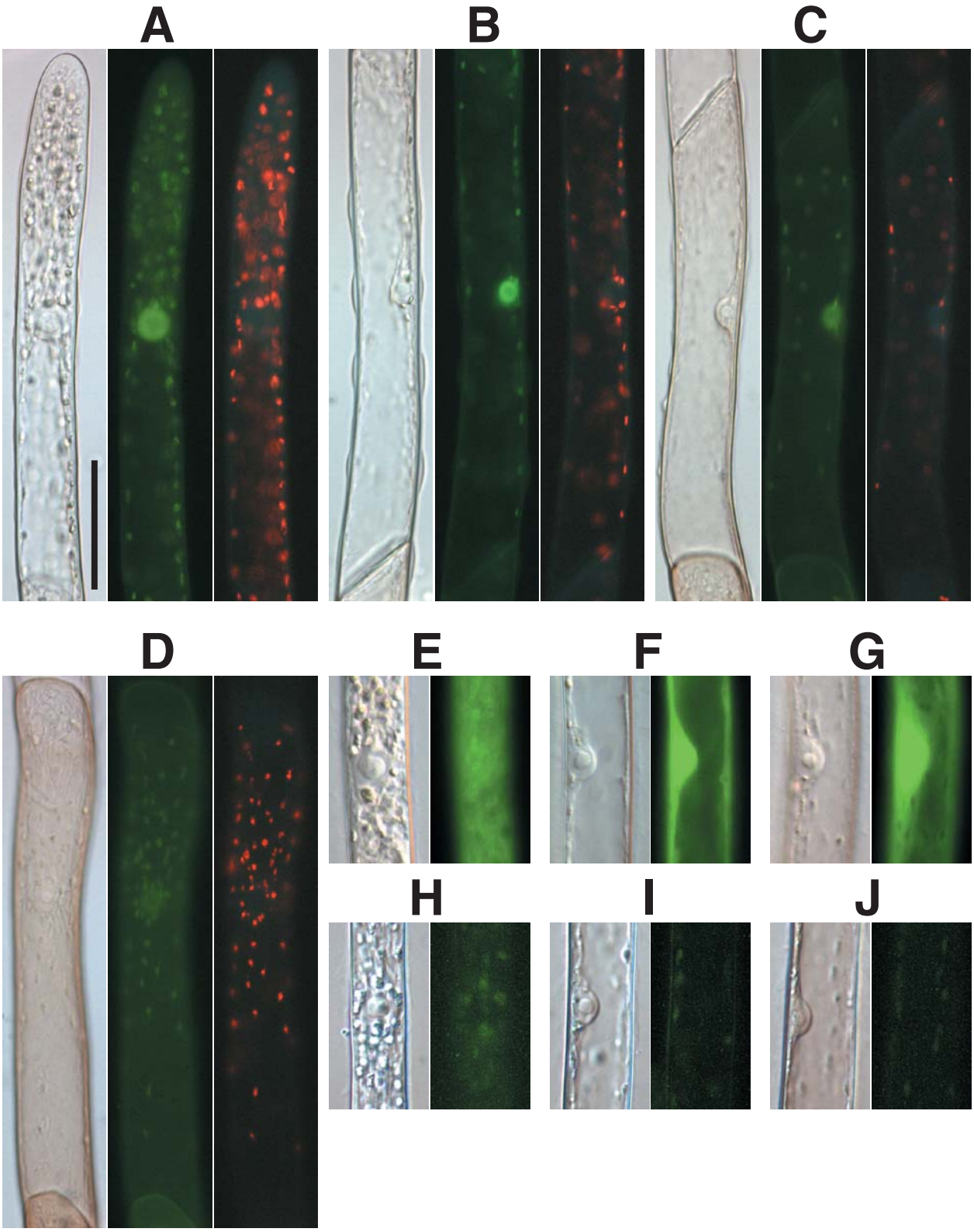

Figure 12. Subcellular localization of the GFP-Pphb7 fusion protein.
(A-D) A rhizoid from GFP-Pphb7-1. The apical (A), second (B), third (C), and fourth (D) cells were examined using Nomarski optics (left), by GFP fluorescence (middle), and by chlorophyll fluorescence (right). (E-J) A rhizoid that expressed an intact GFP under the control of the GH3 promoter (E-G) and a wild-type rhizoid (H-J). The apical (E,H), third (F,I), and fourth (G,J) cells were examined using Nomarski optics (left) and GFP fluorescence images (right). Bar = 50 μm for all panels.

within 1 hour (Fig. 13A). To examine the effect of exogenous auxin on the spatial expression patterns of Pphb7 protein, gametophores of the Pphb7-GUS-1 line were soaked in NAA solution. The GUS signals on gametophore stems were stronger closer to the apex (Fig. 11E,F), where exogenous auxin induced ectopic rhizoids (Fig. 10A). The GUS signals in rhizoids were stronger than in those without NAA treatment (Fig. 11E,F).

Exogenous plant hormones induce several HD-Zip I genes (Söderman et al., 1996; Lee and Chun, 1998; Söderman et al., 1999). I examined the effect of the plant hormones BA, GA, ABA, and the ethylene precursor ACC on the expression of *Pphb7* (Fig. 13B). Treatment with water without any plant hormone for 24 hours resulted in an increased level of *Pphb7* expression. The *Pphb7* expression levels increased more with BA treatment than with water. Although GA treatment increased the expression of *Pphb7*, the increase was less than that with water, indicating that GA represses the expression of *Pphb7*. ABA treatment decreased the expression of *Pphb7*. When treated with ACC, no signals of *Pphb7* or *GAPDH* were detected, probably because of the immediate senescence of gametophores just after incubation in ACC (Fig. 13B). To examine the spatial change in *Pphb7* expression with water, BA, GA, and ABA treatments, gametophores of the Pphb7-GUS-1 line were soaked in 1- or 10-µM solutions of BA, GA, and ABA, respectively. The spatial expression patterns after GA (Fig. 11M), and ABA (Fig. 11N) treatments were not distinguishable from the pattern with no treatment, although the GUS signals became weaker with the GA and ABA treatments than with the water treatment. By contrast, gametophores soaked in 10-µM BA formed adventitious buds within 24 hours, and the basal parts where rhizoids differentiate showed GUS activity (Fig. 11J-L). The expression patterns of Pphb7-GUS were unchanged, except for the additional signals in the buds.

As dehydration and osmotic stress induce the expression of several HD-Zip I genes (Söderman et al., 1996; Lee and Chun, 1998; Söderman et al., 1999), gametophores with rhizoids were left without water or were soaked in 6% mannitol (Fig. 13C). Dehydration induced *Pphb7* expression 1 and 6 hours after it was started, while 6% mannitol treatment did not induce *Pphb7* expression (Fig. 13C).

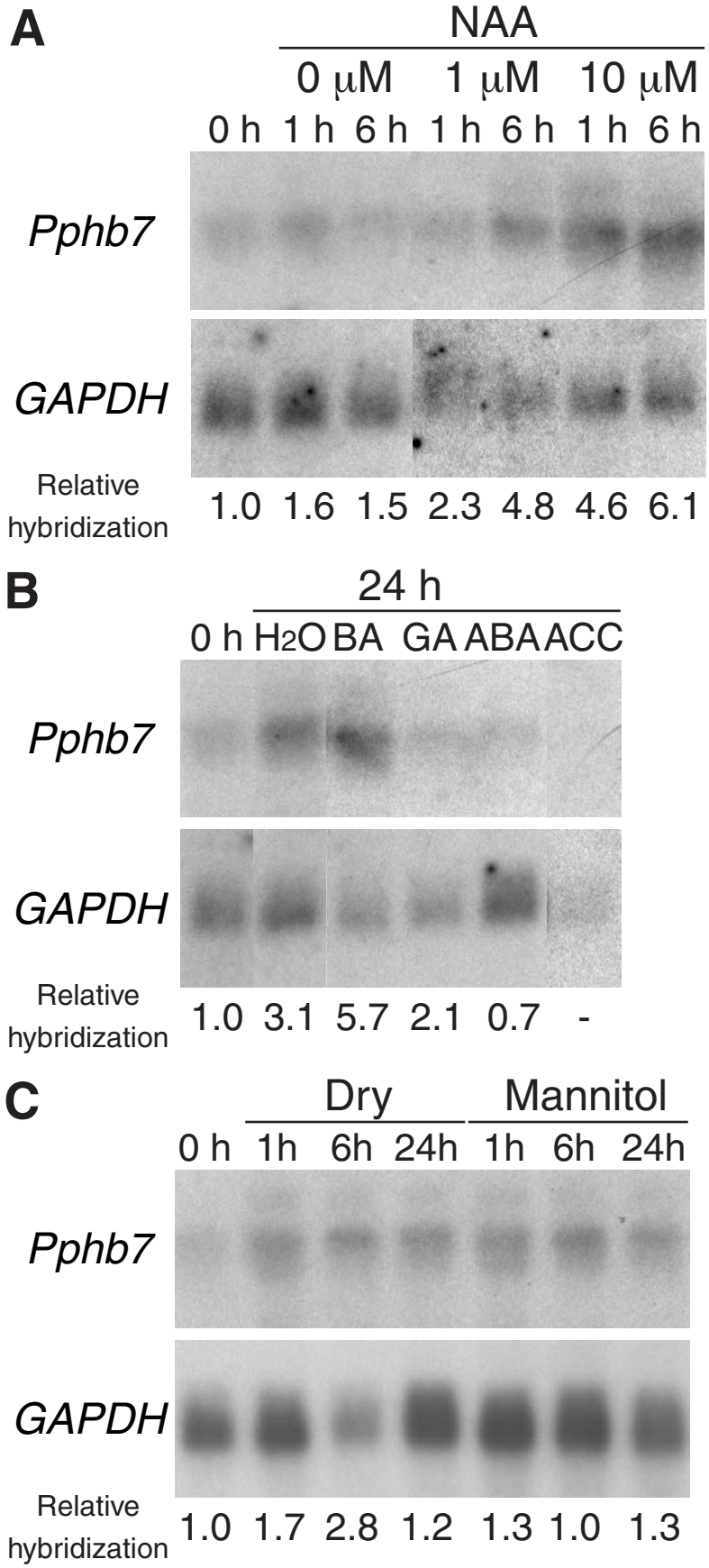

Figure 13. RNA gel blot analyses of *Pphb7*.
(A-C) Poly $(A)^+$ RNA of 1.0 μg from gametophores treated with exogenous NAA (A), other plant hormones (BA, GA, ABA, and ACC; B), and dehydration and osmotic stress (6% mannitol) (C). As an internal control, the DNA fragment encoding glyceraldehyde 3-phosphate dehydrogenase (*GAPDH*) was used as a probe (Leech et al., 1993). The relative expression levels are indicated below each panel.

***Pphb7* disruption alters rhizoid characterization**

Pphb7 encodes a homeodomain that is a putative DNA-binding motif (Laughon, 1991). Loss of the homeodomain is expected to cause a loss of DNA-binding activity and to result in aberrant *Pphb7* function. A 4.0-kb DNA fragment that contained the NPT II cassette was inserted upstream from the homeobox of *Pphb7*. When this DNA fragment was introduced into Physcomitrella, 107 independent stable transformants were obtained. Five of 20 randomly selected stable lines were found by PCR analysis to have a disrupted *Pphb7* locus. DNA gel blot analysis showed that two lines (Pphb7dis-2 and -3) contained a single insertion in the *Pphb7* locus, while the other lines contained multiple copies of the inserted sequence (Fig. 7D,G).

The wild-type rhizoids contained brown pigment, while those of both *Pphb7* disruptants were greener (Fig. 14A). Light transmittance in the red, green, and blue channels was estimated for rhizoid cells using CCD images. The mean light transmittance of Pphb7dis-2 (Fig. 15A) at the fifth cell stage was significantly higher than that of the wild type ($P<0.001$ by the Student's *t*-test), which indicates that rhizoids of the *Pphb7* disruptants were less pigmented than those of the wild type.

Since the rhizoids of the *Pphb7* disruptants were greener in appearance than the wild type (Fig. 14A), the number and size of chloroplasts in the rhizoid cells of wild type and *Pphb7* disruptants were compared. The numbers of chloroplasts per cell in the second, third, and fourth cells from the rhizoid apical cell were determined. The number of chloroplasts in the apical cell could not be determined reliably. The number of chloroplasts in the wild type was constant at around 30 through the second to fourth cell stages, while the numbers in the *Pphb7* disruptants increased, and the fourth cell of the *Pphb7* disruptants contained twice as many chloroplasts as the wild type (Fig. 15B).

The projected areas of the chloroplasts were measured to quantify chloroplast size in the rhizoid cells. The mean chloroplast size was significantly larger in the *Pphb7* disruptants than in the wild type ($P<0.01$), which indicates that *Pphb7*-disrupted rhizoids contain larger chloroplasts than the wild-type rhizoids (Fig. 15C).

In order to assess whether *Pphb7* disruption affected the size and shape of rhizoid cells, the width and length of the fifth cell from the rhizoid apical cell were measured. The width of the rhizoid cells from *Pphb7* disruptants (Pphb7dis-2, 22.1±4.9 μm; Pphb7dis-3,

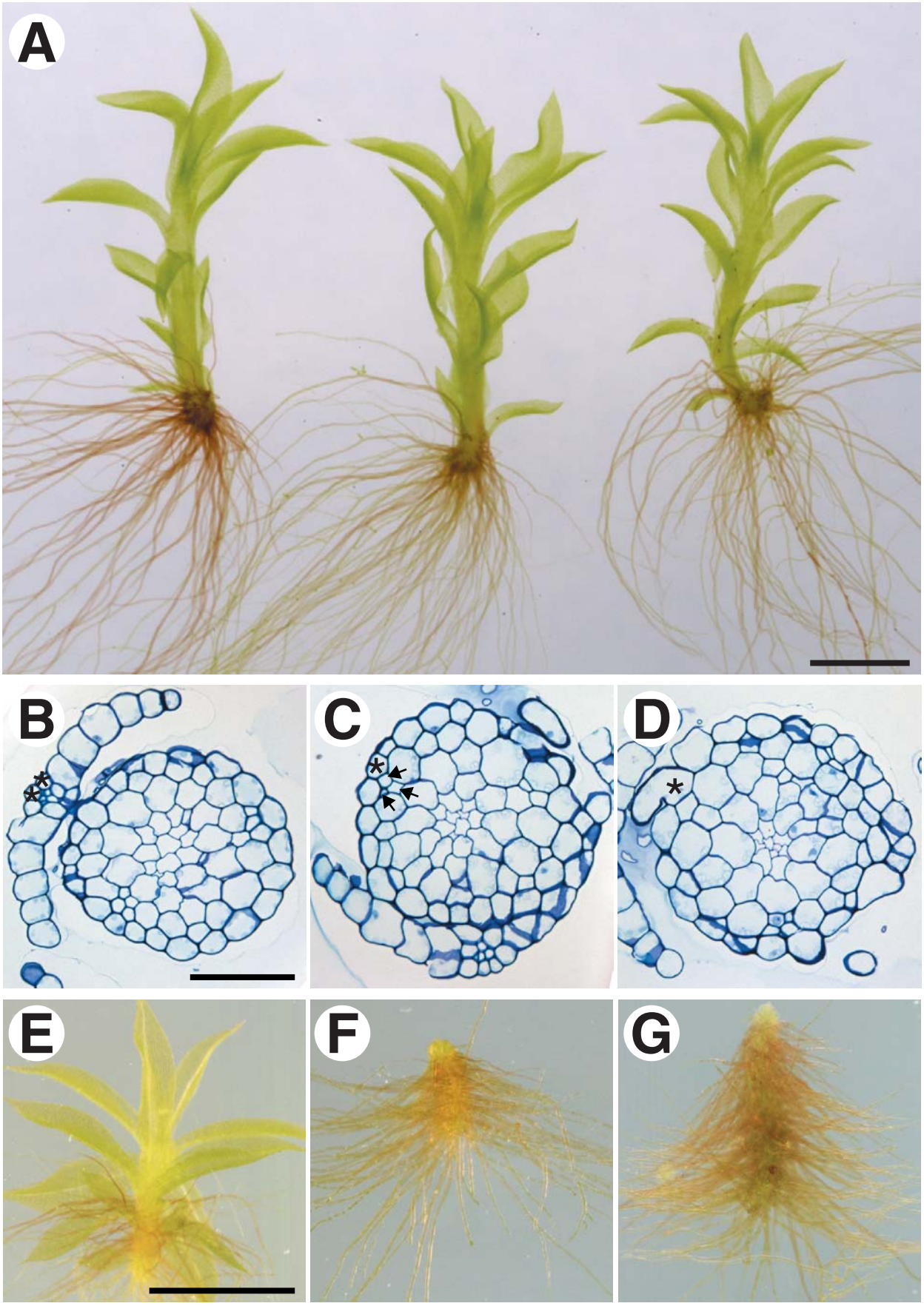
A
B
C
D
E
F
G

Figure 14. Gametophores with rhizoids from the wild type and from the *Pphb7* disruptants. (A) Six-week old gametophores with 12 leaves in the wild type (left), Pphb7dis-2 (middle), and Pphb7dis-3 (right). (B-D) Serial transverse sections of a gametophore with 18 leaves of the Pphb7dis-3 at a position on the leaf above the uppermost mid-stem rhizoid (B), at the position where the leaf merges to a stem (C), and at the position where the uppermost mid-stem rhizoid emerges (D). Asterisks indicate the uppermost mid-stem rhizoid cell (D). The abaxial leaf epidermal cells (B) and the stem epidermal cells (C) in the same longitudinal cell file as the uppermost mid-stem rhizoid. The arrows indicate cells of the leaf traces. (E-G) Gametophores of the Pphb7dis-3 that were grown for 6 weeks in the presence of 0.1- (E), 1- (F), and 10-μM (G) NAA. Bars in (A) and (E) = 1 mm for (A) and (E-G); bar in (B) = 100 μm for (B-D).

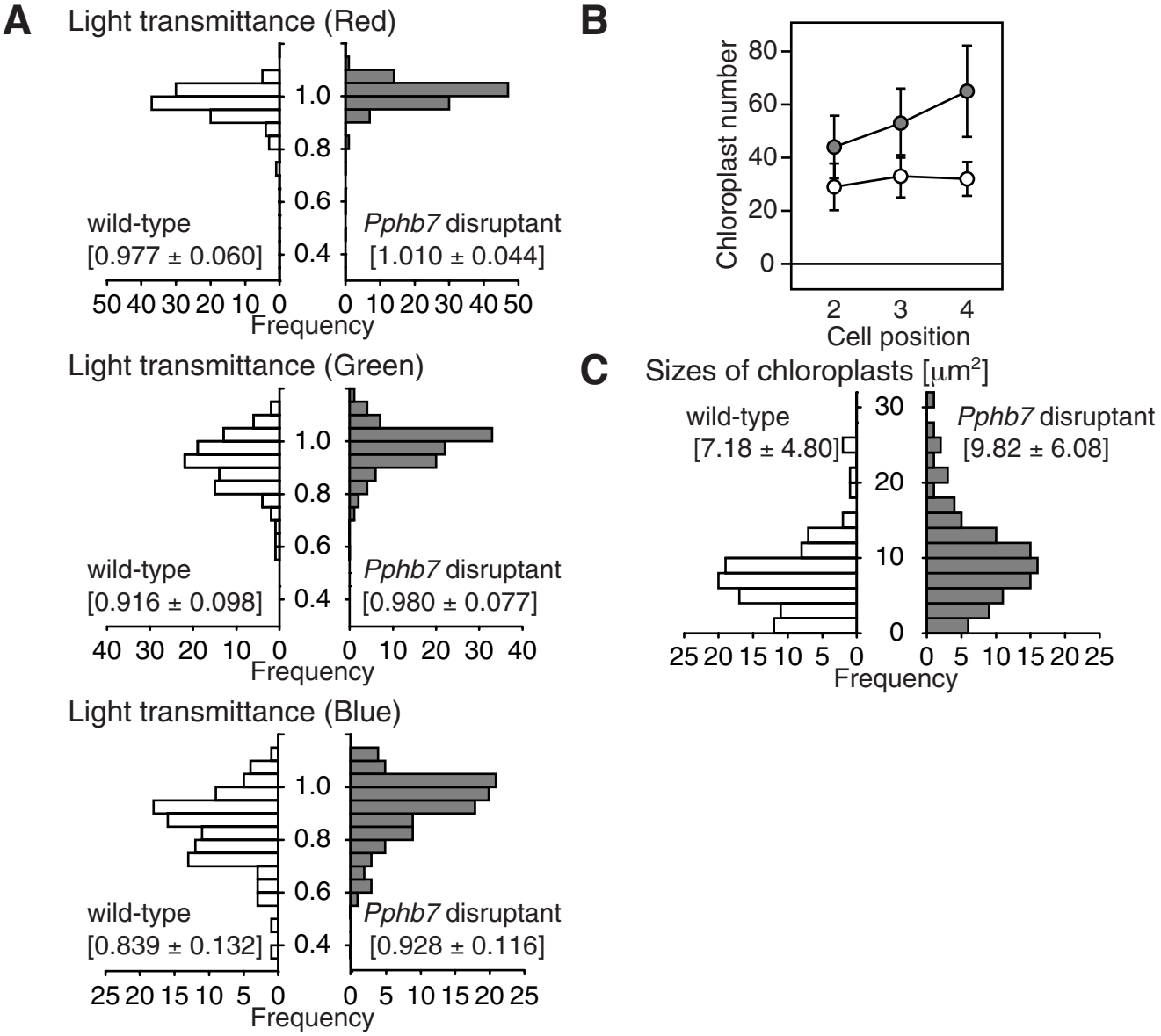

Figure 15. Comparison of the rhizoid characters of the wild type and of the *Pphb7* disruptant.

(A) Frequency distributions of the light transmittance of rhizoids in the wild type (left) and in the Pphb7dis-3 (right). The red, blue, and green channels from RGB images are shown. One hundred cells were quantified for each line. The means and standard deviations of light transmittance are indicated in brackets. (B) The number of chloroplasts per cell at each cell position from the rhizoid apical cell. The white and gray circles indicate the means of the wild type and Pphb7dis-3, respectively. Bars indicate the standard deviations. Ten rhizoids each from the wild type and from the *Pphb7* disruptant were examined. (C) Frequency distribution of chloroplast size in rhizoid cells from the wild type (left) and from the Pphb7dis-3 (right). The means and standard deviations of chloroplast size are indicated in the brackets. The images of the fifth cell from the rhizoid apical cell were taken with a CCD camera, and one randomly selected chloroplast was traced for each cell. Rhizoid cells (100 of each) from the wild type and from the *Pphb7* disruptant were examined.

19.8±3.7 μm, n = 50) was not significantly different from that of the wild type (22.2±5.1 μm; n = 50). The rhizoid cell from the *Pphb7* disruptants (Pphb7dis-2, 214.0±51.3 μm; Pphb7dis-3, 210.9±50.0, n = 50) was shorter than the wild-type rhizoid (222.1±53.4 μm; n = 50), although the differences were not statistically significant.

To compare the structure of chloroplasts between the wild type and *Pphb7* disruptants, nucleoids were observed by staining with SYBR Green I (Fig. 16A,B). The number and size of nucleoids of the wild type and of *Pphb7* disruptants were similar. The internal structure of chloroplasts was further observed with transmission electron microscopy. Well-developed thylakoid membranes with a grana structure were observed in both the wild type and *Pphb7* disruptants (Fig. 16C,D).

Pphb7 regulation of representative gene functions in chloroplasts

To further characterize the effects of *Pphb7* on chloroplasts, mRNA expression of the following genes involved in the photosynthesis was compared between wild-type and *Pphb7*-disruptant rhizoids by RT-PCR: a ribulose-1,5-bisphosphate carboxylase/oxygenase large subunit gene (*rbcL*) and a small subunit gene (*PprbcS1*) as Calvin cycle enzymes (reviewed in Hartman and Harpel, 1994), NADPH-protochlorophyllide oxidoreductase genes (*PpPOR1* and *2*) and light-independent protochlorophyllide reductase gene (*chlB*) as the key enzymes in chlorophyll biosynthesis (reviewed by Armstrong, 1998), and the *psbA* gene encoding D1 protein as a component of photosystem II (reviewed by Zhang and Aro, 2002). Levels of *rbcL* and *PprbcS1* expression were higher in disruptants than in the wild type, while levels of *PpPOR1, PpPOR2, chlB,* and *psbA* did not differ from those of the wild type (Fig. 17).

Disruption of *Pphb7* does not affect the number and position of rhizoids with or without exogenous auxin

Pphb7 functions in rhizoid characterization, and I examined whether *Pphb7* is also involved in rhizoid determination. The number and position of rhizoids in the wild type and in *Pphb7* disruptants were compared. The number of mid-stem and basal rhizoids per gametophore with 11-14 leaves did not differ between the two (Table 9). The number of

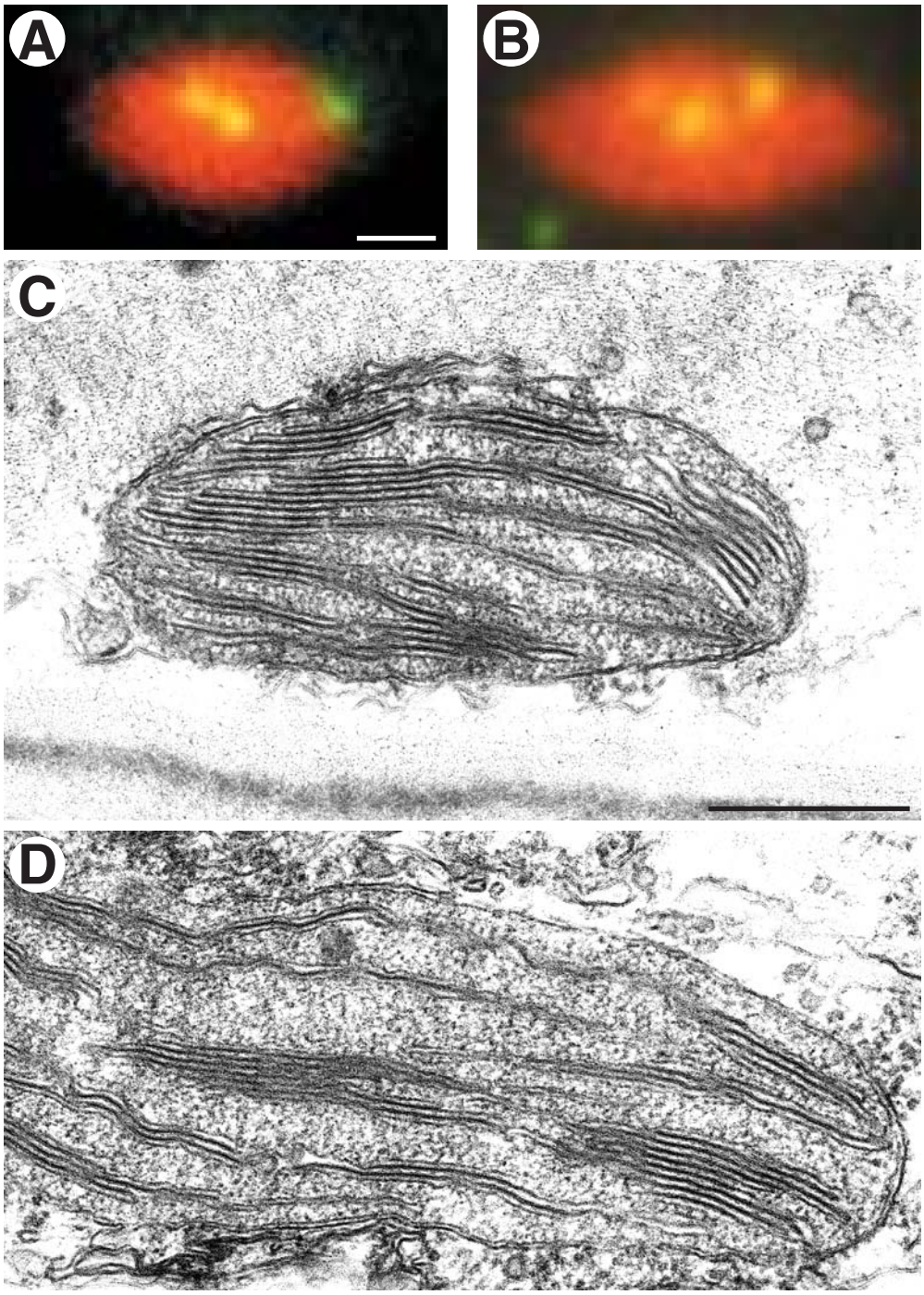

Figure 16. Chloroplast nucleoids and ultrastructure of chloroplasts in wild-type and Pphb7dis-3 rhizoids.
(A,B) Merged images of chlorophyll auto-fluorescence by UV excitation and SYBR Green I staining of chloroplasts in the fifth cell from the rhizoid apical cell of the wild type (A) and Pphb7dis-3 (B). The yellow spots are chloroplast nucleoids. (C,D) Transmission electron micrographs of rhizoid chloroplasts in the wild type (C) and Pphb7dis-3 (D). Bar in (A) = 2.5 μm for (A,B); bar in (C) = 0.5 μm for (C,D).

leaves above the uppermost rhizoid was similar in the wild type and disruptants (Table 8), which indicates that the position of the uppermost mid-stem rhizoid of *Pphb7* disruptants was indistinguishable from that of the wild type. The relationship between the leaf trace and mid-stem rhizoid cell of the *Pphb7* disruptant was identical to that of the wild type (Fig. 14B-D).

To compare the effects of exogenous auxin on the wild type and on the *Pphb7* disruptants, both Pphb7dis-2 and -3 lines were cultured with various concentrations of NAA. Although the *Pphb7*-disrupted rhizoids were less pigmented and greener (Fig. 14E-G), the number of rhizoids in the *Pphb7* disruptant increased to the same extent as in the wild type during both short (Table 8) and long (Table 9) culture periods, and the overall number of rhizoids was not different from that of the wild type.

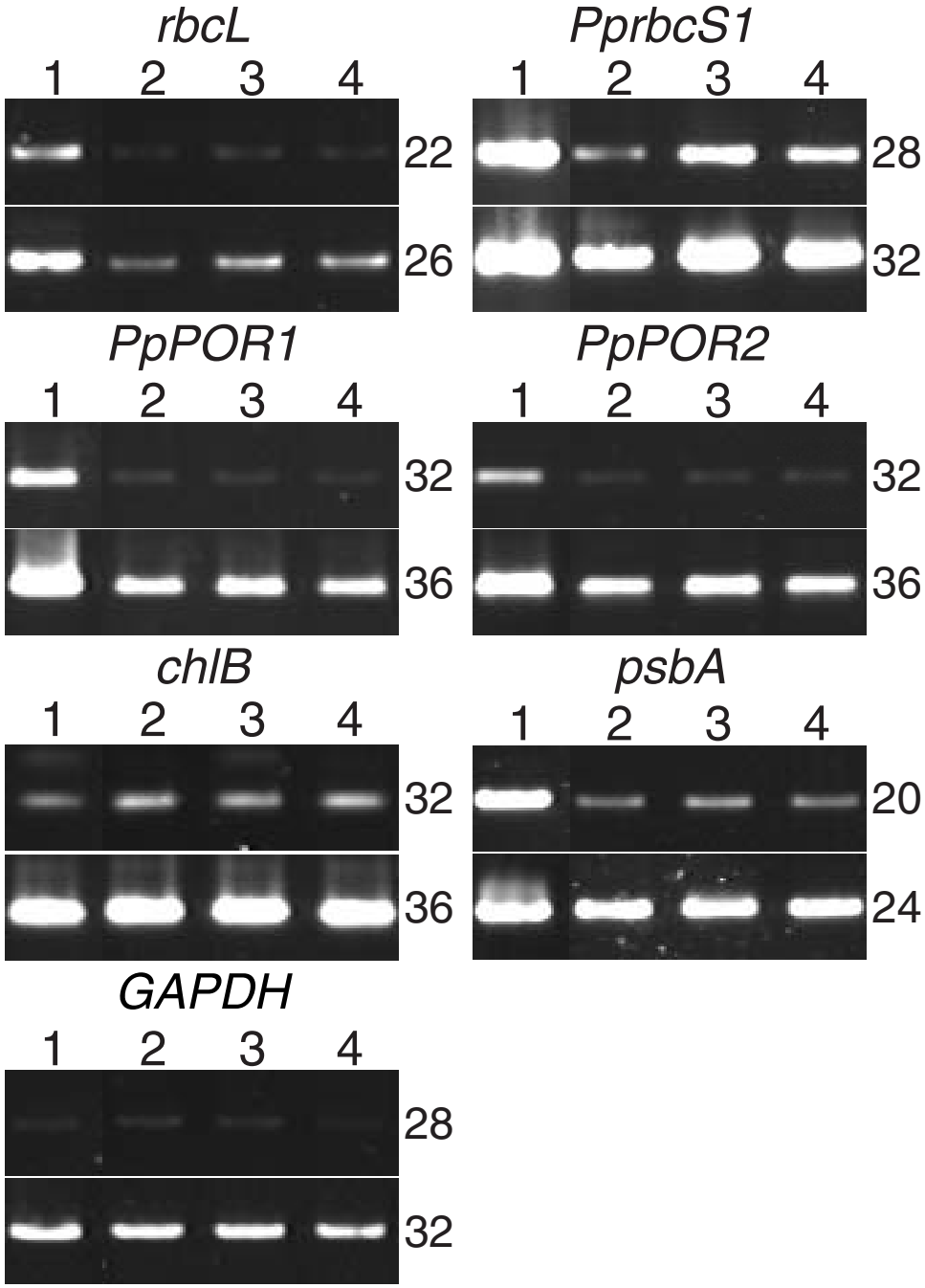

Figure 17. Expression of the genes involved in photosynthesis.
RT-PCR analyses of transcripts of photosynthesis genes in the wild type and in the *Pphb7* disruptants. The number of PCR cycles is indicated to the right of each panel. Gametophores of the wild type (lane 1), rhizoids of the wild type (lane 2), and rhizoids of Pphb7dis-2 and -3 (lanes 3 and 4).

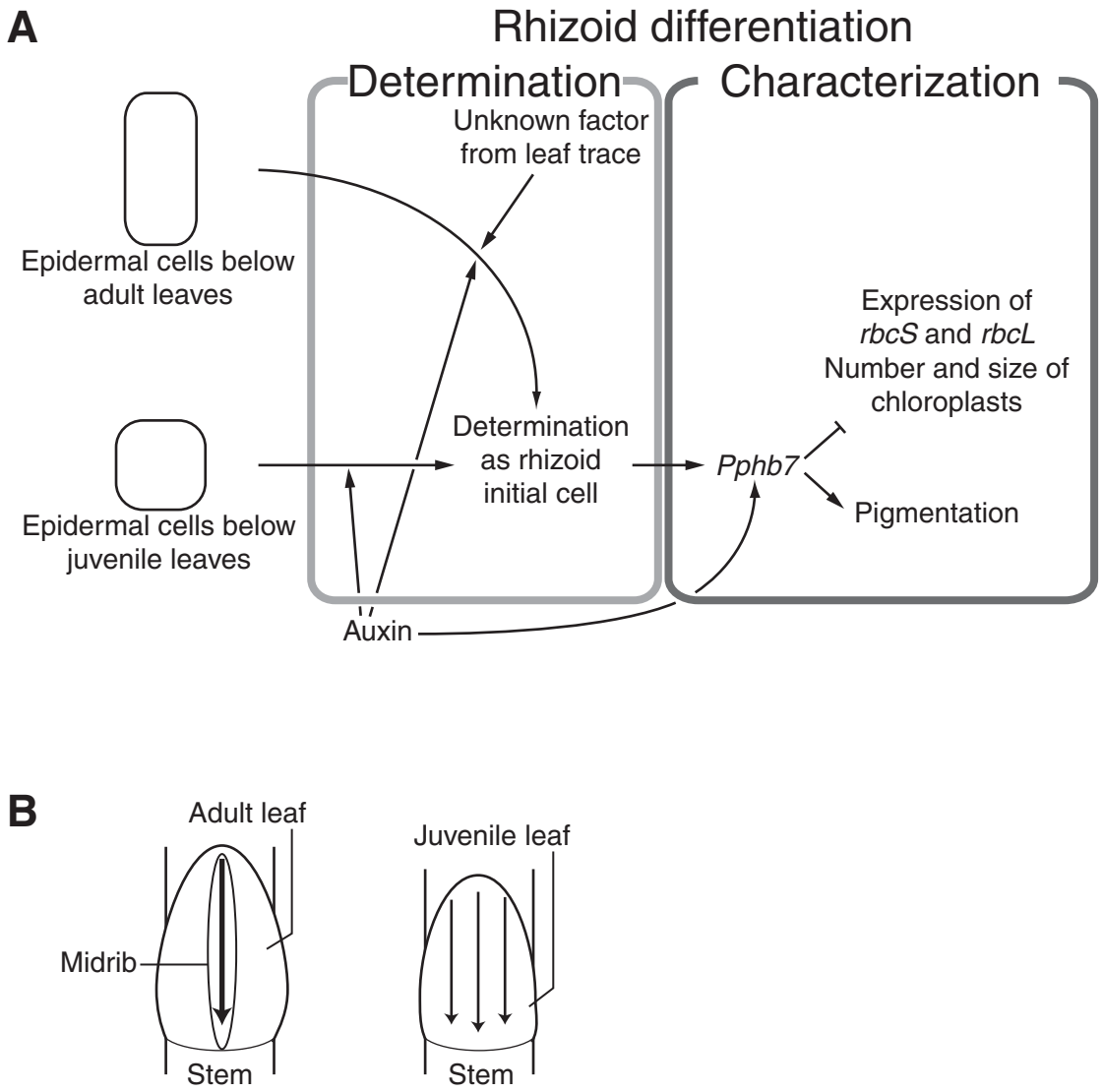

Figure 18. A model of rhizoid differentiation.
(A) Arrows and crossbars indicate the positive and negative interactions, respectively. (B) An explanation for the different differentiation patterns observed between mid-stem and basal rhizoids. The arrows in (B) indicate the hypothetical flow of an unknown factor.

2-5. Discussion

A scheme for rhizoid differentiation

The results of this study enable me to propose a model of rhizoid differentiation in Physcomitrella gametophores (Fig. 18A). My model suggests that rhizoid differentiation can be separated into two processes, which I call determination and characterization. Differentiation is progressive, and the stage and fate of cells become determined at different times and places. To understand the complex differentiation process, I need to subdivide it into components. The determination of presumptive cells and the subsequent signal transduction cascades of cell characterization have been recognized as important processes in epidermal cell differentiation. Hülskamp et al. (1994) suggested that trichome differentiation could be separated into these two processes, because several mutants that regulate only one of the two processes were identified. These processes have not been clearly identified in other model systems of epidermal cell differentiation, such as root hairs and stomatal guard cells.

Mechanisms of rhizoid determination

Rhizoids differentiate from epidermal cells of a gametophore stem below the leaves. Basal and mid-stem rhizoids are distinguished according to their differentiation patterns. The former rhizoid differentiates below a juvenile leaf, while the latter differentiates below an adult leaf. A mid-stem rhizoid always originates from an epidermal cell that lies close to a leaf trace (Fig. 8). Basal rhizoids differentiate at epidermal cells below juvenile leaves, which do not have a midrib (Fig. 8), and no stereotypic spatial pattern of rhizoid differentiation was observed. My model distinguishes between the two types of rhizoid differentiation mentioned above, which are likely caused by different determination processes (Fig. 18A,B).

The number of mid-stem rhizoids increased with the concentration of exogenous NAA (Tables 8, 9), which indicates that auxin promotes mid-stem rhizoid differentiation from stem epidermal cells below adult leaves. The number of basal rhizoids increased when juvenile gametophores were cultured in the presence of 0.1-μM NAA (Table 9), but did not increase when adult gametophores were cultured in NAA (Table 8). This indicates that auxin promotes basal rhizoid differentiation from epidermal cells below juvenile leaves, before the epidermal cells are fully matured. While auxin plays inductive roles in both mid-stem and basal rhizoids, the patterns of additional rhizoid differentiation differ. The increased mid-stem rhizoids always differentiated from stem epidermal cells that lay adjacent to a leaf trace (Fig. 8K),

whereas additional basal rhizoids originated from epidermal cells in a random manner (Fig. 8M). These results suggest that auxin is sufficient for the induction of basal rhizoids, but that an unknown factor that is related to leaf traces is required for mid-stem rhizoid induction (Fig. 18A).

The midrib differentiates in the adult leaf, and probably functions as a conducting tissue (Ligrone et al., 2000). The aforementioned unknown factor may be produced in the leaf and pass through the midrib and the leaf trace as a signal, which, in conjunction with auxin, directs the epidermal cells around the leaf trace to form rhizoids. In the absence of NAA, the uppermost mid-stem rhizoid is usually associated with the 8th leaf from the gametophore apex, which implies that it takes a set amount of time for the unknown factor to accumulate in sufficient amounts to induce rhizoid formation. Although ectopic induction of root hairs by ethylene or its precursor ACC has been reported (Tanimoto et al., 1995), ACC did not increase the number of rhizoids (Fig. 11O), suggesting that different signals are involved in rhizoid induction.

Gametophores grown without NAA formed several mid-stem rhizoids around the first mid-stem rhizoid during later stages of development (Fig. 8L). Rose and Bopp (1983) reported that auxin was transported basipetally in rhizoids. The transport of auxin from the rhizoid to the stem, together with the unknown factor from the leaf trace, may enhance the induction of mid-stem rhizoids. During Arabidopsis trichome differentiation, previously differentiated trichomes inhibit the differentiation of surrounding cells into trichomes (Marks, 1997). However, mid-stem rhizoids promote subsequent rhizoid differentiation.

Two explanations are possible for the differences in patterning between mid-stem and basal rhizoids. First, the different patterns may reflect differences in the distribution of the unknown factor (Fig. 18B). If the unknown factor is abundant in the basal part of a gametophore and is restricted around the leaf trace in the middle, every epidermal cell in the basal part can form a rhizoid in response to auxin, whereas only the epidermal cells around the leaf trace can form rhizoids. The structural differences between juvenile and adult leaves probably account for differences in the distribution of the unknown factor. In juvenile leaves, the unknown factor emanates from leaves, passes through the entire juvenile leaf, and broadly diffuses in epidermal cells, below the juvenile leaves without a midrib. Second, the differences in patterning may reflect different mechanisms for the determination of basal and

mid-stem rhizoids. When basal rhizoids differentiate, the epidermal cells are formed while the gametophore is juvenile, but when mid-stem rhizoids differentiate, the epidermal cells are formed after the gametophore reaches adulthood. Different mechanisms could be involved during different developmental stages. Therefore, the unknown factor that is required for mid-stem rhizoid differentiation may not be essential for basal rhizoid differentiation.

Pphb7 functions not in the determination of rhizoid cells, but in their characterization

The specific expression of *Pphb7* was observed in the rhizoid initial and rhizoid cells (Fig. 11), which indicates that *Pphb7* is involved in rhizoid differentiation. Since the *Pphb7* disruptants formed rhizoids in positions that were spatially indistinguishable from wild-type plants (Fig. 14), it appears that *Pphb7* is not involved in the positional determination of rhizoids, but is involved in the characterization process of rhizoids (Fig. 18A).

Once an epidermal cell is fated to become a rhizoid initial, *Pphb7* regulates various features of the rhizoids, including pigmentation and the size and number of chloroplasts in the rhizoid cell. *Pphb7* is an HD-Zip gene that encodes a putative transcription factor with a DNA-binding motif (Laughon, 1991). Presumably, the GFP-Pphb7 fusion protein functions in the GFP-Pphb7-1, which expresses GFP-Pphb7 instead of Pphb7 but does not show the disruption phenotype. A stronger GFP-Pphb7 signal was detected in the nucleus of the rhizoid cell with slight pigmentation than in the cytoplasm, while intact GFP was localized both in the nucleus and cytoplasm (Fig. 12E-G). This indicates that Pphb7 is localized in the nuclei of rhizoid cells. The signal for GFP-Pphb7 diminished when the rhizoid cells became pigmented, which suggests that *Pphb7* is not required in a fully differentiated rhizoid cell.

Pphb7 regulates the size and number of rhizoid chloroplasts

A rhizoid is composed of a rhizoid apical cell and rhizoid subapical cells. It was difficult to measure the number and size of plastids of an apical cell, probably because of its rich cytoplasm. The discussion that follows focuses on rhizoid subapical cells.

Chloroplasts in wild-type rhizoids are smaller than those in protonemata and gametophores (Figs. 1,8), consistent with the notion that rhizoids are not predominant photosynthetic organs (Duckett et al., 1998). However, the structure of a rhizoid plastid resembles that of a chloroplast in photosynthetic organs (Kasten et al., 1997). Rhizoid plastids

possess chlorophylls, as observed by UV excitation (Fig. 9C,D,F,G), well-developed thylakoid membranes with grana stacks at maturity (Fig. 16C), and randomly distributed plastid nucleoids (Fig. 16A). Rhizoid chloroplasts of *Pphb7* disruptants had all three of the characteristics observed in wild-type rhizoid chloroplasts, although the size and number of chloroplasts in disruptants were increased compared to the wild type (Fig. 15C). This indicates that *Pphb7* does not affect plastid differentiation, but regulates chloroplast size and number in rhizoid subapical cells. This is concordant with the results in Arabidopsis, in which different genes regulate these two processes. The mutant with loss of function of both the *AtGlk1* and *2* genes exhibits a reduction in granal thylakoids, but not in the number of plastids in a cell (Fitter et al., 2002). The *accumulation and replication of chloroplasts* (*arc*) mutants display a phenotype in which chloroplast division is affected, but the chloroplasts develop normally in these loss-of-function mutants (Pyke, 1999).

The size and number of chloroplasts are negatively correlated in many Arabidopsis mutants, suggesting that the corresponding genes in these mutants are involved in chloroplast division (Pyke, 1997; Marrison et al., 1999; Pyke, 1999). The phenotype of *Pphb7* disruptants is clearly different from that of these mutants. Both the size and number of plastids were increased in the rhizoids of disruptants; therefore, *Pphb7* can be considered a new class of regulator that downregulates the total chloroplast mass in a cell. Comparisons of mRNA expression due to several chloroplast genes suggest the molecular mechanism of *Pphb7*. *Pphb7* directly or indirectly downregulates *rbcL* and *PprbcS* genes encoding ribulose-1,5-bisphosphate carboxylase/oxygenase in the wild type (Fig. 17), which often constitutes more than 50% of the total chloroplast protein (Alberts et al., 2002). This suggests that an increase in chloroplast structural proteins per cell causes the increased chloroplast mass per cell. However, the mRNA expression of other chloroplast genes involved in chlorophyll synthesis and a component of photosystem II were not increased in the disruptants, and further analyses of the amounts of protein produced by these genes are necessary to examine this hypothesis, although rhizoids are small and it is difficult to obtain sufficient materials with present techniques.

Regulation of *Pphb7* expression

When the whole gametophytes were treated with NAA, the expression of *Pphb7* mRNA was increased within 1 hour and further increased for up to 6 hours (Fig. 11A). The

time course of induction was comparable to that of auxin-responsive genes, such as *PpIAA1* (Imaizumi et al., 2002), suggesting that *Pphb7* is regulated by auxin fairly directly. Histochemical staining of GUS activity in the Pphb7-GUS line confirmed that the expression was upregulated in rhizoid cells (Fig. 11F). As auxin induces *Pphb7*, which is involved in rhizoid characterization, auxin is likely a positive regulator of both rhizoid characterization and determination (Fig. 18A). BA also induced *Pphb7* expression in the RNA gel blot analysis (Fig. 13B). Microscopic observation showed that new adventitious buds differentiated after BA treatment, and new rhizoids formed at the bases of the newly formed adventitious buds. The GUS signals of the Pphb7-GUS lines were visible at the bases of the adventitious buds, but those in rhizoid cells were not different from those in the controls. Therefore, the induction of *Pphb7* by BA is likely caused by an increase in the number of rhizoid initials with new adventitious bud formation.

While exogenous cytokinin induces chloroplast division in protonemata (Abel et al., 1989), division in rhizoids is not related to exogenous cytokinin, because the numbers of plastids in wild-type and *Pphb7*-disrupted rhizoids treated with 10 µM cytokinin for 48 hours were similar to that in non-treated rhizoids. This implies that the regulation of plastid division in rhizoids differs from that in protonemata.

Other plant hormones (ABA and gibberellin), dehydration, and osmotic stress did not induce *Pphb7* more than water, which induced *Pphb7* three fold. This is concordant with the observation that rhizoids are induced by low nutrient conditions in some mosses (Duckett, 1994).

Physcomitrella rhizoids as a new model system for epidermal cell differentiation

Rhizoids are widely observed in algae and land plants, but their patterns of differentiation have not been elucidated. To understand the molecular mechanisms of rhizoid differentiation and the general rules for epidermal cell differentiation, it is necessary to analyze the genes that are involved in rhizoid differentiation. The Physcomitrella rhizoid appears to be a good model system for the study of rhizoid differentiation in plants. Gene targeting, including gene disruption and modification, is useful for the characterization of gene functions, and can be carried out effectively in Physcomitrella because of its high homologous recombination rate (Schaefer, 2001; Schaefer and Zrÿd, 2001). In addition to the

reverse genetic approaches used in this study, the screening of gene- and enhancer-trap lines with rhizoid-specific expression and of mutants with defects in rhizoid differentiation should provide useful information. Tagged mutant libraries and gene- and enhancer-trap lines have been established in Physcomitrella (Nishiyama et al., 2000; Hiwatashi et al., 2001). Thirty gene-trap lines and 59 enhancer-trap lines with expression in rhizoids have been reported, and a method to identify trapped genes has been established (Hiwatashi et al., 2001). These resources will be useful in future studies of rhizoid differentiation.

General Discussion

As a first step to understand the molecular mechanisms of gametophyte cell differentiation, 10 HD-Zip genes were isolated from Physcomitrella gametophytes. According to the phylogenetic analysis (Fig. 5), Physcomitrella HD-Zip genes belong to three of the four HD-Zip subfamilies, and the four HD-Zip subfamilies diverged before the divergence of the moss and vascular plant lineages. Most of the Physcomitrella HD-Zip genes form sister relationships with angiosperm genes.

Expression and loss-of-function analyses of the Physcomitrella HD-Zip I gene, *Pphb7*, reported in Chapter 2, demonstrate that this gene is involved in rhizoid cell differentiation in gametophytes. Although no mutant of HD-Zip I genes has been identified from angiosperms, expression analyses and the phenotype of overexpressing transformants indicate that HD-Zip I genes are likely involved in cell differentiation in angiosperm sporophytes (Aoyama et al., 1995; Tornero et al., 1996; Hiwatashi and Fukuda, 2000; Nishitani et al., 2001). These findings imply that HD-Zip I genes regulate cell differentiation in the sporophytes of angiosperms and the gametophytes of mosses.

During the evolution of the metazoan body plan, the duplication and modification of a set of developmental genes was likely related to developmental complexity (Force et al., 1999). For example, large-scale genome duplications at the base of the vertebrate lineage greatly increased the number of developmental genes. Such duplications created genetic redundancy; these genes initially regulated the same developmental pathway, but subsequently acquired new or different roles in development (Carroll, et al., 2001).

The gene duplications and modification of the duplicated gene functions also provided developmental complexity in angiosperms. MADS-box genes encode transcription factors and form a large gene family (Hasebe and Banks, 1997; Theissen et al., 2001), and several of them function as floral organ identity genes (reviewed in Weigel and Meyerowitz, 1994; Jack, 2001). Phylogenetic analyses of the MADS-box gene family indicate that the MADS-box genes involved in flower development arose after the divergence of the seed plant and fern lineages (Hasebe et al., 1998; Hasebe, 1999; Theissen et al., 2001). The duplication of MADS-box genes in angiosperms and the functional differentiation of these genes likely played important roles in the evolution of floral organs (reviewed in Hasebe, 1999; Theissen et al., 2001). Thus, gene duplication and the functional differentiation of these genes led to

innovations in morphology in both metazoans and land plants. Genes of each HD-Zip I subfamily increased extensively within each lineage (mosses, ferns, and angiosperms). Although the functions of moss HD-Zip genes are unknown, the duplication of HD-Zip genes and the modification of these gene functions may have been related to the increased cell type complexity in moss gametophytes. This possibility will be assessed using functional analyses of other *Pphb* genes in gametophytes.

Acknowledgments

I am deeply indebted to Professor Mitsuyasu Hasebe for his general support and helpful discussion. I am grateful to Dr. Murata Takashi and Dr. Tomomichi Fijita for helpful discussion and technical advice. I deeply thank Professor Masahiro Kato for his support and collaboration in this work.

I sincerely wish to thank Dr. Tomoaki Nishiyama, Dr. Rumiko Kofuji and Ms. Naomi Sumikawa for collaboration in this work. I show my sincere thanks to Mrs. Satoko Arakawa-Kobayashi and Dr. Toku Kanaseki for providing TEM photos in Fig. 16C,D. I would like to thank Dr. Hiroyoshi Takano for suggestion on the chloroplast experiments in Chapter 2. I also appreciate Dr. Mamoru Sugita kindly provided unpublished sequence data for *chlB* and *psbA*, Dr. Y. Niwa for pTH-2, Ms. Hisako Sakaguchi for the GH3:GFP-containing transformant, Dr. Misako Mishima for advice about morphological analyses, Dr. Hirokazu Tanaka, Dr. Yasunori Machida, and Dr. Chiyoko Machida for preliminary analyses using SEM, Ms. Masae Umeda, Ms. Yoshimi Bitoh, Mrs. Kana Yano, Mrs. Etsuko Aoki, Mrs. Yukiko Dodo-Tanikawa, and Ms. Mayumi Naruse for technical help. I would like to thank Futamura Chemical Industries Co., Ltd. for providing the cellophane used to culture Physcomitrella and Kyowa Hakko Kogyo Co., Ltd. for Driserase. I thank all the past and present members of Dr. Hasebe's laboratory for giving me many help.

The computations were partly done on a SUN Enterprize 3000 or a SGI Origin 2000 in the Computer Lab of NIBB. The NIBB Center for Analytical Instruments provided sequence facilities.

List of references

Abel, W.O., Knebel, W., Koop, H.U., Marienfeld, J.R., Quader, H., Reski, R., Schnepf, E., and Sporlein, B. (1989). A cytokinin-sensitive mutant of the moss, *Physcomitrella patens*, defective in chloroplast division. Protoplasma **152,** 1-13.

Adachi, J., and Hasegawa, M. (1996). MOLPHY version 2.3: programs for molecular phylogenetics based on maximum likelihood. Comput. Sci. Monogr. **28,** 1-150.

Alberts, B., Johnson, A., Lewis, J., Raff, M., Roberts, K., and Walker, P. (2002). Molecular biology of the cell. 4th ed. (New York: Garland Science).

Altschul, S. F., Madden, T. L., Schäffer, A. A., Zhang, J., Zhang, Z., Miller, W., and Lipman, D. J. (1997). Gapped BLAST and PSI-BLAST: a new generation of protein database search programs. Nucl. Acids Res. **25**, 3389-3402.

Aoyama, T., Dong, C.H., Wu, Y., Carabelli, M., Sessa, G., Ruberti, I., Morelli, G., and Chua, N.H. (1995). Ectopic expression of the *Arabidopsis* transcriptional activator *Athb-1* alters leaf cell fate in tobacco. Plant Cell **7,** 1773-1785.

Armstrong, G.A. (1998). Greening in the dark: light-independent chlorophyll biosynthesis from an oxygenic photosynthetic bacteria to gymnosperms. J. Photochem. Photobiol. **43,** 87-100.

Ashton, N.W., and Cove, D.J. (1977). The isolation and preliminary characterization of auxotrophic and analogue resistant mutants of the moss, *Physcomitrella patens*. Mol. Gen. Genet. **154**, 87-95.

Ashton, N.W., Grimsley, N.H., and Cove, D.J. (1979). Analysis of gametophytic development in the moss, *Physcomitrella patens*, using auxin and cytokinin mutants. Planta **144,** 427-435.

Aso, K., Kato, M., Banks, J.A., and Hasebe, M. (1999). Characterization of homeodomain-leucine zipper genes in the fern *Ceratopteris richardii* and the evolution of the homeodomain-leucine zipper gene family in vascular plants. Mol. Biol. Evol. **16,** 544-552.

Baima, S., Nobili, F., Sessa, G., Lucchetti, S., Ruberti, I., and Morelli, G. (1995). The expression of the *Athb-8* homeobox gene is restricted to provascular cells in *Arabidopsis thaliana.* Development **121,** 4171-4182.

Baima, S., Possenti, M., Matteucci, A., Wisman, E., Altamura, M.M., Ruberti, I., and

Morelli, G. (2001). The Arabidopsis *ATHB-8* HD-zip protein acts as a differentiation-promoting transcription factor of the vascular meristems. Plant Physiol. **126,** 643-655.

Bates, J.W., and Bakken, S. (1998). Nutrient retention, desiccation and redistribution in mosses. In Bryology for the twenty-first century, J.W. Bates, N.W. Ashton, and J.G. Duckett, ed. (British Bryological Society), pp. 293-304.

Bell, P.R. (1992). Green plants: Their origin and diversity. (Cambridge: Cambridge University Press).

Berger, D., and Altmann, T. (2000). A subtilisin-like serine protease involved in the regulation of stomatal density and distribution in *Arabidopsis thaliana*. Genes Dev. **14,** 1119-1131.

Bharathan, G., Janssen, B.J., Kellogg, E.A., and Sinha, N. (1997). Did homeodomain proteins duplicate before the origin of angiosperms, fungi, and metazoa? Proc. Natl. Acad. Sci. USA **94,** 13749-13753.

Bold, H.C., Alexopoulos, C.J., and Delevoryas, T. (1987). Morphology of plants and fungi. 5th ed. (New York: Harper Collins Publishers).

Brownlee, C. (2000). Plant development: Keeping your distance. Curr. Biol. **10,** 555-557.

Bürglin, T.R., Finney, M., Coulson, A., and Ruvkun, G. (1989). *Caenorhabditis elegans* has scores of homeobox-containing genes. Nature **341,** 239-243.

Bürglin, T.R. (1998). The PBC domain contains a MEIKNOX domain: coevolution of Hox and TALE homeobox genes? Dev. Genes. Evol. **208**, 113-116.

Carroll, S.B., Grenier, J.K., and Weatherbee, S.D. (2001). From DNA to diversity: Molecular genetics and the evolution of animal design. (Malden, Massachusetts: Blackwell science).

Chan, R.L., Gago, G.M., Palena, C.M., and Gonzalez, D.H. (1998). Homeoboxes in plant development. Biochim. Biophys. Acta **1442**, 1-19.

Chan, S.K., Jaffe, L., Capovilla, M., Botas, J., and Mann, R.S. (1994). The DNA binding specificity of *Ultrabithorax* is modulated by cooperative interactions with extradenticle, another homeoprotein. Cell **78,** 603-615.

Chiu, W.-l., Niwa, Y., Zeng, W., Hirano, T., Kobayashi, H., and Sheen, J. (1996). Engineered GFP as a vital reporter in plants. Curr. Biol. **6,** 325-330.

Church, G.M., and Gilbert, W. (1984). Genomic sequencing. Proc. Natl. Acad. Sci. USA **81,**

1991-1995.

Cove, D. J. (1992). Regulation of development in the moss, *Physcomitrella patens*. In Development: The molecular genetic approach, V.E. Russo, S. Brody, D.J. Cove, S. Ottolenghi eds. (Berlin: Spring-Verlag), pp. 179-193.

Cove, D.J., Knight, C.D., and Lamparter, T. (1997). Mosses as model systems. Trends Plant Sci. **2,** 99-105.

Dengler, N.G. (2001). Regulation of vascular development. J. Plant Growth Regul. **20,** 1-13.

Di Cristina, M., Sessa, G., Dolan, L., Linstead, P., Baima, S., Ruberti, I., and Morelli, G. (1996). The *Arabidopisis Athb-10* (*GLABRA2*) is an HD-Zip protein required for regulation of root hair development. Plant J. **10,** 393-402.

Doolittle, R.F., Feng, D.-F., Tsang, S., Cho, G., and Little, E. (1996). Determining divergence times of the major kingdoms of living organisms with a protein clock. Science **271,** 470-477.

Duckett, J.G. (1994). Studies of protonemal morphogenesis in mosses VI. The foliar rhizoids of *Calliergon stramineum* (Brid.) Kindb. function as organs of attachment. J. Bryol. **18,** 239-252.

Duckett, J.G., Schmid, A.M., and Lignore, R. (1998). Protonemal morphogenesis. In Bryology for the twenty-first century, J.W. Bates, N.W. Ashton, and J.G. Duckett, eds. (British Bryological Society), pp. 223-246.

Esau, K. (1977). Anatomy of seed plants. (New York: John Wiley & Sons, Inc.).

Fitter, D.W., Martin, D.J., Copley, M.J., Scotland, R.W., and Langdale, J.A. (2002). *GLK* gene pairs regulate chloroplast development in diverse plant species. Plant J. **31,** 713-727.

Force, A., Lynch, M., Pickett, F.B., Amores, A., Yan, Y.L., and Postlethwait, J. (1999). Preservation of duplicate genes by complementary, degenerative mutations. Genetics 151, 1531-1545.

Fukuda, H. (1996). Xylogenesis: Initiation, progression, and cell death. Annu. Rev. Plant Physiol. Plant Mol. Biol. **47,** 299-325.

Girke, T., Schmidt, H., Zahringer, U., Reski, R., and Heinz, E. (1998). Identification of a novel Delta 6-acyl-group desaturase by targeted gene disruption in *Physcomitrella patens*. Plant J. **15,** 39-48.

Girod, P.A., Fu, H.Y., Zrÿd, J.P., and Vierstra, R.D. (1999). Multiubiquitin chain binding

subunit MCB1 (RPN10) of the 26S proteasome is essential for developmental progression in *Physcomitrella patens.* Plant Cell **11,** 1457-1471.

Glover, B.J. (2000). Differentiation in plant epidermal cells. J. Exp. Bot. **51,** 497-505.

Gonzalez, D.H., Valle, E.M., Raquel, G.G., and Chan, R.L. (1997). Interaction between proteins containing homeodomains associated to leucine zippers from sunflower. Biochim. Biophys. Acta **1351,** 137-149.

González-Crespo, S., Abu-Shaar, M., Torres M., Martínez, C., Mann, R. S. and Morata, G. (1998). Antagonism between *extradenticle* function and *Hedgehog* signaling in the developing limb. Nature **394**, 196-200.

Graham, L.E. (1993). Origin of land plants. (New York: John Wiley & Sons, Inc.).

Grimsley, N.H., Ashton, N.W., and Cove, D.J. (1977). The production of somatic hybrids by protoplast fusion in the moss, *Physcomitrella patens*. Mol. Gen. Genet. **154**, 97-100.

Grueneberg, D.A., Simon, K.J., Brennan, K., and Gilman, M. (1995). Sequence-specific targeted expression of nuclear signal transduction pathway by homeodomain protein. Mol. Cell. Biol. **15,** 3318-3326.

Hasebe, M., and Banks, J.A. (1997). Evolution of MADS gene family in plants. In Evolution and Diversification in Land Plants, K. Iwatsuki and P.H. Raven, eds (Tokyo: Springer-Verlag), pp. 179-197.

Hasebe, M., Wen, C.-K., Kato, M., and Banks, J.A. (1998). Characterization of homeotic genes in the fern *Ceratopteris richardii*. Proc. Natl. Acad. Sci. USA 95, 6222-6227.

Hasebe, M. (1999). Evolution of reproductive organs in land plants. J. Plant Res. 112, 463-474.

Hasegawa, M., and Kishino, H. (1994). Accuracies of the simple methoods for estimating the bootstrap probability of a maximum-likelihood tree. Mol. Biol. Evol. **11**, 142-145.

Hartman, F.C., and Harpel, M.R. (1994). Structure, function, regulation, and assembly of D-ribulose-1,5-bisphosphate carboxylase/oxygenase. Annu. Rev. Biochem. **63,** 197-234.

Hiwatashi, Y., and Fukuda, H. (2000). Tissue-specific localization of mRNA for carrot homeobox genes, *CHB*s in carrot somatic embryo. Plant Cell Physiol. **41,** 639-643.

Hiwatashi, Y., Nishiyama, T., Fujita, T., and Hasebe, M. (2001). Establishment of gene-

trap and enhancer-trap systems in the moss *Physcomitrella patens*. Plant J. **28,** 105-116.

Hu, J.C., O'Shea, E.K., Kim, P.S., and Sauer, R.T. (1990). Sequence requirements for coiled-coils: analysis with lambda repressor-GCN4 leucine zipper fusions. Science **250**, 1400-1403.

Hülskamp, M., Misera, S., and Jürgens, G. (1994). Genetic dissection of trichome cell-development in *Arabidopsis.* Cell **76,** 555-566.

Imaizumi, T., Kadota, A., Hasebe, M., and Wada, M. (2002). Cryptochrome light signals control development to suppress auxin sensitivity in the moss *Physcomitrella patens*. Plant Cell **14,** 373-386.

Jack, T. (2001). Relearning our ABCs: new twists on an old model. Trends Plant Sci. **6**, 310-316.

Jefferson, R.A., Kavanagh, T.A., and Bevan, M.W. (1987). GUS fusions: b-glucuronidase as a sensitive and versatile gene fusion marker in higher plants. EMBO J. **6,** 3901-3907.

Jones, D.T., Taylor, W.R., and Thornton, J.M. (1992). The rapid generation of mutation data matrices from protein sequences. Comput. Appl. Biosci. **8**, 275-282.

Karnovsky, M.J. (1965). A formaldehyde-glutaraldehyde fixative of high osmolality for use in electron microscopy. J. Cell. Biol. **27,** 137A.

Kasten, B., Buck, F., Nuske, J., and Reski, R. (1997). Cytokinin affects nuclear- and plastome-encoded energy- converting plastid enzymes. Planta **201,** 261-272.

Kenrick, P., and Crane, P.R. (1997a). The origin and early evolution of plants on land. Nature **389,** 33-39.

Kenrick, P., and Crane, P.R. (1997b). The origin and diversification of early land plants: A cladistic study. (Washington, DC: Smithonian Institution Press).

Kishino, H., Miyata, T., and Hasegawa, M. (1990). Maximum likelihood inference of protein phylogeny and the origin of chloroplasts. J. Mol. Evol. **30**, 151-160.

Kissinger, C.R., Liu, B., Martin-Blanco, E., Kornberg, T.B., and Pabo, C.O. (1990). Crystal structure of an engrailed homeodomain-DNA complex at 2.8 Å resolution: A framework for understanding homeodomain-DNA interactions. Cell **63,** 579-590.

Knight, C.D., Cove, D.J., Boyd, P.J., and Ashton, N.A.W. (1988). The isolation of biochemical and developmental mutants in *Physcomitrella patens*. In Methods in

bryology, J.M. Glime, ed (Miyazaki, Japan: The Hattori Botanical Laboratory), pp. 47-58.

Knight, C.D., Sehgal, A., Atwal, K., Wallace, J.C., Cove, D.J., Coates, D., Quatrano, R.S., Bahadur, S., Stockley, P.G., and Cuming, A.C. (1995). Molecular responses to abscisic acid and stress are conserved between moss and cereals. Plant Cell **7,** 499-506.

Kolukisaoglu, H.Ü., Braun, B., Martin, W.F., and Schneider-Poetsch, H.A.W. (1993). Mosses do express conventional, distantly B-type-related phytochromes: Phytochrome of *Physcomitrella patens* (Hedw.). FEBS Lett. **334,** 95-100.

Koprivova, A., Meyer, A.J., Schween, G., Herschbach, C., Reski, R., and Kopriva, S. (2002). Functional knockout of the adenosine 5'-phosphosulfate reductase gene in *Physcomitrella patens* revives an old route of sulfate assimilation. J. Biol. Chem. **277,** 32195-32201.

Landschulz, W.H., Johnson, P.F., and McKnight, S.L. (1988). The leucine zipper: a hypothetical structure common to a new class of DNA binding proteins. Science **240,** 1759-1764.

Laughon, A. (1991). DNA binding specificity of homeodomains. Biochemistry **30,** 11357-11367.

Lee, M.M., and Schiefelbein, J. (1999). *WEREWOLF*, a *MYB*-related protein in *Arabidopsis*, is a position-dependent regulator of epidermal cell patterning. Cell **99,** 473-483.

Lee, Y.H., and Chun, J.Y. (1998). A new homeodomain-leucine zipper gene from *Arabidopsis thaliana* induced by water stress and abscisic acid treatment. Plant Mol. Biol. **37,** 377-384.

Leech, M.J., Kammerer, W., Cove, D.J., Martin, C., and Wang, T.L. (1993). Expression of *myb*-related genes in the moss, *Physcomitrella patens*. Plant J. **3,** 51-61.

Li, Y., Wu, Y.H., Hagan, G., and Guilfoyle, T. (1999). Expression of the auxin-inducible GH3 promoter/GUS fusion gene as a useful molecular marker for auxin physiology. Plant Cell Physiol. **407,** 675-682.

Ligrone, R., Duckett, J.G., and Renzaglia, K.S. (2000). Conducting tissues and phyletic relationships of bryophytes. Phil. Trans. R. Soc. Lond. B **355,** 795-813.

Liu, Y.-G., Mitsukawa, N., Oosumi, T., and Whittier, R.F. (1995). Efficient isolation and mapping of *Arabidopsis thaliana* T-DNA insert junctions by thermal asymmetric

interlaced PCR. Plant J. **8,** 457-463.

Mann, R. S., and Chan, S.-K. (1996). Extra specificity from *extradenticle*: the partnership between HOX and PBX/EXD homeodomain proteins. Trends Genet. **12**, 258-262.

Mann, R. S., and Affolter, M. (1998). Hox proteins meet more partners. Curr. Opin. Genet. Dev. **8**, 423-429.

Marks, M.D. (1997). Molecular genetic analysis of trichome development in *Arabidopsis*. Annu. Rev. Plant Physiol. Plant Mol. Biol. **48**, 137-163.

Marrison, J.L., Rutherford, S.M., Robertson, E.J., Lister, C., Dean, C., and Leech, R.M. (1999). The distinctive roles of different *ARC* genes in the chloroplast division process in *Arabidopsis*. Plant J. **18,** 651-662.

McConnell, J.R., Emery, J., Eshed, Y., Bao, N., Bowman, J., and Barton, M.K. (2001). Role of *PHABULOSA* and *PHAVOLUTA* in determining radial patterning in shoots. Nature **411,** 709-713.

McGinnis, W., Garber, L., Wirz, J., Kurokawa, A., and Gehring, W.J. (1984). A homologous protein-coding sequence in *Drosophila* homeotic genes and its conservation in other metazoans. Cell **37,** 403-408.

Meijer, A.H., Scarpella, E., Van Dijk, E.L., Qin, L., Taal, A.J.C., Rueb, S., Harrington, S.E., McCouch, S.R., Schilperoort, R.A., and Hoge, J.H.C. (1997). Transcriptional repression by *Oshox1*, a novel homeodomain leucine zipper protein from rice. Plant J. **11,** 263-276.

Murray, M.G., and Thompson, W.F. (1980). Rapid isolation of high molecular weight plant DNA. Nucl. Acids Res. **8**, 4321-4325.

Nishitani, C., Demura, T., and Fukuda, H. (2001). Primary phloem-specific expression of a *Zinnia elegans* homeobox gene. Plant Cell Physiol. **42,** 1210-1218.

Nishiyama, T., Hiwatashi, Y., Sakakibara, K., Kato, M., and Hasebe, M. (2000). Tagged mutagenesis and gene-trap in the moss, *Physcomitrella patens* by shuttle mutagenesis. DNA Research **7,** 9-17.

O'Shea, E.K., Rutkowski, R., and Kim, P.S. (1991). Evidence that the leucine zipper is a coiled coil. Science **243,** 538-541.

Oppenheimer, D.G., Herman, P.L., Sivakumaran, S., Esch, J., and Marks, M.D. (1991). A *myb* gene required for leaf trichome differentiation in *Arabidopsis* is expressed in stipules. Cell **67,** 483-493.

Payne, C.T., Zhang, F., and Lloyd, A.M. (2000). *GL3* encodes a bHLH protein that regulates trichome development in *Arabidopsis* through interaction with *GL1* and *TTG1*. Genetics **156,** 1349-1362.

Ptashne, M. (1988). How eukaryotic transcriptional activators work. Nature **335,** 683-689.

Pyke, K.A. (1997). The genetic control of plastid division in higher plants. Am. J. Bot. **84,** 1017-1027.

Pyke, K.A. (1999). Plastid division and development. Plant Cell **11,** 549-556.

Raghavan, V. (1989). Developmental biology of fern gametophytes. (Cambridge: Cambridge University Press).

Rerie, W.G., Feldmann, K.A., and Marks, M.D. (1994). The *GLABRA2* gene encodes a homeodomain protein required for normal trichome development in *Arabidopsis*. Genes Dev. **8,** 1388-1399.

Reski, R. (1998). Development, genetics and molecular biology of mosses. Bot. Acta **111,** 1-15.

Rose, S., and Bopp, M. (1983). Uptake and polar transport of indoleacetic acid in moss rhizoids. Physiol. Plant. **58**, 57-61.

Russell, A.J., Cove, D.J., Trewavas, A.J., and Wang, T.L. (1998). Blue light but not red light induces a calcium transient in the moss *Physcomitrella patens* (Hedw.) B., S. & G. Planta **206,** 278-283.

Saitou, N., and Nei, M. (1987). The neighbor-joining method: a new method for reconstructing phylogenetic tree. Mol. Biol. Evol. **4**, 406-425.

Scarpella, E., Rueb, S., Boot, K.J.M., Hoge, J.H.C., and Meijer, A.H. (2000). A role for the rice homeobox gene *Oshox1* in provascular cell fate commitment. Development **127,** 3655-3669.

Schaefer, D., Zrÿd, J.P., Knight, C.D., and Cove, D.J. (1991). Stable transformation of the moss *Physcomitrella patens*. Mol. Gen. Genet. **226**, 418-424.

Schaefer, D.G., and Zrÿd, J.P. (1997). Efficient gene targeting in the moss *Physcomitrella patens*. Plant J. **11,** 1195-1206.

Schaefer, D.G. (2001). Gene targeting in *Physcomitrella patens.* Curr. Opin. Plant Biol. **4,** 143-150.

Schaefer, D., and Zrÿd, J.P. (2001). The moss *Physcomitrella patens*, now and then. Plant Physiol. **127,** 1430-1438.

Schena, M., and Davis, R.W. (1992). HD-Zip proteins: members of an *Arabidopsis* homeodomain protein superfamily. Proc. Natl. Acad. Sci. USA **89**, 3894-3898.

Schofield, W.B., and Hébant, C. (1984). The morphology and anatomy of the moss gametophore. In New manual of bryology. Vol. 2., R.M. Schuster, ed. (Miyazaki, Japan: The Hattori Botanical Laboratory).

Sessa, G., Morelli, G., and Ruberti, I. (1993). The *Athb-1* and *-2* HD-Zip domains homodimerize forming complexes of different DNA binding specificities. EMBO J. **12,** 3507-3517.

Sessa, G., Steindler, C., Morelli, G., and Ruberti, I. (1998). The *Arabidopsis Athb-8*, *-9* and *-14* genes are members of a small gene family coding for highly related HD-ZIP proteins. Plant Mol. Biol. **38,** 609-622.

Stewart, W., and Rothwell, G.W. (1993). Paleobotany and the evolution of plants. 2nd ed. (Cambridge: Cambridge University Press).

Strepp, R., Scholz, S., Kruse, S., Speth, V., and Reski, R. (1998). Plant nuclear gene knockout reveals a role in plastid division for the homolog of the bacterial cell division protein *FtsZ*, an ancestral tubulin. Proc. Natl. Acad. Sci. USA **95,** 4368-4373.

Swofford, D.L. (2000). PAUP*. Phylogenic analysis using parsimony (* and other methods). Version 4.0 b4a. (Sunderland: Sinauer Associates).

Söderman, E., Mattsson, J., and Engström, P. (1996). The *Arabidopsis* homeobox gene *Athb-7* is induced by water deficit and by abscisic acid. Plant J. **10,** 375-381.

Söderman, E., Hjellstrom, M., Fahleson, J., and Engström, P. (1999). The HD-zip gene *ATHB6* in *Arabidopsis* is expressed in developing leaves, roots and carpels and up-regulated by water deficit conditions. Plant Mol. Biol. **40**, 1073-1083.

Tanimoto, M., Roberts, K., and Dolan, L. (1995). Ethylene is a positive regulator of root hair development in *Arabidopsis thaliana.* Plant J. **8,** 943-948.

Theissen, G. (2001). Development of floral organ identity: stories from the MADS house. Curr. Opin. Plant Biol. 4, 75-85.

Thompson, J.D., Higgins, D.G., and Gibson, T.J. (1994). CLUSTAL W: improving the sensitivity of progressive multiple sequence alignment through sequence weighting, positions-specific gap penalties and weight matrix choice. Nucl. Acids Res. **22**, 4673-4680.

Tornero, P., Conejero, V., and Vera, P. (1996). Phloem-specific expression of a plant homeobox gene during secondary phases of vascular development. Plant J. **9,** 639-648.

Tsuge, T., Tsukaya, H., and Uchimiya, H. (1996). Two independent and polarized processes of cell elongation regulate leaf blade expansion in *Arabidopsis thaliana* (L) Heynh. Development **122,** 1589-1600.

Wada, T., Tachibana, T., Shimura, Y., and Okada, K. (1997). Epidermal cell differentiation in *Arabidopsis* determined by a *Myb* homolog, *CPC*. Science **277,** 1113-1116.

Weigel, D., and Meyerowitz, E.M. (1994). The ABCs of floral homeotic genes. Cell 78, 203-209.

Wiencke, C., and Schulz, D. (1983). The fine structural basis of symplasmic and apoplasmic transport in the nerv of the *Funaria* leaflet. Z. Pflanzenphysiopl. **112**, 337-350.

Ye, Z.H. (2002). Vascular tissue differentiation and pattern formation in plants. Ann. Rev. Plant Biol. **53,** 183-202.

Zappavigna, V., Sartori, D., and Mavilio, F. (1994). Specificity of HOX protein function depends on DNA-protein and protein-protein interactions, both mediated by the homeo domain. Genes Dev. **8,** 732-744.

Zhang, L., and Aro, E.-M. (2002). Synthesis, membrane insertion and assembly of the chloroplast-encoded D1 protein into photosystem II. FEBS Lett. **512,** 13-18.

Zhong, R.Q., and Ye, Z.H. (1999). *IFL1*, a gene regulating interfascicular fiber differentiation in *Arabidopsis*, encodes a homeodomain-leucine zipper protein. Plant Cell **11,** 2139-2152.